CHARACTERIZATION OF MARINE EXOPOLYMERIC SUBSTANCE (EPS) RESPONSIBLE FOR BINDING OF THORIUM (IV) ISOTOPES

A Dissertation

by

NICOLÁS GABRIEL ALVARADO QUIROZ

Submitted to the Office of Graduate Studies of
Texas A&M University
in partial fulfillment of the requirements for the degree of

DOCTOR OF PHILOSOPHY

May 2004

Major Subject: Oceanography

CHARACTERIZATION OF MARINE EXOPOLYMERIC SUBSTANCE (EPS) RESPONSIBLE FOR BINDING OF THORIUM (IV) ISOTOPES

A Dissertation

by

NICOLÁS GABRIEL ALVARADO QUIROZ

Submitted to Texas A&M University
in partial fulfillment of the requirements
for the degree of

DOCTOR OF PHILOSOPHY

Approved as to style and content by:

Peter H. Santschi (Chair of Committee)	Luis A. Cifuentes (Member)
John R. Schwarz (Member)	James L. Pinckney (Member)
Paul A. Lindahl (Member)	Wilford D. Gardner (Head of Department)

May 2004

Major Subject: Oceanography

ABSTRACT

Characterization of Marine Exopolymeric Substance (EPS) Responsible for Binding of Thorium (IV) Isotopes. (May 2004)

Nicolás Gabriel Alvarado Quiroz, B.Sc., University of Ottawa;

M.Sc., University of Ottawa

Chair of Advisory Committee: Dr. Peter H. Santschi

The functional group composition of acid polysaccharides was determined after isolation using cross-flow ultrafiltration, radiolabeling with ^{234}Th(IV) and other isotopes, and separation using isoelectric focusing (IEF) and polyacrylamide gel electrophoresis (PAGE). Phosphate and sulphate concentrations were determined from cultured bacterial and phytoplankton colloid, particulate and colloidal samples collected from the Gulf of México (GOM). Characterization of the ^{234}Th(IV)-binding biomolecule was performed using ion chromatography (IC), and gas chromatography-mass spectrometry (GC-MS). Radiotracer experiments and culture experiments were conducted in determining the binding environment of the ^{234}Th(IV)-binding ligand (i.e., sorption onto suspended particles), as well as the origin of the ligand in seawater systems. In all samples, ^{234}Th(IV) isoelectric focusing profiles indicated that 49% to 65% of the ^{234}Th(IV) labeled EPS from *Roseobacter gallaeciensis*, *Sagittula stellata*, *Emiliania huxleyi*, *Synechococcus elongatus* and GOM Station 4-72m was found at a pH_{IEF} of 2 in the IEF spectrum. The carboxylic acid group appeared at the same pH_{IEF} as ^{234}Th(IV) for EPS from *Roseobacter gallaeciensis*, *Emiliania huxleyi*, *Synechococcus elongatus*

and GOM colloidal organic matter sample. The phosphate group appeared at the same pH_{IEF} as ^{234}Th(IV) for EPS from *Roseobacter gallaeciensis*, and *Synechococcus elongatus* sample. The sulphate group was found at the same pH_{IEF} as ^{234}Th(IV) for EPS from *S. elongatus* and GOM colloidal organic matter sample. The total polysaccharide content was only 14% and 8%, uronic acids were approximately 5.4% and 87.1%, and total protein content was 2.6% and 6.2% of total carbon content of *Sagittula stellata* and *Synechococcus elongatus*, respectively. Monosaccharides identified in both *Sagittula stellata* and *Synechococcus elongatus* were galactose, glucose, and xylose in common. In addition, *Sagittula stellata* contained mannose and *Synechococcus elongatus* had galactoglucuronic acid. Thus, depending on the species, the size, structural composition, and functional groups of the ^{234}Th(IV)-binding, acidic polysaccharides will vary. From these observations, it is concluded that the steric environment and not necessarily the exact functional group might actually be responsible for thorium-234 complexation to macromolecular organic matter. This research helped to improve our understanding of the observed variability in POC/^{234}Th ratios in the ocean and provided insights into factors that regulate organic carbon export fluxes.

Quiero dedicar mi doctorado a mi familia.

ACKNOWLEDGEMENTS

I thank my advisor, Dr. Peter H. Santschi, who took me on for this project, introduced me to colloidal and radio-chemistry, broadened my career in the environmental field and was a constant source of encouragement and information.

I give many thanks to my committee, Dr. James L. Pinckney, Dr. Luis A. Cifuentes, Dr. John R. Schwarz, and Dr. Paul A. Lindahl at Texas A&M University, College Station and Texas A&M University at Galveston, for their source of information and guidance throughout the duration of the project. I am grateful to Dr. Gary S. Schultz and Dr. Chin-Chang Hung for their expertise in microbiology, polysaccharide characterization and GC-MS work involved with this project and for introducing me to their fields of study. Thanks to Dr. G. Alvarado Urbina for his insight and assistance on techniques in molecular biology.

A special thanks to Dr. John Schwarz, Dr. Jaime Alvarado Bremer, Dr. Alexandru Balaban and Dr. Marc Ilies for the use of their laboratory and equipment throughout the project.

I express my gratitude to NSF for the selection and funding of this project [NSF OCE-9633125 and OCE-9906823].

I recognize the staff of the Department of Oceanography at the Texas A&M University, which includes Mary Howley, Sandy Drews, Amanda Wotkins-Borth, Laura Caldwell and Sheri Shaklovitz for their continuous assistance and support with academic administration. Thanks are also due to Mona S. Hochman at the Texas A&M University

at Galveston Seafood Safety Lab. I would like to express my gratitude to former graduate students for their advice Dr. Kent Warnken, Dr. Lao-Dong Guo, Dr. Kathleen Schwehr and Dr. Matt Quigley. Thanks to fellow grad-students Erick Huchzermeyer and Kimberly Roberts for lending me their ears and a very special thank you to Ron Lehman for technical assistance.

I personally would like to give my gratitude to the deliverEdocs and Interlibrary Loan (ILL) Services and Thesis office at Texas A&M University, College Station for their prompt turnaround time.

Finally, I give thanks to my family who continually encouraged and supported me. I give my gratitude to my father, Dr. Gabriel G. Alvarado Urbina, my mother Mrs. Gladys Quiroz Alvarado, who provided an endless source of advice and encouragement. I also give a special thanks to Constanza, Sebastian, Margaret, and Sergio. Finally, I thank Cristina Urizar for her help and encouragement.

TABLE OF CONTENTS

Page

Page

LIST OF FIGURES

Page

Page

Page

Page

LIST OF TABLES

Page

Page

I. INTRODUCTION

Atmospheric carbon dioxide (CO_2) concentration has increased in the last 60 years, from 280 ppm to 360 ppm, due largely to anthropogenic discharge of excess CO_2 through burning of fossil fuels (Keeling and Whorf, 1994). Since the ocean is vast and undersaturated with respect to CO_2, the ocean represents a large potential sink for CO_2 emissions (Reichle *et al.*, 1999). The cycling of carbon begins with the production of organic matter from CO_2 fixation by phytoplankton. The phytoplankton produce dissolved organic matter (DOM) and particulate organic matter (POM), as a result of photosynthesis.

New production is the portion of primary production stimulated by new nutrient inputs. New production provides a central framework for oceanographers studying upper ocean biogeochemical cycles. The gross fluxes of bioactive elements through the euphotic zone thus become linked, in one way or another, by the rates of new production. At steady state, the balance of the import flux for a particular nutrient element minus its export flux must equal its net biological uptake within a given region. The balance must in turn translate to an export flux as dissolved and particulate organic matter (Aufdenkampe and Murray, 2002). The global carbon export fluxes can be assessed by measuring biogenic particle fluxes caught in sediment traps (Buesseler *et al.*, 1992, 1995). In the last decade, carbon export fluxes have been evaluated by measuring particulate organic carbon (POC)/^{234}Th(IV) ratios in suspended matter.

This dissertation follows the style of Marine Chemistry.

Thorium-234 (^{234}Th(IV), $t_{halflife}$=24.1 days) is a naturally occurring highly particle-reactive radionuclide continuously produced from alpha decay of Uranium-238 ($t_{halflife}$ =4.47 X 10^9 years) in seawater. Uranium in seawater exists as the dissolved carbonate species [$UO_2(CO_3)_3^{4-}$] and is relatively unreactive to particulates (less than 0.1% of uranium is particulate in seawater). Thus, uranium exhibits a rather conservative distribution in the open ocean (Ku *et al.,* 1977; Edwards *et al.*, 1987) with an average U-concentration of 13.9 nM (10^{-9} M) at a salinity of 35. On the other hand, total Th(IV) occurs in seawater at about 43-47fM (femtomolar, 10^{-15} M) (Choppin and Wong, 1998) and ^{234}Th(IV) at about aM (attomolar, 10^{-18} M) concentrations compared to natural seawater cation concentrations which are in the millimolar (10^{-3} M) concentrations (Table 1). According to Choppin and Wong (1998) Th(IV) will form a humic acid complex in seawater.

Table 1 Concentrations of major constituents in surface seawaters (Pilson, 1998).

	At salinity S = 35.000%	
	g/kg	**mM**
Na^+	10.781	480.57
K^+	0.399	10.46
Mg^+	1.284	54.14
Ca^{2+}	0.4119	10.53
Sr^{2+}	0.00794	0.0928
Cl^-	19.353	559.40
SO_4^{2-}	2.712	28.93
HCO_3^-	0.126	2.11
Br^-	0.0673	0.865
$B(OH)_3$	0.0257	0.426
F^-	0.0013	0.070

Matijevic *et al.* (1960) proposed that, in the absence of organic matter, dissolved thorium exists as the hydrolysis product of $Th(OH)^{3+}$, which is a reactive species with a high tendency to sorb onto particles. Bhat *et al*. (1969) and Matsumoto (1975) showed that these reactive species of $^{234}Th(IV)$ can be removed from the dissolved state by adsorption onto marine particles, a process which lends itself to box modeling and computation of removal rates and residence times (Bacon and Anderson, 1982). Figure 1 is an example for the degree of radioactive disequilibrium that can occur in the water column between $^{234}Th(IV)$ (particle reactive daughter) and ^{238}U (its soluble parent). This can be used to quantify removal rates for $^{234}Th(IV)$ by adsorption to settling particles. Thus, the resulting $^{234}Th(IV)$ loss from surface waters indicates a direct rate of removal of $^{234}Th(IV)$ via sinking particles (particle flux) from the upper ocean (Bacon and Anderson, 1982; Coale and Bruland, 1985; Buessler *et al.*, 1992, 1995, 1998; Bacon *et al.*, 1996; Baskaran *et al.*, 1996; Murray *et al.*, 1989, 1996; Moran and Buessler, 1992; Gustaffson *et al.*, 1997; Buessler, 1998; Santschi *et al.*, 1999; Benitez-Nelson *et al.*, 2001).

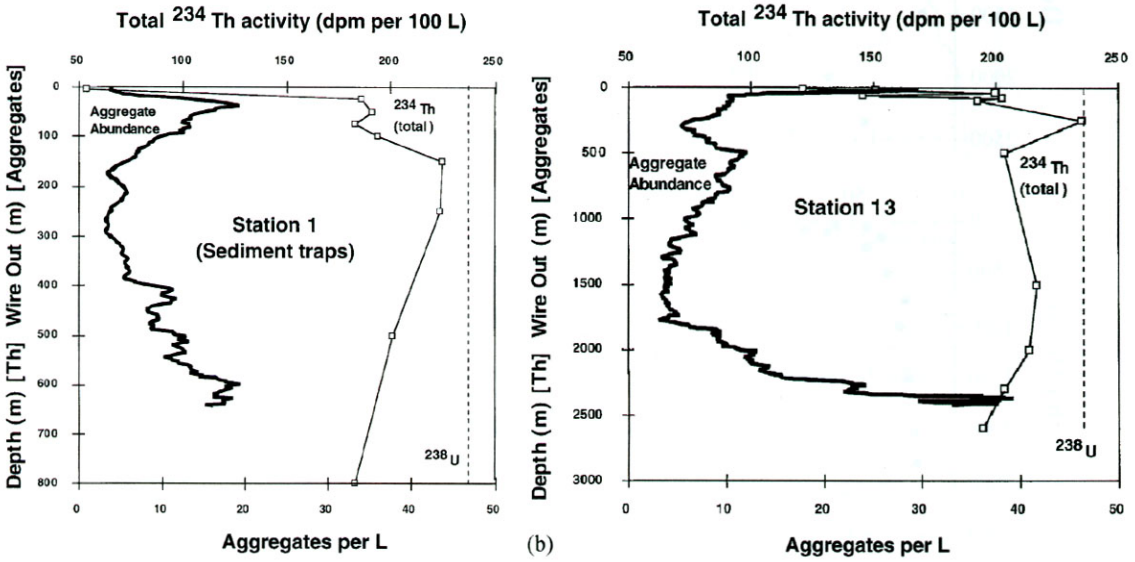

Figure 1 $^{234}Th/^{238}U$ disequilibrium in the Middle Atlantic Bight (Reprinted from Continental Shelf Research, Vol 19, Santschi, P. H., Guo, L.-D. Walsh, I. D., Quigley, M. S. and Baskaran, M.. Boundary exchange and scavenging of radionuclides in continental margin water of the Middle Atlantic Bight: implications for organic carbon fluxes. pp 609-636 Copyright (1999), with permission from Elsevier).

I.1. Carbon Flux Model

Coale and Bruland (1985) derived a relationship between organic carbon flux or new production as particulate organic carbon (POC) in the upper ocean and $^{234}Th(IV)/^{238}U$ disequilibrium (Eq.1). The extent of $^{234}Th(IV)$ removal rates in the open ocean is depicted in equation 1.

$$P_{POC} = \lambda_{234}\left(A_{\mathrm{U}} - A_{\mathrm{Th}}\right)\frac{POC}{Th_p} \qquad \textbf{Eq. 1}$$

Relationship between organic carbon flux or new production (POC) in the upper ocean and ^{234}Th(IV)/^{238}U disequilibrium where POC and Th_p represent the concentration of organic carbon (OC) and ^{234}Th(IV) activity determined in certain particle size class (e.g., the >53μm; sinking particles), and A_U and A_{Th} are the total activities of ^{238}U and ^{234}Th(IV), respectively. However, the POC/^{234}Th(IV) ratio can vary with kind (suspended or sinking particles), particle size, and depth (Moran *et al.*, 2003). Figure 2 shows that ^{234}Th(IV) is preferentially complexed with a highly surface reactive subfraction (~13kDa) of natural organic matter and this subfraction is rich in acidic polysaccharides (Quigley, 2000; Quigley *et al.*, 2001). These acidic polysaccharide fibrils have been identified as important biopolymers in different aquatic systems (Alldredge *et al.*, 1993; Leppard, 1995, Santschi *et al.*, 1998).

Quigley *et al.* (2001) list typical concentrations of colloidal organic carbon (COC), particulate organic carbon (POC), and dissolved organic carbon (DOC) in surface waters and deep waters, which are ~30μM-C and 10μM-C (COC), 1-10 μM-C (POC), and 100 μM-C and 40 μM-C (DOC), respectively. Thus, DOC and COC outweigh the POC concentrations. Organic carbon to ^{234}Th(IV) ratios in suspended matter, used to determine new production rates, decrease with increasing depth, particle size, and are often different for settling particles caught in sediment traps than for large (>53 μm) suspended particles (Buesseler *et al.,* 1995, 1998; Murray *et al.,* 1996; Bacon *et al.,* 1996; Moran *et al.,* 1997; Santschi *et al.,* 2003). The variability present along a water column profile is due to the organic matter aggregating or coagulating and subsequently settling out of the water column.

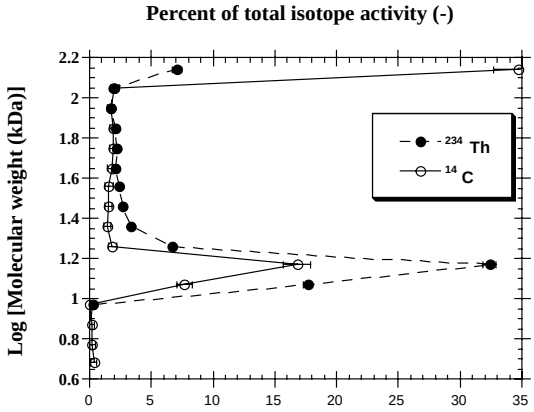

Figure 2 Results from one-dimensional SDS-PAGE resulting in a molecular weight of 13 kDa for the ^{234}Th(IV) complexing and ^{14}C labeled (to sugar hydroxyl groups) ligand [Reprinted with permission from Quigley et al., 2000].

Higher polysaccharide content material exhibited stronger sorption with ^{234}Th(IV), as well as numerous other trace metals (Quigley *et al.*, 2002). The fraction of organic matter that ^{234}Th(IV) is most likely tracing is thus the recently produced, surface active, polysaccharide rich macromolecules (Santschi *et al.,* 1998) with an acidic functional group (Figure 3; Quigley, 2000; Quigley *et al.*, 2001). Acid polysaccharides, even though only a small fraction of the polysaccharide pool (~10% of total polysaccharide) (Santschi *et al.*, 2003), are present in both particulate and colloidal material, play a critical role in the formation of marine snow flocs, mucilaginous aggregates, and the removal of trace elements and radionuclides from the water. Quigley *et al.* (2001) identified this Th(IV) binding ligand in the colloidal phase, a transitory phase (e.g., particle aggregates such as marine snow can produce colloids by enzymatic release), which also contains smaller segments of acid polysaccharide fibrils. Moreover,

colloids extracted from particulates, have a greater number of surface complexation sites per unit mass present compared to suspended particles (Wen *et al.*, 1999). Since these colloids are surface active, they can coagulate again into the particle phase. These coagulating macromolecules can in turn take with them newly adsorbed/complexed ^{234}Th(IV) into the particle phase. Thus, colloids may be a reactive intermediary in the biologically mediated decomposition of large particles. A better understanding of ^{234}Th(IV) interactions with marine colloidal organic matter to trace geochemical pathways of ^{234}Th is thus of critical importance.

Furthermore, it will be important to show that the same ^{234}Th(IV) binding ligand that was found in the colloidal phase also exists in the particulate phase. The organic carbon to ^{234}Th(IV) ratio, which is used to determine new production, could differ between particulate and colloidal fractions significantly; thus, the interactions between ^{234}Th and marine organic matter could be ligand or concentration dependent. Natural organic matter consists of hundreds of (unknown) compounds. Many of these compounds are hydrophobic and are not likely complexing agents for ^{234}Th(IV).

^{234}Th(IV) binding ligand was surface active (Quigley *et al*., 2001) but acidic. Quigley *et al.* (2002) suggested that this ligand is amphiphilic (i.e. contains both hydrophobic and hydrophilic parts), similar to surfactants.

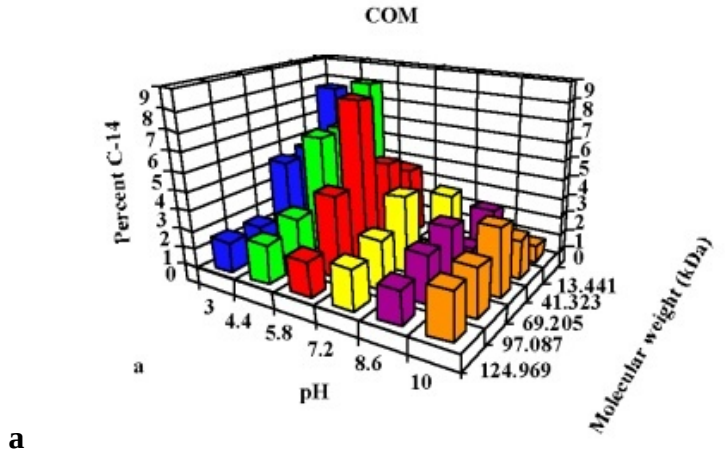

a

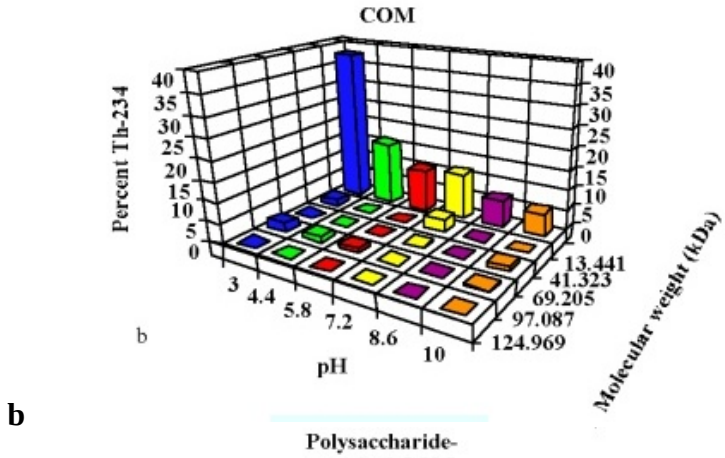

b

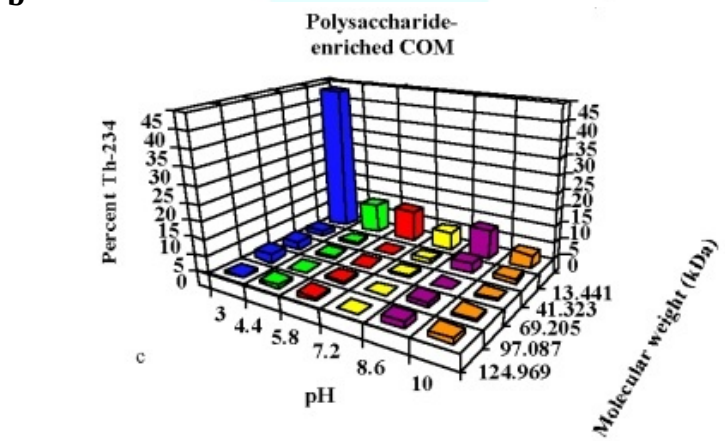

c

Figure 3 2-D PAGE results of ^{234}Th(IV) and ^{14}C labeled (to sugar hydroxyl groups) colloidal macromolecular organic matter (COM) a) isolated from the Gulf of México; b) as compared to (^{234}Th(IV) labeled) COM c) and polysaccharide enriched COM. [Reprinted with permission from Quigley, 2000].

Field measurements illustrated highest K_d and K_c values for marine particulate and colloidal phases, whereby colloids are mostly organic in nature (Quigley *et al.*, 2002). Inorganic ligands (Si, Fe, Al, and Mn oxides) cannot compete with acid polysaccharides for Th(IV) complexation as their K_d values are low (Table 2).

Table 2 Solid-ligand partition coefficients constants of Th(IV) with different sorbents (according Quigley *et al,*. 2002).

Sorbent	**Log K_c (l/kg)**
Chitin	1.72
SiO_2	2.6-3.3 (pH 3) 0.9 (pH 8)
$CaCO_3$	2.7-3.7
FeOOH	5.1
MnO_2	4.5
COM	5.0-6.8
Polysaccharide-enriched COM at 100% enrichment	7.9
Acid polysaccharide standard compounds	7.3-8.1

I.2. Microbial Exopolymeric Substances (EPS)

The plasma membrane encloses and defines a cell's boundaries, separating the cytosol from the environment. It is highly selective (acting as a filter) as it is the site for active transport (Sweadner and Goldin, 1980; Cantley, 1981; West, 1983; Hopkins,

1986; Scott, 1987). The membrane controls the entry of nutrients and the exit of waste products in addition to the ionic potential difference between the interior of the cell and the exterior (Sweadner and Goldin, 1980; West, 1983; Olden *et al*. 1985; Hopkins, 1986; Scott, 1987). Although membranes are valuable as a way to segregate the interior of the cell from its environment, or to segregate intracellular events from one another, they have other important functions.

Microbes send information to one another by releasing signaling molecules. The plasma membrane is responsible for chemotaxis, since it acts as a sensor for external signals allowing the cell to change in response to environmental cues (West, 1983; Holden *et al*., 1999; Marx and Aitken, 2000; Marketon *et al*., 2003). The membrane is composed of assemblies of lipids and proteins, which are fluid and dynamic, and allows them to move about its plane (Singer and Nicolson, 1972; Bretscher, 1973; Kornfeld and Kornfeld, 1980; Storch and Kleinfeld, 1985; Edindin, 1987; Kleinfeld, 1987). The outer membrane's proteins, known as *receptors,* bind the circulating signaling molecules. Microbes are usually in contact with a network of secreted extracellular macromolecules referred to as extracellular matrix. This gel-like matrix acts as glue that holds on to neighboring cells and provides a network for cells to migrate and interact with one another (Reddi, 1984; Watt, 1986; McDonald, 1988; Potts, 1999, Wang *et al.*, 2000,).

Microbial exopolymeric substances (or EPS) are essentially biosynthetic polymers or biopolymers. Geesey (1982) defined EPS as "extracellular polymeric substances of biological origin that participate in the formation of microbial aggregates." Wingender *et al*., (1999) defined EPS as "organic polymers of microbial origin, which

in biofilm systems are frequently responsible for binding cells and other particulates materials together (cohesion) and to the substratum (adhesion)". Proteins and nucleic acids have been shown to appear in trace amounts in EPS from environmental samples (Wingender *et al*., 1999).

These biopolymers are responsible for various environmental responses important to cellular survival. Such survival responses are the reduction of trace metal toxicity (Christensen, 1989; Pistocchi *et al.*, 2000; Croot *et al.*, 2000; De Philippis *et al.*, 2001; Lombardi *et al.*, 2002), uptake and or loss of water from cells (Potts, 1999), protection from swelling and shrinkage (Caoila *et al.*, 1993, 1996), UV defense mechanism (Franklin and Forster 1997; Ehling-Schulz and Scherer, 1999; Potts, 1999; Gröniger *et al.*, 2000; Wolfe 2000; Zimmer and Butman, 2000), defense mechanism against pathogens (Bouarab *et al,*. 1999; Potin *et al.*, 1999), protection of soil erosion (Falchini *et al.,* 1996), hypersalinity (Liu and Buskey, 2000), tolerance to desiccation (Hill *et al.,* 1997; De Philippis and Vincenzini, 1998; Potts 1999) and adhesion onto solid surfaces (Tsuneda *et al.*, 2003).

Cyanobacteria exhibit three general types of stress response against harmful effects of ultraviolet (UV) rays (Ehling-Schulz and Scherer, 1999):

I) Stress avoidance by gliding mechanisms
II) Stress defense by synthesis of UV-absorbing compounds, antioxidants and extracellular polysaccharides
III) Repair mechanisms such as DNA repair and resynthesis of UV-sensitive proteins

The synthesis of extracellular polysaccharides may help limit UV damage because the EPS-containing sheath of cyanobacteria forms a buffer zone between the environment and the cell (Ehling-Schulz and Scherer, 1999). For example, the cyanobacteria *Nostoc commune*, exhibits a series of physiological responses under UV-B radiation. The first response is a rapid increase of carotenoids as a fast active emergency response to detrimental stimuli. The secondary response is an increase of extracellular UV-A/B-absorbing mycosporine associated with glycan synthesis, and lastly scytonemin a passive UV screen against long-term exposure (Ehling-Schulz and Scherer, 1999; Gröniger *et al.*, 2000).

Moreover, a consequential outcome from exopolysaccharides production is the direct impact on cellular organisms aggregating (Burdman *et al.*, 2000; Koblizek *et al.*, 2000) to form colonies. Thus, aggregation and emulsifying properties of biopolymers, that usually depend on their amphiphilic properties and the presence of hydrophobic parts such as proteins or lipids in acid polysaccharides (Dickinson, 2003), can influence the size of colonies and stimulate interactions betweens colonies (Wolfe 2000; Passow, 2002, McDougald *et al*., 2003), and decreases light absorption by enhancing self-shading (Koblizek *et al*., 2000).

Strong ^{234}Th(IV)-binding ligands can be directly related to the scavenging of particle reactive metals by particulate organic matter. Thus, it is important to understand the sources and fates of such ligands in the marine environment. The sources of the strong ^{234}Th(IV)-binding ligand in the ocean are believed to be marine organisms such

as phytoplankton and bacteria (Hirose and Tanoue, 2001). Hirose and Tanoue (2001) proposed production pathways for the production of such ligands:

i) Intracellular chelators;
ii) Synthesis and release of extracellular chelators.

As a result, an attempt is made to overview major functional groups that are in excess, and accessible to the organism.

I.2.1 Carboxylic Acids

The carboxylic acid functional group (COOH) is an important and a fundamental component in small biomolecules. Macromolecules are polymers of monomers and important macromolecules are proteins (from amino acids), polysaccharides (from monosaccharides), and lipids (from fatty acids).

Amino acids are subunits of proteins that contain a carboxylic acid group and an amino group attached to one carbon atom but with varying side group (R) (Figure 4). There are 20 common amino acids each with a different side chain (R) attached to the α-carbon. When individual amino acids are joined together by a peptide bond (bond between the carboxylic acid of one amino acid to the amino group of the next amino acid) they synthesize a protein.

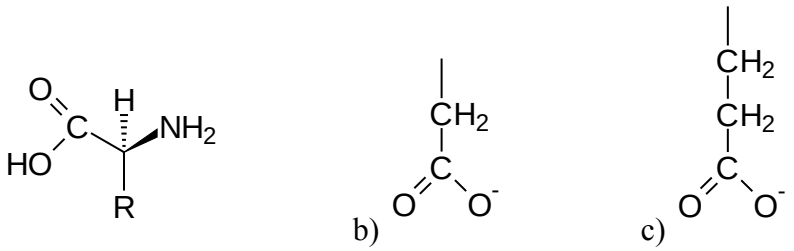

a) b) c)

Figure 4 Amino acid formula illustrating a) amino group (NH_2), carboxylic acid group (COOH), and side chain (R) from α-carbon; b) aspartic acid side chain; c) glutamic acid side chain

Out of the 20 amino acids, two have acidic side groups, aspartic acid (Asp) and glutamic acid (Glu) (Alberts *et al*., 1989). The shape of a protein is determined by the amino acid sequence (primary structure) (Anfinsen, 1973; Baldwin, 1986) and intrinsic H-bonding interactions within the contiguous length of polypeptide results in α-helices and β sheets (secondary structure) (Doolittle, 1985; Milner-White and Poet, 1987). Proteins can be brought together to form larger structures (tertiary structure) such as binding sites for enzymes (Bajaj and Blundell, 1984). Thus, biological functions of proteins depend on the detailed chemical properties of its surface (Chothia, 1984; Altman *et al.*, 1986). Binding sites are formed as surface cavities in which precisely positioned amino acid side chains are brought together by protein folding (2^{ary} and 3^{ary} structures) that are responsible for Na^+-K^+ ATPase pump (Hokin, 1976; Tanford, 1983), regulate metabolism (Koshland, 1984), and thus involved in cell signaling (Nishizuka, 1984).

$$6\,CO_2 + 6\,H_2O \underset{\text{respiration}}{\overset{\text{photosynthesis}}{\rightleftharpoons}} C_6H_{12}O_6 + 6\,O_2$$

Figure 5 Photosynthesis

Carbohydrates are organic compounds containing carbon, hydrogen and oxygen, produced during photosynthesis, where light energy from the sun is converted into chemical energy by combining carbon dioxide with water to form carbohydrate (CH_2O) and molecular oxygen (Figure 5). Thus, light energy is stored as chemical energy in the form of carbohydrates in photoautotrophic phytoplankton and bacteria. The most biologically relevant carbohydrates are those containing 5 and 6 carbon atoms sugars. Five carbon atoms sugars (pentoses) are significant in their role in the structural backbone of DNA. Six carbon sugars (Figure 6) are the monomeric constituents of cell wall polymers and energy reserves.

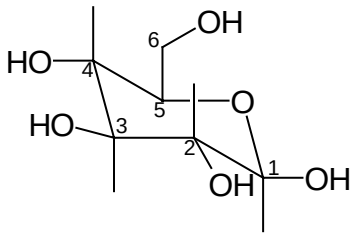

Figure 6 Structure of β-D-glucopyranose.

Derivatives of simple carbohydrates are formed by replacing the hydroxyl groups (OH) with other functional groups (i.e. carboxylic acid, phosphate, or sulphate).

Polysaccharides are high-molecular-weight carbohydrates containing monomeric units connected to each other by a glycosidic bond. The glycosidic bond can exist in the axial (α) and equatorial (β) orientation. Polysaccharides with a repeating structure can be composed of glucose units linked between carbons 1 and 4 in the alpha orientation (i.e. glycogen). A glucose unit linked by beta 1-4 orientation is typical of polysaccharide present in phytoplankton (cellulose) (Brock *et al*., 1984). Polysaccharides are divided into homopolysaccharides, consisting of one repeating monomer, and heteropolysaccharides, consisting of two or more monomers. Given the many combinations of polysaccharides that exist (α or β; 1-4 or 1-6; homo- or heteropolymeric) polysaccharides exhibit a great diversity of structure.

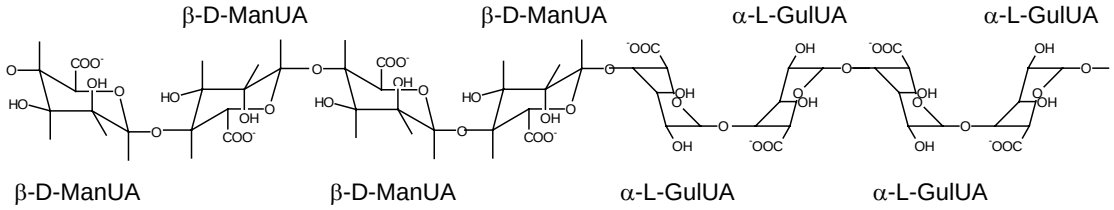

Figure 7 Alginic acid polymer with mannuronic acid and guluronic acid structure.

Alginic acid or polysaccharide algin is found in cell walls and is a linear polysaccharide composed of two monosaccharide units of β-D-mannopyranosyl uronic acid and α-L-gulopyranosyl uronic acid (Figure 7). Each unit is linked in a 1-4 orientation (Hirst *et al.*, 1964, 1965). D-mannuronic acid and L-guluronic acid are in a 2:1 ratio for most algins; however, the ratio can vary slightly from algal species. The

bacterial algins are rich in D-mannuronic acid with a ratio of 0.4 to 2.4, depending on bacterial species and growth conditions (Larsen and Haug, 1971). Murein is a polysaccharide composed of N-acetyl-2amino-2deoxy-D-glucopyranose units linked β-1→4, and is a major component of bacterial cell walls (Tipper *et al.*, 1965). One of the N-acetyl-D-glucosamine units (NAG) is substituted at the C-3 carbon with an O-lactic acid group through an ether linkage to yield N-acetyl-D-muramic acid (NAM) (Figure 8) (Robyt, 1997).

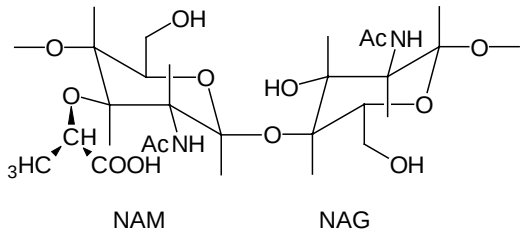

Figure 8 Bacterial polysaccharide Murein with NAM and NAG monomers.

Fatty acids have two distinct regions: a long hydrocarbon chain (hydrophobic) and a carboxylic acid group (hydrophilic), which is ionized in solution (COO^-) (i.e. palmitic acid, Figure 9). The most important function of fatty acids is in the construction of cell membranes. These thin impermeable membranes are largely composed of phospholipids (see I.2.2 below). Acid dissociation constants (pK_a) for carboxylic acid functional groups range from 3.74 to 6.40 (Table 3). The stability constants of Th(IV) with HPO_4^{2-} should be strongest, then SO_4^{2-}, and acetic acid should

be most weakly bound. Dicarboxylic acids would be bound at strengths almost similar to that of phosphate.

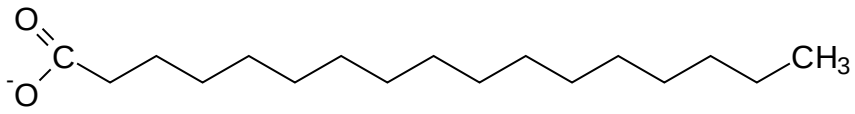

Figure 9 Palmitic acid.

Table 3 List of pK_a values and stability constants for Thorium/Ligand Complexes $Th^{4+} + L^{n-} = ThL(^{4-n})^{+}$.

Ligand	Log β_1	Log β_2	pK_a of acid	Ref.
OH^-	10.2		14	1
CO_3^{2-}	11.0		10.25 (6.3)	1
F^-	7.3	3.2	3.2	1
SO_4^{2-}	3.67		2.0 (-9)	1
Cl^-	0.36		-7	1
HPO_4^{2-}	10.8	22.8	7.2 (2.15) 2.15 (pK_1), 7.20 (pK_2), 12.74 (pK_3)	1 4
NO_3^-	0.94	2.0	-1.4	1
Acetic acid	3.1		4.72	2
Oxalic acid	9.3	18.5	1.2	1
Malonic acid	5.58		5.07	2
Succinic acid	6.44		4.21 (pK_1), 5.64 (pK_2) 4.2	1 2
Humic acids	10-11	15-17	4.5	3
$ThH_3PO_4^{4+}$			1.91	1
$ThH_2PO_4^{3+}$			4.52	1
$Th(H_2PO_4)_2^{2+}$			8.88	1
$ThSO_4^{2+}$			5.45	1
$Th(SO_4)_2^0$			9.73	1

1. Langmuir and Herman (1980); Choppin (1989)
2. Martel and Smith (1990)
3. Nash and Choppin (1980)
4. Harris (1991)

I.2.2 Organophosphate

Preliminary isoelectric focusing experiments showed that the ^{234}Th(IV) binding biomolecule contains phosphate (Santschi *et al.*, 2003). Organophosphate (likely as a polyphosphate) is believed to be one of these ligand types produced by phytoplankton and bacteria that binds strongly to ^{234}Th(IV), as orthophosphate forms stable compounds with ^{234}Th(IV) (Figure 10).

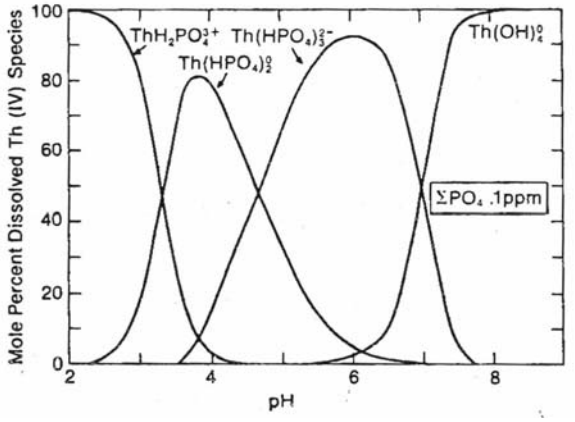

Figure 10 Distribution of thorium-hydroxy and phosphate complexes vs. pH at 25ºC with ΣTh = 0.01 ppb and ΣPO_4 = 0.1ppm (Reprinted from Geochimica et Cosmochimica Acta, Vol 44, No 11, Langmuir, d., and Herman, J. The mobility of thorium in natural waters at low temperatures pp 1753-1766 1980, with permission from Elsevier).

Phosphorus is an important biophilic element and a fundamental component of biomolecules that are key players in metabolic processes at the cellular level (Raghothama, 2000). Phosphorus is involved in processes that involve energy transfer such as Adenosine Tri-Phosphate (ATP), signal transduction (Sciorra and Morris, 2002), biosynthesis of macromolecules (i.e. DNA, RNA), catalysis of enzymatic reactions (i.e.

dephosphorylation), and photosynthesis and respiration (Plaxton and Carswell, 1999; Raghothama, 1999). At the bacterial level, phosphorus is a component of bioactive lipid mediators (i.e. lipid phosphate phosphatases, lysophosphatidic acid, sphingosine 1-phosphate, and phosphatidic acid) that exert diverse effects on cells through both extracellular and intracellular targets (Sciorra and Morris, 2002). Aside from these features, the principal reason why organophosphate is of interest is the role it performs and its ubiquity on the cell surface. Phospholipids are major constituents of cell membranes and play a role in the formation of liposome structures that can protect labile organic matter from decomposition (Suzumura and Ingall, 2001). They are small amphiphilic molecules composed of two fatty acids coupled to two glycerol sites and a phosphate coupled to the third glycerol site. Thus, there is a hydrophobic tail (fatty acids) and a polar head group where the phosphate is located. In addition to the phospholipids, there are lipopolysaccharides and peptidoglycans (Beveridge *et al.,* 1982), which are more complex biomolecules found in the cell walls of gram-negative and gram-positive bacteria. In addition, the outer cell walls of gram-positive bacteria are also composed of P-containing teichoic acid and teichuronic acids in their outer cell walls. However, in natural waters most of these organophosphorus compounds have not been quantified.

Suzumura and Ingall (2001) determined concentrations of total lipid phosphorus from coastal waters (Tokyo Bay and Corpus Christi Bay) and reported ranges from 30 to 300 nM corresponding to 5-14% of particulate phosphorus. Dissolved lipid phosphorus concentrations ranged from 0.7 to 6.0 nM, which indicates that it is a minor component

in seawater (less than 1% of total dissolved organic phosphorus). Dissolved organic phosphorus concentrations ranged from 490 to 670 nM. To gain an understanding of how organic phosphorus could be incorporated into the ^{234}Th(IV) mechanics for new production at the phytoplankton and bacterial level, identification and characterization of Th(IV) binding biomolecules is necessary.

Phytoplankton cells secrete surface-bound polysaccharides or muco-polysaccharides during all growth phases (Gilbeaut, 2000), which are collectively referred to as photosynthetic extracellular release (PER) or transparent exopolymers (TEP). PER is influenced by nutrient availability (Leppard, 1995; Myklestad, 1995; Biersmith and Benner, 1998). These high molecular weight, polysaccharide-rich biomolecules are often resistant to bacterial degradation (Fajon *et al.*, 1999; Goldthwait and Alldredge, 2004). This production, combined with relatively slow degradation rates, facilitates the accumulation and aggregation of this material under stagnant water conditions (Myklestad, 1995; Fajon *et al.*, 1999). Bacterially mediated reactions play a key role in the degradation of these aggregates. This is due to the presence of hydrolytic enzymes located on the surfaces of cells which can hydrolyze polymers at the phytoplankton surface (Leppard, 1995; Smith *et al.*, 1995). Knowledge of the interactions of ^{234}Th(IV) with the various fractions of polysaccharides produced by phytoplankton and bacteria is essential for a better understanding of factors controlling the biogenic flux in the oceans.

I.2.3 Organosulphate

Beside the above mentioned polymers, phytoplankton and bacteria also produce other polysaccharides that surround and form part of the cell membrane. Sulphated polysaccharides also serve various purposes in the survival of the cell (Bouarab *et al.*, 1999). Carrageenans are a family of polysaccharides composed of three linear D-galactans. Kappa (κ)-carrageenan and iota (ι)-carrageenan consist of alternating sequences of β-1→4 D-galactopyranose and α-1→3 3,6-anhydro-D-galactopyranose. The only variability that exists between them is the number and position of O-sulphate groups. Kappa (κ)-carrageenan has the sulphate group at the C-4 carbon of the D-galactopyranose unit and iota (ι)-carrageenan has a sulphate group at the C-4 carbon of the D-galactopyranose unit and at the C-2 carbon on the 3,6-anhydro-D-galactopyranose unit (Figure 11).

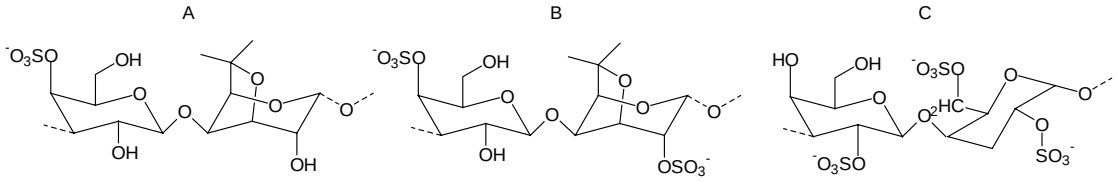

Figure 11 Structure of sulphated polysaccharide a) κ-, b) ι-, and c) λ- carrageenan.

Glycosaminoglycan is another group of polysaccharides synthesized in the Golgi apparatus that finds its way to the cellular interface. These polymers combine the carboxylic acid functional group and the sulphate functional group. Glycosaminoglycans

are unbranched, acidic polysaccharides covalently linked to a protein core to form a proteoglycan (Islam and Linhardt, 2003). Proteoglycans generally consist of glucuronic acid (GlcAp), galactose (Galp), and xylose (Xylp) linked to the hydroxyl group of serine in the polypeptide core (Figure 12). These polysaccharides are generally attached to a protein backbone forming a proteoglycan. Proteoglycans are macromolecular complexes with a protein central core to which several polysaccharide chains are covalently attached (Robyt, 1997).

Thus, microbial EPS are essentially biopolymers produced by organisms for a myriad of functions. Organisms, such as phytoplankton, use nutrients (i.e. iron) to build enzymes. These enzymes catalyze biochemical reactions in the carbon cycles involved in the photosynthetic transformation of carbon from inorganic forms to organic forms.

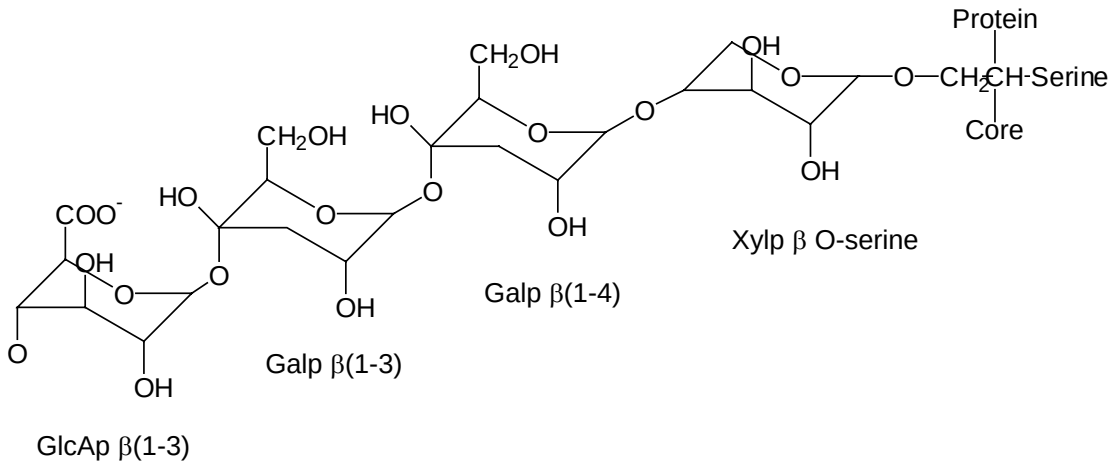

Figure 12 Glycosaminoglycan structure.

Primary production is the ultimate source of the organic carbon molecules forming the bulk of the tissue of living organisms, and it is nature's way of removing a greenhouse gas, CO_2, from the atmosphere. Clearly, biopolymers are involved in the acquisition or chelation of trace metals. This phenomenon occurs due to electrostatic interactions between positive a charge on the metal and a negative charge on the functional groups on biopolymers. Bear in mind that such biopolymers may be one or a combination of proteins, carboxylic acids, lipids, phospholipids, lipopolysaccharides, peptidoglycans, and glycosaminoglycans. Carboxylic acid, phosphate and sulphate are functional groups on the biopolymers that may be responsible for the regular metabolic maintenance of microorganisms. Thus, metal affinity for an acidic polysaccharide increases with an increase in functional group (carboxylic acid, phosphate or sulphate) density on the polysaccharide. Salt bridging, where polyvalent metals bond to two negatively charged (anionic) groups on separate polymer chains, has been known to occur resulting in increasing overall stability (Geesey and Jang, 1989). Alginic acid (Figure 7) is known to chelate calcium in the egg-box model (Geesey and Jang, 1989; Moe *et al*., 1995).

Polysaccharides are produced through the natural growth and the metabolic processes of phytoplankton and bacteria. Phytoplankton growth and metabolic processes also include maintenance of the cell membrane, synthesizing structural proteins, phospholipids and polysaccharides to cover the surface of the membrane. Polysaccharides are an important component of the cell membrane (2% cell membrane composition), (Alberts *et al.*, 1989), the formation of structure for cell adhesion, in the

response to environmental stressors (such as trace metal-possibly toxic concentrations) and in the acquiring of essential metal nutrients for organism's sustenance. These polysaccharides, in turn, play a vital role in the formation of gel layers surrounding all living organisms in the ocean (De Philippis and Vincenzini, 1998; Schuster and Sleyter, 2000).

I.3. Specimens

Santschi *et al.* (2003) demonstrated the importance of cyanobacteria and prymnesiophytes for ^{234}Th(IV) binding and removal in the Gulf of México. Cyanobacteria are a major group of Gram-negative prokaryotes possessing the unifying ability to photosynthesize oxygen photoautotrophically as the dominant mode of nutrition, much like terrestrial plants. They also have the ability to grow chemolithoautotrophically and under anaerobic conditions with sulfide as the electron donor. Cyanobacteria are characterized by their morphological diversity, which ranges from unicellular species to filamentous species and colonial (De Phillipis *et al*. 1998). Prymnesiophytes are an algal class that includes all coccolithophores and flagellates. *Synechococcus elongatus* is an ubiquitous and abundant cyanobacterium in the ocean (Waterbury *et al.*, 1979, Chisholm *et al.*, 1988), and *Emiliania huxleyi* is a prymnesiophyte that is dominant in coastal waters (Berger *et al.*, 1977).

Marine bacteria are obligate aerobic marine phototrophs and chemoorganotrophs. *Sagittula stellata* and *Roseobacter gallaeciensis* are coastal marine bacteria that are commonly associated with surfaces and are widespread in marine environments (Gonzales *et al*., 1997; Ruiz-Ponte *et al.*, 1998). Thus, in addition to the cyanobacterium

Synechococcus elongatus and prymnesiophyte *Emiliania huxleyi*, the bacteria *Sagittula stellata and Roseobacter gallaeciensis* are commercially available cultures that were cultivated in order to obtain a significant amount of EPS.

Hung *et al.* (2003a,b) reported that diatom and cyanobacteria dominated the shelf waters from the Gulf of México; while cyanobacteria and prymnesiophytes were dominant in slope waters. In March 2001, prymnesiophytes were the main phytoplankton group in a cold core ring eddy (CCR) and warm core ring eddy (WCR); while in July 2000, prochlorophytes and cyanobacteria were the most abundant algal groups (Hung *et al.*, 2003a,b). The abundance of cyanobacteria and prymnesiophyte, both producers of mucilaginous acid polysaccharides (APS), closely correlated with APS and uronic acid (URA) abundance (Hung and Santschi, 2001; Santschi *et al*., 2003). Phytoplankton and bacteria cultures were also used to obtain polysaccharide- and APS-enriched isolates from particle phases using established procedures (Staats *et al*., 1999). Thus, the species used to extract APS in this dissertation for cultivation were the marine bacteria *Roseobacter gallaeciensis* (Strain ATCC 700781) and *Sagittula Stellata (*Strain ATCC 700073) and the phytoplankton *Emiliania huxleyi* (Strain CCMP 374) and *Synechococcus elongatus* species (Strain CCMP 1379).

I.4. Importance of Study

Thorium-234 is being used as a tracer to quantify the fluxes of organic carbon (new production) from the euphotic zone to the deep ocean (Buesseler 1998 and references therein; Santschi *et al*., 1999). Global research projects, such as the Joint Global Ocean Flux Study (JGOFS), have used POC fluxes, calculated as the product of

the ^{234}Th(IV) export flux and the POC:^{234}Th(IV) ratio. However, POC/^{234}Th(IV) ratios in suspended and sinking particles are not constant; they vary with particle size, water depth, and study area. Thus, understanding the factors that control the POC/^{234}Th(IV) ratio in the ocean is of paramount importance in global carbon cycle studies. Recent studies have shown that ratios of organic carbon to thorium-234 (OC:^{234}Th(IV)), which are used to determine new production (i.e., ^{234}Th flux multiplied by OC:^{234}Th ratio), could be significantly different in different particulate and colloidal size fractions (e.g., Guo and Santschi, 1997; Buesseler, 1998 and references therein; Santschi *et al.*, 1999). If the interactions between ^{234}Th(IV) isotopes and marine organic matter are ligand dependent, then the use of controlled laboratory experiments is a promising approach to evaluate the nature of ^{234}Th(IV) binding with different fractions of marine organic matter.

I.5. Objective of Study

The primary objective of this research is to improve the understanding of the processes that regulate the POC/^{234}Th(IV) ratio in oceanic particles. This was accomplished by investigations through field and controlled laboratory experiments to isolate and characterize the organic matter [from pure cultures of phytoplankton (*S. elongatus, E. Huxleyi*), bacteria (*R. gallaeciensis, S. stellata*), and natural water samples collected from the Gulf of México] responsible for ^{234}Th(IV) binding.

I.5.1 Hypotheses

I. Acidic polysaccharides (those containing acidic functional groups) are mainly responsible for surface complexation of ^{234}Th(IV) compared to neutral polysaccharides. If there is no observed correlation between acidic region and ^{234}Th(IV), then the null (H_o) will have to be accepted.

H_{o1} ^{234}Th(IV) will have no correlation with acidic functional groups for all samples

II. Carboxylic acid functional group is a potential functional group candidate for ^{234}Th(IV) adsorption

H_{o2} Carboxylic Acid functional group has no correlation with ^{234}Th(IV) for all samples

III. Phosphate functional group is a potential functional group candidate for ^{234}Th(IV) adsorption.

H_{o3} Phosphate functional group has no correlation with ^{234}Th(IV) for all samples

IV. Sulphate functional group is a potential functional group candidate for ^{234}Th(IV) adsorption.

H_{o4} Sulphate functional group has no correlation with ^{234}Th(IV) for all samples

II. STUDY AREA – GULF OF MÉXICO

II.1. Sampling Location

Colloidal organic matter (COM) water samples (GOM Station 4) were taken along a N-S transect in the Gulf of México (GOM) aboard the R/V Gyre during March 17-25, 2001. Water column samples were obtained from a cold core ring (CCR) and a warm core ring (WCR) extending from the coastal to the continental shelf to the open Gulf region

(Figure 13, Table 4).

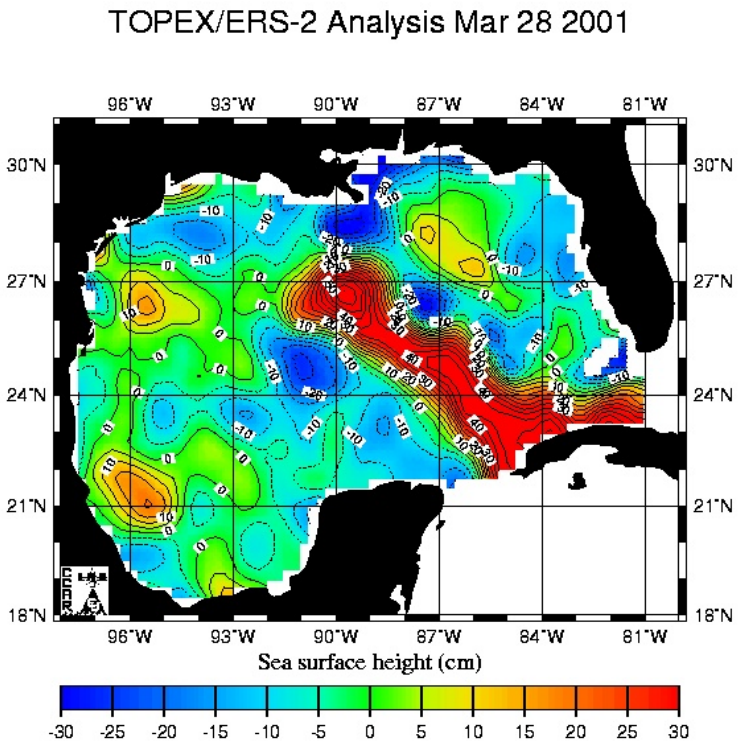

Figure 13 Sampling locations of WCR and CCR sampled in the GOM 2001 (http://www-ccar.colorado.edu/~realtime/gsfc_gom-real-time_ssh/).

Table 4 Sampling locations, water depth, surface water temperature, and salinity at Gulf of México stations in 2001 (Santschi *et al.*, 2003; Hung *et al.*, 2003a,b).

Station no.	Date of collection	Latitude	Longitude	Water depth (m)	Temperature (° C)	Salinity
1	18-03-2001	28°52'N	94°59'W	17	25.92	27.841
2	18-03-2001	28°29'N	94°59'W	30	26.24	28.954
3	19-03-2001	27°59'N	95°00'W	81	25.86	34.451
4 (CCR)	19-03-2001	27°38'N	94°59'W	638	26.04	33.640
5	21-03-2001	27°00'N	94°59'W	1400	26.34	34.998
6 (WCR)	22-03-2001	26°19'N	95°00'W	1632	26.50	36.420

CCR: cold core ring; WCR: warm core ring.

II.2. Site Selection Rationale

The Gulf of México is oligotrophic (low in nutrients and in primary production) with warm core (nutrient depleted) eddies of down welling water and cold core rings (nutrient enriched) of upwelling water created from the Gulf Stream. The vertical profiles from warm core rings and cold core ring eddies that spin off from the Gulf Stream are associated with the existence of a subsurface biomass maxima (Lohrenz *et al.*, 1999, 2002). These subsurface maxima may exchange between surface and subsurface layers leading to a decrease in nutrient concentrations (Lohrenz *et al.*, 1999), and this is presumed to be the flux of carbon in the form of particulate organic matter (POM). The rates of export are variable (Guo *et al.* 2002; Hung *et al.*, 2003a,b) and indicate that cold core rings have elevated fluxes compared to warm core rings. Primary productivity is variable and dependent on phytoplankton species (Lohrenz *et al.*, 1999). The downward flux of POC to below the mixed layer is the impetus behind carbon sequestration in the oceans. Since the oceans are vast and undersaturated with respect to CO_2, the ocean represents a large potential sink for the sequestered CO_2 emissions

(Reichle *et al.*, 1999). The exact biological and chemical implications of POC composition are not well-characterized. Very little is known about the composition of exopolymeric exudates from phytoplankton and bacterial species in the oligotrophic GOM. This dissertation, to the best of my knowledge, is the first attempt to determine the composition of functional groups involved in the complexation of ^{234}Th(IV).

III. Methods

III.1. Field Sampling

Cross-flow ultrafiltration (CF-UF) was used to extract the colloidal fraction from large volumes of seawater (Guo *et al*., 1994, 1996, 2000a,b). CU-UF attempts to minimize artifacts caused by aggregation, adsorption, and solute polarization using a high shear rate across the membrane interface (Guo *et al.,* 1994). Organic matter (OM) was fractionated according to nominal molecular weight cut-offs of 1,000 and 10,000 Dalton (Da), by a cross-flow ultrafiltration technique. Surface seawater samples were pumped directly through an acid and base rinsed 0.1 μm Nuclepore cartridge and subsequently through the 1,000 Da or 1 kDa ultrafiltration systems. Colloidal organic carbon is defined operationally as the fraction between 1 kDa and 0.1 μm pore size. Ultrafilters were calibrated using compounds of different molecular weights. An Amicon DC10L ultrafiltration system was used with 1 kDa spiral-wound polysulfone cartridges (Amicon, S10N1). At deep stations (stations 4 and 6 water depth were approximately 638, and 1632 m, respectively), seawater was collected from various depths which correspond to surface and bottom waters above and below the chlorophyll a maxima. About 200 1iters of seawater were processed, and the concentrated colloidal fraction was reduced to ~ 2 1iters. All ultra-filtration experiments were done aboard ship within 6-10 h of seawater collection (Guo *et al.*, 1994).

III.2. Laboratory Techniques

III.2.1 Thorium Purification

Pure ^{234}Th(IV), used in all spike experiments, was separated from its parent ^{238}U (in the form of uranium acetate, Pfaltz and Bauer, Lot No.: 038337) by an ion exchange resin (Biorad AG1-X8 100-200 mesh, Lot No.: 48389B) column (Quigley et al., 2001). During evaporation, the thorium solution in a Teflon beaker was placed on a hot plate inside a polycarbonate case that was open in the back to allow the fumes to escape. This design allowed for the evaporation of an acid solution in a fume hood while minimizing contamination from airborne particles. Once the ^{234}Th(IV) solution had completely evaporated, the ^{234}Th(IV) was repeatedly dissolved (four to five times) and evaporated in hot, ultrapure, concentrated HNO_3 and a few drops of 30% H_2O_2. The final ^{234}Th(IV) residue was dissolved in 2 ml ultrapure, concentrated HNO_3 and diluted to 10 ml with high-purity (18 MΩ) H_2O. The Th spike solution was assayed by use of a calibrated liquid scintillation counter (Beckman 8100 LSC) with Ecolume liquid scintillation cocktail (ICN, Lot No.69221) (Quigley et al., 1996, 2001). Final ^{234}Th(IV) activity was c. 2.0 X 10^6 dpm ml^{-1}. Natural organic matter (NOM) were also used in electrophoresis experiments.

III.2.2 Bacterial Cultures

Bacterial cultures were obtained from the American Type Culture Collection (ATCC). The bacterial species *S. stellata* and *R. gallaeciensis* occurred in 2 l Erlenmeyer flask in Marine Broth 2216 (Difco Laboratories) composed of peptone (5.00

g), yeast extract (1.00 g), Fe(III) citrate (0.10 g), NaCl (19.45 g), $MgCl_2$ (5.90 g), $NaSO_4$ (3.24 g), $CaCl_2$ (1.80 g), KCl (0.55 g), Na_2CO_3 (0.16 g), KBr (0.08 g), $SrCl_2$ (34.00 mg), H_3BO_3 (22.00 mg), Na-silicate (4.00 mg), NaF (2.40 mg), $(NH_4)NO_3$ (1.60 mg), and Na_2HPO_4 (8.00 mg). The incubations were carried out in 1000 ml cultures. The bacteria were grown for 36-48 hours at 36° C under constant agitation using a shaker (Glass and Col Bench top shaker, at a speed of 50 rpm) in an incubator (Precision Mechanic convection Incubator at 28° C). A preculture (2h) in the corresponding media was used to inoculate the flasks.

III.2.2.1 Strain ATCC 700781 *Roseobacter gallaeciensis*

Bacterial strain $BS107^T$, isolated from seawater off the coast of Spain from larval cultures of the scallop *Pecten maximus*, and was obtained from the American Type Culture Collection (ATCC 700781). The cells are Gram-negative ovoid rods having a length of 1.7-2.5 μm and width of 0.7-1 μm. They are motile by means of a polar flagella. Cells grow in marine broth 2216 [DIFCO 279110] for 72-96 hours of incubation at temperatures ranging from 15° to 37°C with optimal growth occurring between 23° to 27° C with a pH of 7.0. Cell growth also occurs in the presence of 0.1 to 2.0M NaCl with optimal concentration of 0.2M requiring thiamin and demonstrate non-fermentive metabolism. *R. gallaeciensis* exhibits oxidase and catalase activities, however it does not demonstrate any denitrification activity. Cells do not contain bacteriochlorophyll *a*. Phylogenetic analysis places isolates in a distinct monophyletic

group of the α subclass of the *Proteobacteria* containing Roseobacter species (Ruiz-Ponte *et al.*, 1998).

III.2.2.2 Strain ATCC 700073 *Sagittula stellata*

Bacterial strain E-37 (Figure 14) was originally found in seawater from the coast of Georgia in the U.S., and was obtained from the American Type Culture Collection (ATCC 700073). The cells are Gram-negative and rod shaped with a length of 1.7-2.5 μm and width of 0.7-1 μm. They are motile by means of a polar flagella. Cells grow in marine broth 2216 [DIFCO 279110] for 72-96 hours of incubation at temperatures ranging from 15° to 37°C with optimal growth occurring between 23° to 27° C with a pH of 7.0. Cell growth also occurs in the presence of 0.1 to 2.0 M NaCl with optimal concentration of 0.2M requiring thiamin and demonstrate non-fermentive metabolism. *S. stellata* exhibits oxidase and catalase activities, however it does not demonstrate any denitrification activity. Cells do not contain bacteriochlorophyll *a*. Phylogenetic analysis places isolates in a distinct monophyletic group of the α subclass of the *Proteobacteria* containing Roseobacter species (Gonzalez *et al.*, 1997). This specimen is known to produce polysaccharide fibrils on the cell surface (Figure 15).

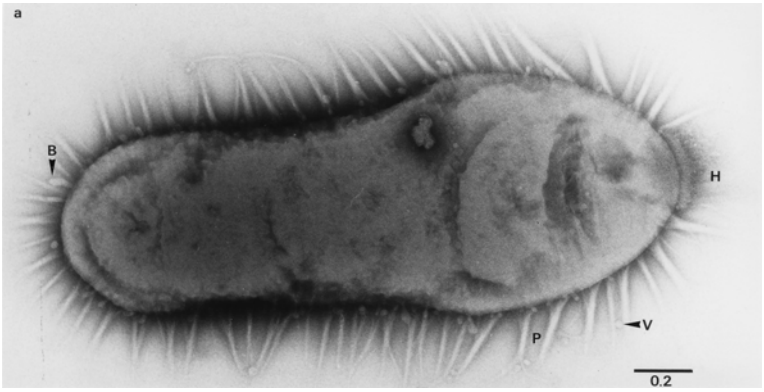

Figure 14 Transmission electron microscopy of negatively stained isolate E-37T samples. Cell covered by polysaccharide fibrils (P) aggregated into bundles. Bar=0.2μm (Reprinted from International Journal of Systematic Bacteriology, 47 (3): Gonzalez, J. M., Mayer, F., Moran, M. A., Hodson, R. E. and Whitman, W. B., pages.773-780, Copyright (1997), with permission from International Union of Microbiological Societies).

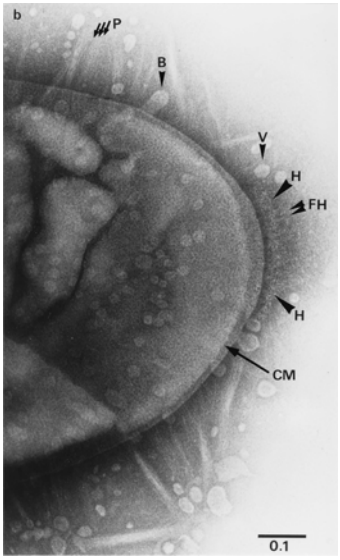

Figure 15 Transmission electron microscope of polysaccharide fibrils attached to the cell surface and the fibrillar components of the holdfast structure (FH). CM, cytoplasmic membrane. Bar=0.1μm. (Reprinted from International Journal of Systematic Bacteriology, 47 (3): Gonzalez, J. M., Mayer, F., Moran, M. A., Hodson, R. E. and Whitman, W. B., pp.773-780, Copyright (1997), with permission from International Union of Microbiological Societies).

III.2.3 Phytoplankton Cultures

Axenic phytoplankton cultures were obtained from the Bigelow Center for the Culture of Marine Phytoplankton (CCMP) collection. Phytoplankton cultures were prepared using standard filtered seawater media (salinity = 26). All glassware was rinsed thoroughly with soap and water and covered with foil and materials (media, sterile flasks, sterile pipettes, and cultures) were autoclaved prior to use. Gulf of México seawater was filtered through a 0.4 μm polycarbonate filter (Osmonics/Poretics 0.4mm, 47mm Lot. No.: 215880) into a 2 l flask. To 1.5 l filtered seawater, sodium nitrate stock (1 ml $8.83X10^{-4}$ M $NaNO_3$), sodium phosphate stock (1 ml $3.63X10^{-5}$ M $NaH_2PO_4 \cdot H_2O$) and trace metal stock solutions were added (1.0 ml of f/2 trace metal stock solution and 0.5 ml vitamin solution per liter of seawater) [f/2 trace metal solution has final concentrations of $1X10^{-5}$ M $FeCl_3 \cdot 6H_2O$, $1X10^{-5}$ M $Na_2EDTA \cdot 2H_2O$, $4X10^{-8}$ M $CuSO_4 \cdot 5H_2O$, $3X10^{-8}$ M $NaMoO_4 \cdot 2H_2O$, $8X10^{-8}$ M $ZnSO_4 \cdot 7H_2O$, $5X10^{-8}$ M $CoCl_2 \cdot 6H_2O$, $9X10^{-7}$ M $MnCl_2 \cdot 4H_2O$; f/2 vitamin solution has final concentrations of $1X10^{-10}$ M Vitamin B_{12} (cyanocobalamin), $2X10^{-9}$ M Biotin, $3X10^{-7}$ M Thiamine HCl]. The seawater was subsequently autoclaved 15 minutes, and removed from autoclave after 30-40 minutes to prevent burning of media. The seawater media was allowed to cool, and f/2 trace metal solution (1 ml stock prepared solution per liter of seawater) and f/2 vitamin solution (0.5 ml stock solution per liter of seawater) were added.

Phytoplankton incubations involved inoculating sterile seawater media with 10 ml of phytoplankton culture of interest and returned to incubator. The light cycle was programmed to be 12 hours on, 12 hours off. All cultures were kept at a temperature of

20° C. Every 10-14 days, each of the respective phytoplankton species line were transferred to fresh media. 50 ml of sterile, 0.4 μm filtered seawater was added sterile 250 ml Erlenmeyer flasks. Flasks were allowed to reach room temperature if the media came straight out of the refrigerator or the autoclave. Nutrients were then added (per instructions for each species), and then 2 ml of previous week's culture was used as inoculum (avoiding contamination prior to sampling).

III.2.3.1 Strain CCMP 374 *Emiliania huxleyi*

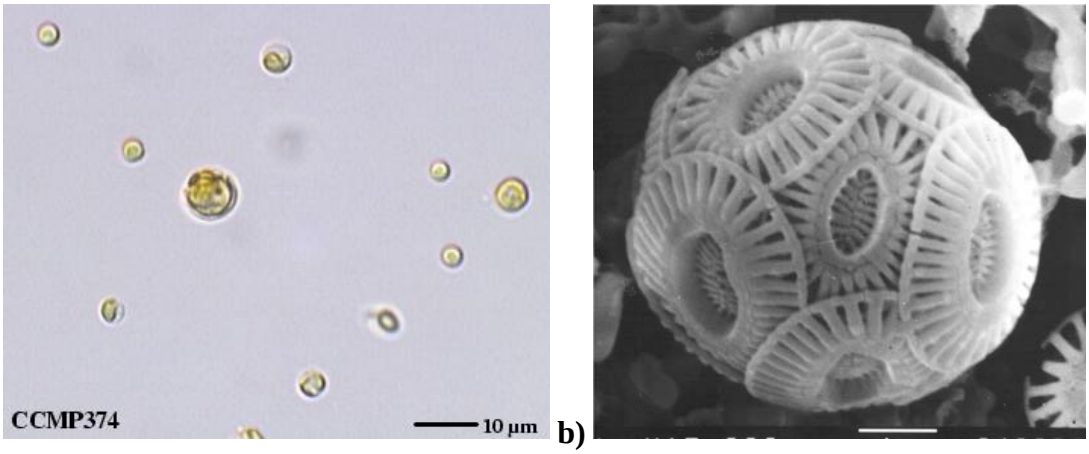

Figure 16 a) A light microscope image (Reprinted with permission from the Provasoli-Guillard Center for Culture of Marine Phytoplankton - ccmp374_40x_1) and b) Scanning Electron Microscope image of *E. huxleyi* (Reprinted with permission from V. Pariente, 2004).

Emiliania huxleyi strain CCMP374 (Figure 16), originally isolated in 1989 at a latitude of 42.5N and longitude of 69.0W near the Gulf of Maine, North Atlantic by T. Skinner. A culture was obtained from the Bigelow Center for the Culture of Marine

Phytoplankton (CCMP374). *E. huxleyi* strain required a f/2-Si growth medium with a temperature range from 11°C to 22°C. It has an observed cell length of 4 to 8 μm and a cell width of 4 to 6 μm. Strain CCMP347 was routinely maintained in autoclaved Gulf of México seawater supplemented by f/2-Si nutrients (silicate omitted) at 20° C in a Precision 818 low temperature illuminated incubator under a 12:12 h LD irradiance cycle. These lighting conditions were maintained during the experiments.

III.2.3.2 Strain CCMP 1379 *Synechococcus elongatus*

Synechococcus elongatus strain CCMP1379, isolated in 1985 at 14.9S and 148.7W near Mataiva, Tahiti by R. Lewin, was obtained from the Bigelow Center for the Culture of Marine Phytoplankton (CCMP1379). This *Synechococcus elongatus* strain required an f/2-Si growth medium with a temperature range from 18° C to 26° C. It has an observed cell length of 3μm and cell width of 2-3μm. Strain CCMP1379 was routinely maintained in autoclaved Gulf of México seawater supplemented by f/2-Si nutrients (silicate omitted) at 20° C in a Precision 818 low temperature illuminated incubator under a 12:12 h LD irradiance cycle. These lighting conditions were maintained during the experiments.

III.2.4 Radioisotopic Incubation [^{32}P, ^{35}S and $^{234}Th(IV)$]

Incubations were conducted in parallel but on smaller scale (30 ml) on all species. Triplicate cultures of each species were incubated with ^{32}P in the form of H_3PO_4 in 0.02N HCl, ^{35}S in the form of H_2SO_4 in water and $^{234}Th(IV)$ in d.d.H_2O. The primary purpose was to verify the mass balance of the extraction procedure and the

resulting data was the extraction efficiency of the Staats *et al.*, (1999) method. In addition a small quantity of radiolabeled material was extracted and results will follow in section IV.1.

III.2.5 Extraction, Precipitation and Purification Procedure

Exopolymeric substance (EPS) extraction and precipitation procedure was performed on cultured matter in order to study the differences in exopolymeric substance composition. Natural organic matter (NOM) sample was collected during a Gulf of México cruise on board the R/V *Gyre* (see section III.1). The cultured organic matter was obtained from the two bacterial species (*S. stellata* and *R. gallaeciensis*) and two phytoplankton species (*S. elongatus* and *E. huxleyi*). Detailed procedures of extraction method are described in Staats *et al.* (1999) illustrating the preferred solvent for extraction and minimizing cell lysis (Figure 17).

After the bacterial and phytoplankton incubations (III.2.2 & III.2.2.2), 35 ml of media solution (marine broth or seawater and bacteria or phytoplankton, respectively) was placed into centrifuge tubes. The bacteria and phytoplankton, respectively, were centrifuged (Sorvall RC-5B Refrigerated Superspeed Centrifuge) at 10,000 rpm for a period of 30 minutes at 20° C. This was performed in order to separate phytoplankton and bacteria from seawater and Marine broth media, respectively.

The supernatant seawater and marine broth were decanted. Tap water was used to wash the bacterial and phytoplankton pellet to extract surficial acidic polysaccharides (Staats *et al.*, 1999). The aqueous supernatant was collected and 80% ethanol was added and stored in –20° C overnight to promote precipitation of polysaccharides. The ethanol:water mixture was ultracentrifuged for 30 minutes (temperature set to –20°C, performed total of five times) and the polysaccharide was collected and lyophilized. Material was then run through isoelectric focusing and 2D SDS-PAGE to determine the activity of ^{14}C, ^{32}P, ^{35}S, $^{234}Th(IV)$, and concentrations of phosphate (PO_4^{3+}), and sulphate (SO_4^{2-}).

The natural marine organic matter (NOM), including colloidal organic matter (COM) and particulate organic matter (POM), used in this study was extracted from seawater collected from the Gulf of México (GOM) [see section III.1]. COM (operationally defined here as the fraction between 1 nm and 0.1 μm) was isolated from large volumes of seawater using cross-flow ultra-filtration techniques (Guo *et al.*, 1994; Guo and Santschi 1996). The concentrated COM was further dialfiltered using 1 kDa molecular weight cut off (MWCO) regenerated cellulose ultrafiltration membranes (Amicon/Millipore YM1 Lot No.: K1PN6205) with high-purity (18.3 MΩ) H_2O, to remove residual sea salts or detergent (Triton X-100). The final concentrated COM samples were then freeze-dried and stored at 4°C. Detailed procedures of sample collection and locations are described in Guo *et al*. (1994).

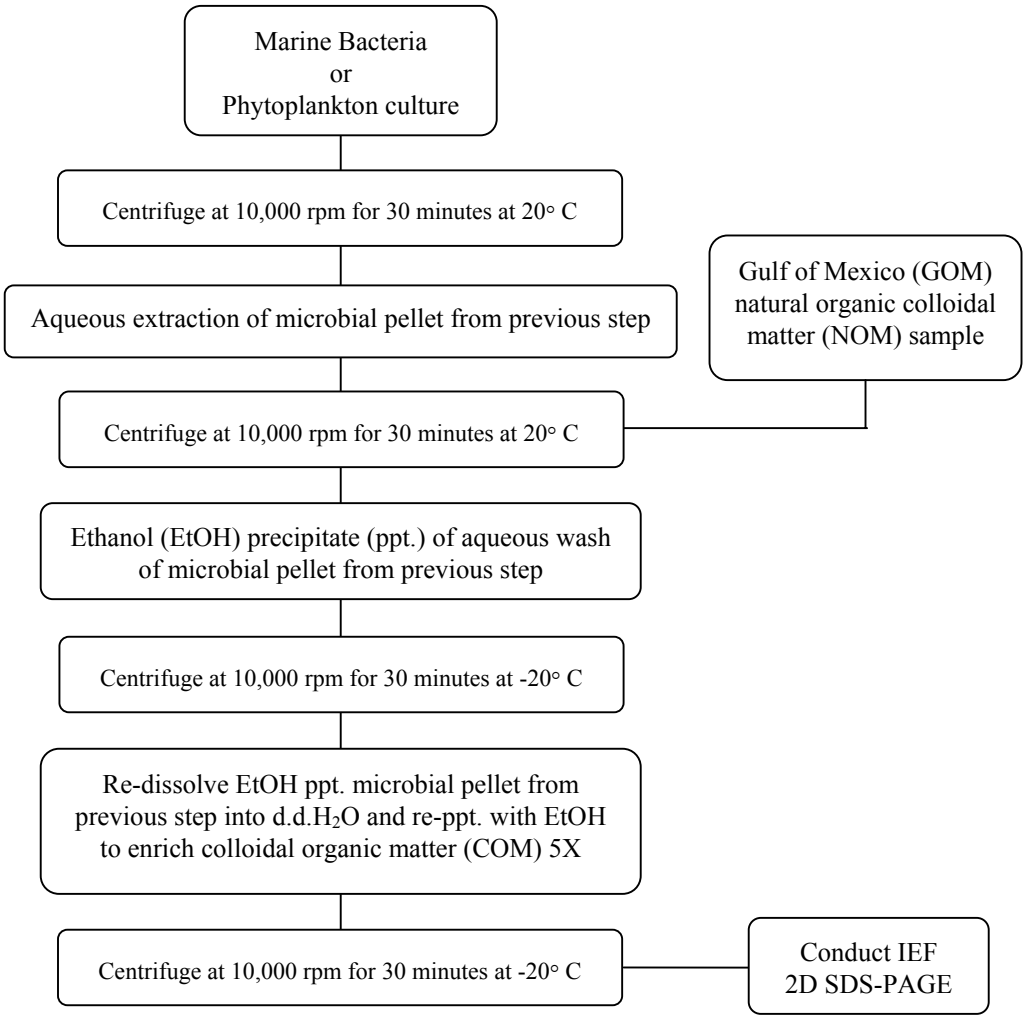

Figure 17 Extraction procedure of microbial cultures and natural organic matter samples.

III.2.6 Electrophoresis

Electrophoresis is the movement of charged particles (ions) in an electric field and is based on the ionic mobility *u* or electrophoretic mobility. When a particle in solution is moving in the direction *E*, its velocity *v* depends on particle charge, frictional coefficient *f* arising from the solution and strength of the field *E* (Eq.2).

$$E = \frac{d\varphi}{dx} = \frac{I}{A\kappa} \qquad \textbf{Eq. 2}$$

The quantity *E* is defined as the difference in potential (ϕ) in volts of two electrodes at distance x, or the current *I* (amps) divided by the product of cross-area (cm^2) and ionic conductance of the solution (κ) (Ω^{-1} cm^{-1}). Two types of electrophoresis were conducted in this research, isoelectric focusing (IEF) and sodium dodecyl sulphate polyacrylamide gel electrophoresis (SDS-PAGE). In the first method, the isoelectric point pI or pH_{IEP} is obtained, which is the point where a molecule moves towards the anode or cathode to a position in the pH gradient where its net-charge is zero. In the second method, SDS-PAGE separates macromolecules on the basis of molecular size as they move through the polyacrylamide gel matrix towards the anode. Larger molecules migrate slowly, whereas smaller molecules migrate at a faster rate. Using these two techniques, it was possible to characterize the composition of the natural and cultured particulate organic samples and colloidal organic samples (Sun, 1994). IEF was used to obtain pH profiles of ^{14}C, ^{32}P, ^{35}S, $^{234}Th(IV)$, PO_4^{3-} and SO_4^{2-} for all samples. 2D SDS-

PAGE technique was used to isolate and purify the organic material fractions responsible for adsorption to ^{234}Th(IV).

III.2.6.1 Isoelectric Focusing Electrophoresis (IEF)

IEF is an electrophoretic method that separates molecules according to their isoelectric point (pI or pH_{IEP}). Molecules under investigation are amphoteric, possessing a positive, negative or zero charge depending of their surrounding pH. The net charge of a molecule is the sum of all the negatively (carboxyl, phosphato or sulphato) and positively charged (amino) functional groups. The isoelectric point (pI) is the specific pH at which the net charge of the molecule is zero. The molecule is positively charged below the pI, and negatively charged above the pI. In a pH gradient under the influence of an electric field, the molecule will migrate to a position in the gradient (strip) where its net charge is zero. A molecule with a positive net charge will migrate towards the cathode, becoming progressively less positively charged as it moves through the gradient until it reaches its pI. A molecule with a negative net charge will move towards the anode becoming less negatively charged until it also reaches a zero net charge. If a molecule diffuses away from its pI, it immediately gains charge and migrates back under current. This focuses the molecules and concentrates them at their pIs and allows the separation of molecules based on very small charge differences (Trubetskoj *et al*., 1992; Berkelman and Stenstedt, 1998). IEF is performed under denaturing conditions to provide the highest resolution and the cleanest results. This is undertaken by mixing urea and detergent to ensure that each sample (polymer) is only present in one

configuration and aggregation and intermolecular interactions are minimized. Each sample (c. 2 mg of microbial EPS) was loaded into each IPG strip (Amersham Biosciences, Immobiline Dry Strip, pH 3-10, 11cm, Lot No: 300135), in addition to 100 μl of rehydration solution [see appendix V.1]. The IPG strips were placed into the reswelling tray for at least 12 hours. Consequently the IPG strips were then placed in the Electrophoresis apparatus (Amersham Biosciences, Multiphor II Electrophoresis System) and run for 17.5 hours with a current profile of 19,701 Volt-hours (V_h) [see appendix V.1], and the pH values calibrated separately.

III.2.6.2 Polyacrylamide Gel Electrophoresis (SDS-PAGE)

SDS-Polyacrylamide gel electrophoresis (SDS-PAGE) was used for the separation of colloidal organic matter (COM). Single-dimension gel electrophoresis in the presence of a detergent (i.e., in the presence of sodium dodecyl sulphate, SDS) separates macromolecules on the basis of molecular size as they move through a polyacrylamide gel matrix towards the anode. The SDS binds to macromolecules to form a complex that carries a negative charge in the form of rods. When subjected to electric field, the molecules migrate at different rates. Larger molecules migrate slowly whereas smaller molecules migrate at a faster rate. The separation of samples is in essence a sieving effect and the mobility of a compound is proportional to its size, which in turn, is proportional to its molecular weight and inversely proportional to its diffusion coefficient (Sun, 1994).

2D SDS-PAGE separates molecules according to two physical properties, i.e., net surface charge (pH) and molecular size. The charged molecules migrate during isoelectric focusing through the gel toward one of the electrophoresis electrodes until protonation or deprotonation within the pH gradient results in a net neutral charge for the molecule (pH_{IEP}) (Trubetskoj *et al*., 1992). The second dimension run, which was carried out on the same sample, was a standard polyacrylamide homogeneous gel (T=15% Amersham Pharmacia Biotech). The Multiphor II system (Amersham Pharmacia Biotech) was used for sample preparation and electrophoresis, according to the manufacturer's recommended procedures. The pH along the length of the isoelectric focusing gel was monitored, and the molecular weight (MW) gradient or homogeneous gel was calibrated by use of rainbow colored MW marker standards (Amersham Pharmacia Biotech). Typically, sample detection is made visually by use of protein-specific stains. However, for this work, detection of the sample within the gel was made by use of detection of radiotracers (^{234}Th(IV)) by liquid scintillation counting. Upon completion of the 2D PAGE run, the gel was sectioned from low pH to high pH sections and according to rainbow colored protein weight markers (Amersham Biosciences, Low molecular weight range RPN 755 Batch No.: 73) into molecular mass sections ranging from less than 1.0 kDa (bromophenol blue), 3.5 kDa (insulin (b) chain), 6.5 kDa (aprotinin), 14.3 kDa (lysozyme), 20.1 kDa (trypsin inhibitor), 30 kDa (carbonic anhydrase) and greater than 45 kDa (ovalbumin) [V.1.1]. Each section was put in a glass liquid scintillation vial with 15 ml of Ecolume liquid scintillation cocktail for 24 h before the vials counted (Quigley *et al*., 2001).

III.2.7 Constraints for Chemical and Instrumental Analysis

From the preliminary results obtained by isoelectric focusing the total measured phosphate concentration for the IEF strip was 0.2 μmoles-P, with 15% of this in the region where Th(IV) peaked. Given that the starting material for IEF analysis was 1 mg of organic matter, equivalent to about 0.2 mg-C (or 16 μmoles-C), an approximate carbon to phosphorus ratio of 83:1 was obtained for the colloidal material. For comparison, Suzumura and Ingall (2001) had values of ~100:1. This indicated that it would be possible to run 15 IEF strips ten times and/or PAGE procedures to produce enough material (at least 10mg) of purified polysaccharide for instrumental analysis. To facilitate matters, it was necessary to cast our own SDS-PAGE gels since the commercially available SDS-PAGE gels were only 0.5mm thick and the loading capacity was of the order of 5-17μl for homogeneous (15%) gels and 1-40 of μl for gradient (8-18%) gels. Our sample solutions were usually around 20 ml of isolated pH triton-X solution that needed to be run on SDS-PAGE. In the preliminary trials, it took approximately 4 weeks and over twenty-five 15% SDS-PAGE commercially available plates. However, by casting our own gels the process was four-fold quicker and more cost effective (for procedure see Appendix V.2). This, to the best of my knowledge, is the first successful attempt to extract, isolate and purify marine microbial EPS associated with ^{234}Th(IV).

III.3. Chemical Characterization and Instrumental Analysis

III.3.1 Radioisotope Labeling of Microbial EPS – ^{32}P, ^{35}S and $^{234}Th(IV)$ Incubation

Both bacteria and phytoplankton were grown in growth media [III.2.2 and III.2.3, respectively] containing radiolabeled solutions of ^{32}P (as $H_3{}^{32}PO_4$ in 0.02N HCl, ICN, Lot No.: 4035P3), ^{35}S (as $H_2{}^{35}SO_4$ in H_2O ICN, Lot No.: 4031S1) and $^{234}Th(IV)$ (in H_2O, see III.2.1) for pathway tracking studies. Phytoplankton and bacteria cultures were used to obtain EPS isolates from the particulate phase using established procedures involving ultra-centrifugation, ultrafiltration, and repeated alcohol precipitations (Staats *et al*. 1999) [III.2.5].

III.3.2 Determination of the Relative Concentration of Carboxylic Acid

The method used for the determining the presence of carboxylic acid functional group was originally outlined in the radiolabeling method of Warwick *et al.*, (1993), which was improved by Reinhardt (pers. commun.). 20.0 mg of Suwannee River Humic Acid Standard (Int. Humic Substances Society) and 5.0 mg of microbial (bacteria and phytoplankton) EPS samples were added to 10.0 ml 0.05M NaCl adjusted to pH of 7.0 and filtered through a 0.22mm white GSWP 47mm filter (Millipore Lot No.: H3BN09995). Under nitrogen atmosphere, 0.322×10^{-4} Moles 1-ethyl-3-(3-dimethylaminopropyl) carbodiimide (Fluka-Chemika, Lot No.:10748/1) was added to the filtered sample. 6.95×10^{-7} M ^{14}C-methylamine (ICN, Lot No.312102), an amount sufficient to react with 1% of the number of carboxylic acid groups present in solution, was added to the Humic acid or microbial samples, respectively (assuming identical

meq/OM from Suwannee River Humic Acid Standard). The basis for labelling only 1% was so that the behaviour of the macromolecule would not be altered and generate different results due to the chemistry. The pH of the solution was adjusted to 7.0, and the reaction vessel allowed to stir overnight. The pH of the solution was then lowered to approximately pH of 2 using concentrated nitric acid (18.5M HNO_3). 30 cm of the dialysis bag Spectrapor (Spectrum CE MWCO 500, Lot No.: 40935) was rinsed for 30 minutes with d.d.H_2O in order to eliminate the sodium azide. The acidic solution was then placed in the dialysis bag, clamped at both ends and inserted in 900ml of 0.05 M NaCl pH 2.0 (acidified with conc. nitric acid to pH 2). The contents of the bag were allowed to equilibrate for 72 hours using a magnetic stir plate. The solution was recovered from the dialysis bag and neutralized to a pH of 7.0, then dialysed again with d.d.H_2O to remove unwanted salts prior to isoelectric focusing. Contents were then freeze-dried and resuspended in d.d.H_2O prior to carrying out isoelectric focusing and 2-D SDS-PAGE [III.2.6.2]; finally, individual parts were sectioned and subsequently analyzed on a liquid scintillation counter [III.3.3].

III.3.3 Liquid Scintillation Counting (LSC) - ^{14}C, ^{32}P, ^{35}S and $^{234}Th(IV)$

^{14}C, ^{32}P, ^{35}S and $^{234}Th(IV)$ analyses were determined by Liquid Scintillation counting. Mechanical pipettes (Eppendorf) were calibrated gravimetrically before being used to transfer 5.00 ml of water to a 22 ml polyethylene scintillation vial. A calibrated dispenser (Brinkmann Dispensette) was used to add 15.00 ml of Ecolume scintillation cocktail (ICN, Lot No.69221). The samples were capped, shaken vigorously, and loaded

into a Beckman Model 8100 Liquid Scintillation Counter (LSC). Samples were counted for 10 minutes. The conventional energy windows for ^{14}C, ^{32}P, ^{35}S and ^{234}Th(IV) used were energy windows of 18 keV to 0.156 MeV, 1.709 MeV, 0.167 MeV and 0.199 MeV, respectively. Using these settings, detection limits for ^{14}C, ^{32}P, ^{35}S and ^{234}Th analyses were 6.36, 8.28, 6.33 and 6.25 dpm, respectively. Analysis yielded ±10% or 2-sigma error (Quigley *et al.,* 2001).

III.3.4 Determination of Organic Phosphate and Sulphate by Ion Chromatography (IC)

The organic phosphorus and sulphate were extracted from the IEF gel sections with Triton X-100 (PlusOne, Lot No.: K21994782545). Determination of organic phosphorus and sulphur is based on the Grotjan *et al.*, (1986) modification of Silvestri *et al*., (1982) method. The method utilizes acid hydrolysis of organic material with subsequent lyophilization followed by pyrolysis with ultimate injection into ion chromatograph (IC). The ion chromatograph consisted of a Dionex gradient pump 120 VAC BioLC pump equipped with anion self-regenerating suppressor ultra (4mm), an injector equipped with a 0.05 ml sample loop (Dionex, Houston, TX, USA), a IonPac AG4A anion guard column (P/N 037042), an IonPac AS4A analytical Anion Column (P/N 037041), Dionex Conductivity detector-II and Dionex 4400 Integrator chart recorder (Dionex, Houston, TX, USA). 1.8 mM Na_2CO_3/1.7 mM$NaHCO_3$ (Dionex Lot No: 971206) solutions were prepared, using 18.3 MΩ d.d.H_2O, as an eluant at a flow rate of 2.0 mL/min. The conductivity detector output scale was set at 30 μS and resulting background conductivity was 17.6 μS. All glassware was washed with dilute

nitric acid and with d.d.H_2O. A standard curve for phosphate (PO_4^{3-}) and sulphate (SO_4^{2-}) was carried for (5 nM, 50 nM, 500 nM, 750 nM, 1μM, 1.25 μM, 1.5 μM, R^2=0.9995 for both PO_4^{3-} and SO_4^{2-}). Detection limits were 2.68 μM/L for phosphate and sulphate ions, respectively.

III.3.5 Determination of Total Carbohydrates

Carbohydrate concentrations were determined by a modified spectrophotometric method (Hung and Santschi, 2001), which is based upon oxidizing the free reduced sugars with the 2, 4, 6-tripyridyl-s-triazine (TPTZ), followed by spectrophotometric analysis (Myklestad *et al*., 1997). For total carbohydrates (TCHO), 4 ml of seawater and 0.4 ml of 1 N HCl were added to a 10 ml glass ampoule. The sealed ampoules were then placed in an oven at 150 °C for 1 hr. After complete hydrolysis, 0.4 ml of 1N NaOH was added to the ampoules. Then, 1 ml of the hydrolysate was added to a dark glass bottle containing 1 ml of 0.7 mM potassium ferricyanide (400 mg NaOH, 20 g Na_2CO_3 and 230 mg $K_3[Fe(CN)_6]$ in 1000 ml of d.d.H_2O), and the well-mixed solution was placed in a boiling water bath for 10 min. A 2 mM solution of ferric chloride was prepared by dissolving 32.4 mg of anhydrous $FeCl_3$ in 100 ml of a solution prepared by adding 16.4 g sodium acetate (anhydrous), 4.2 g citric acid and 30 g acetic acid to 1000 ml of d.d.H_2O. One ml of this 2 mM ferric chloride solution and 2 ml of 2.5 mM TPTZ (2,4,6-Tripyridyl-s-triazine, Sigma Lot No.: 111K2600) solution in 3M acetic acid were immediately added and mixed on a Vortex mixer. After 30 min, the absorbance was read at 595 nm. The control experiments used d.d.H_2O instead of seawater, but followed the

same procedures. The reagent blank in d.d.H_2O was subtracted before calculating the final concentration of the monosaccharide (e.g. glucose). It is important to note that the whole analytical procedure must be conducted in the dark because most of the reagents are light-sensitive. The concentration of TPCHO was expressed as μM-C. The precision of each method was 5 to 10% (one standard deviation).

III.3.6 Determination of Uronic Acids

Uronic acids (UA) contents for marine bacteria and phytoplankton were determined according to Hung and Santschi (2000), which is based on a modification of the method of Filisetti-Cozzi and Carpita (1991), after pre-concentration by cation exchange and freeze drying (Hung and Santschi, 2001). Briefly, 0.4 ml of sample solution was pipetted to a glass vial where 40 μL of 2M sulfamic acid was added and stirred on a vortexer. Subsequently, 2.4 ml of 75 mM sodium tetraborate (Sigma, Lot No.: 19H0760) in concentrated H_2SO_4 was added to the glass vial and covered tightly. The sample was then mixed with a vortexer before it was heated at 100 $^{\circ}$C for 10 min in a boiling water bath. After cooling to room temperature, 30 μL of 0.15% m-hydroxydiphenyl was added to the glass vial and mixed well by a vortexer. The red color, which developed, was complete after 3 ~ 5 min and was measured within 20 min. There is little loss of color with time and after 45 min the absorbance decreased by only 3-7%. The absorbance was measured at 525 nm with a 1-cm disposable cell using a spectrophotometer. Concentrated sulfuric acid was used to auto zero the spectrophotometer. For the procedural blank of the sample, 30 ml of uronic acid free

seawater was used after UV irradiating it for 48 hr and applying the same procedures used for the samples. For the measurement of uronic acid standards, the following solutions were prepared: 0.2 ml and 0.4 ml 200 μM of uronic acids, galacturonic acid, glucuronic acid, and mannuronic acid. Each of these acids was added into 30 ml of uronic acid free seawater to be run as a matrix matched standard calibration solution. The average slopes of the standard curves for galacturonic acid, glucuronic acid, and mannuronic acid were used for the calculation of the total uronic acid concentration in the sample. The procedural blank (~ 0.1 μM) was subtracted from the measured concentrations and reported as "total uronic acids" (URA).

III.3.7 Total Protein Content

The Bicinchoninic acid (BCA) protein assay is a rapid and reliable dye-based assay, which is a variation by Smith *et al.* (1985) of the 1951 Lowry method for determining protein content in solution. The colorimetric reaction is simple to perform, has fewer interfering substances and a more stable end product. Disadvantages are a slower reaction time and irreversible denaturation of protein samples. The protein concentrations were normalized to bovine albumin fraction V protein (BSA) (Pierce, Lot No:DK59769). The sensitivity of method is 0.5-10 μg/ml (micro assay) and 10-1200 μg/ml (standard assay) (Bollag *et al.*, 1996) [V.3]. Purity of the protein was determined using UV-Vis spectrophotometer. A solution, which has no contamination with nucleic acids, will have an absorbance ratio (A_{260}:A_{280}) of less than 0.6. Any value larger than

this is consistent with nucleic acid contamination (Alvarado-Urbina, *person. commun.,* Bollag *et al.*, 1996).

III.3.8 Gas Chromatography Mass Spectrometry (GC-MS)

Monosaccharide determination was carried out on a GC-MS using Doco *et al.*, (2001) method. Following the polysaccharide sample purification (via PAGE), a fraction of total sample obtained from marine bacteria *S. stellata* and phytoplankton *S. elongatus* were dissolved in d.d.H_2O and placed in teflon vials and capped. To each sample solution, 100 μl of alditol (as an internal standard), 100 μl of methanol and 100 μl of 1 M HCl were added and solution was then heated at 80° C on a heating block (Environmental Express Hot block) for 16 hours. Samples were subsequently cooled to 40° and dried under nitrogen gas (N_2) for 4 hours. Once material was dried, 400 μl of Tri-Sil reagent (Sigma) was added and vials were capped and brought up to 80° C for 20 minutes. Temperature was brought down to 40° C, again, with subsequent drying under nitrogen. At this point, material has been derivatized and prior to running on GC-MS, the sample was dissolved in hexane (Aldrich, Lot No.: CO 02244CO). Identification of a polysaccharide compound based on its mass spectrum relies on the fact that every compound has a unique fragmentation pattern. A library of known mass spectra is stored on the computer and is searched by computer software to assist in identifying the unknown compound (Lambert *et al.*, 1987; Fox *et al.,* 1998; Samuelsen *et al.*, 1999).

IV. RESULTS AND INTERPRETATIONS

IV.1. Radioisotope Labeling Incubation Experiment – ^{14}C, ^{32}P, ^{35}S, and $^{234}Th(IV)$

The mass balance for the EPS extraction method [III.2.5] was obtained for all species and each individual step of the method. Recoveries for ^{32}P, ^{35}S, and $^{234}Th(IV)$ ranged from 69-110%, 113-119% and 60-82%, respectively, for marine bacteria *R. gallaeciensis* (Figure 18, Table 19). For the second bacterial sample, *S. stellata*, the recoveries for ^{32}P, ^{35}S, and ^{234}Th ranged from 96-109%, 85-101% and 93-97%, respectively (Figure 19, Table 20). In the phytoplankton species *E. huxleyi*, the mass balance yields for ^{32}P, ^{35}S, and $^{234}Th(IV)$ ranged from 88-118%, 64-106%, and 66-122%, respectively (Figure 20, Table 21). And finally, for *S. elongatus*, the mass balance yields for ^{32}P, ^{35}S, and $^{234}Th(IV)$ ranged from 86-99%, 81-100%, and 93-99%, respectively (Figure 21, Table 22).

In all four cases, little of the ^{35}S labeled sulphate was incorporated into the microorganism nor did it trace any organic matter along the extraction and precipitation procedures. Most of the $^{35}SO_4$ remained in the marine broth or seawater media. The reason why the microbial pellet exhibited a negative activity is due to the fact that from the 30 ml of seawater or marine broth media that was used for incubation, only 25 ml were removed so as not to disturb the microbial pellet. A correcting factor was used from the activity of the seawater media and subtracted this correction factor from the activity of the pellet. Since the activity of the pellet was at background, the net difference from the correcting factor produced a negative activity. Very little, if any, sulphate was detected on the walls of the centrifuge tubes at various steps of the

extraction. Dilution of the $^{35}SO_4^{2-}$ by the large sulphate reservoir of seawater did not allow much tracer to be incorporated during the experiment.

IV.1.1 Bacterial Incubations

For both bacterial samples *R. gallaeciensis* (ATCC700781) and *S. stellata* (ATCC700073), less than 25% of total ^{32}P label existed in the media fraction. Roughly 46-71% of the total ^{32}P activity was accounted for in the bacterial pellet fraction from the various steps. This indicates that $^{32}PO_4$, unlike $^{35}SO_4$, was associated with the bacterial pellet. As the mass balance for the subsequent steps of the extraction was obtained, it was evident that $^{32}PO_4$ was extracted successfully from the pellet in both bacteria. Ultimately, between 12% and 19% of the $^{32}PO_4$ was incorporated by *R. gallaeciensis* and *S. stellata* at the cell surface, respectively. Thus a large portion of the PO_4 still remains on the cell surface indicating that the extraction procedure was effective but did completely remove all of the potential ligand for $^{234}Th(IV)$ (Figure 18 and Figure 19).

In the case of $^{234}Th(IV)$, less than 4% of total activity remained in the marine broth. 56-75% and 79-89% of the total $^{234}Th(IV)$ activity was associated with the microbial pellet for *R. gallaeciensis* and *S. stellata*, respectively. The water extraction of the microbial pellet was 1% and 8% extraction efficiency for *R. gallaeciensis* and *S. stellata*, respectively.

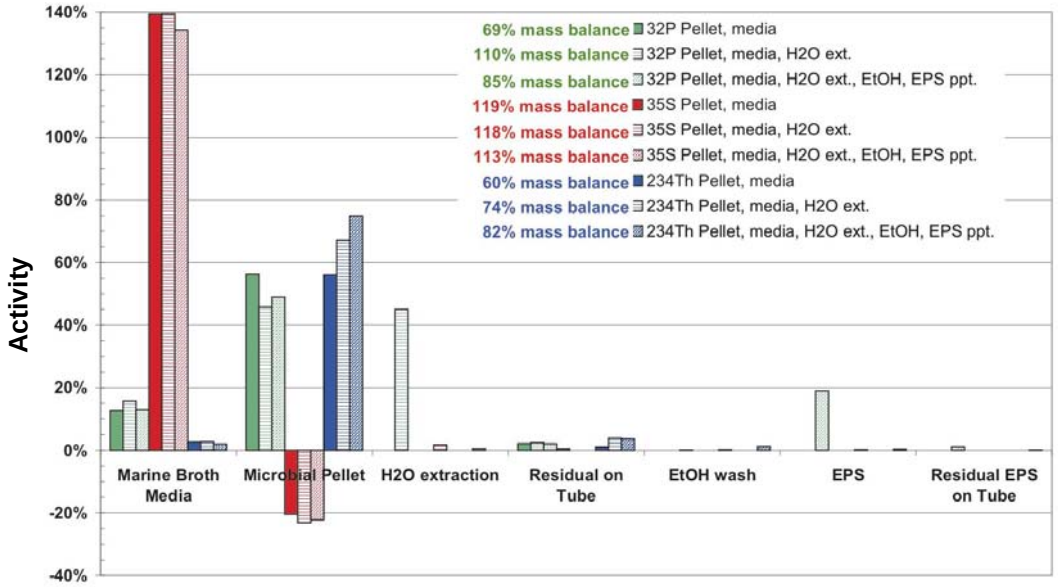

Figure 18 Partitioning experiments of ^{32}P, ^{35}S, and $^{234}Th(IV)$ of *R. gallaeciensis.*

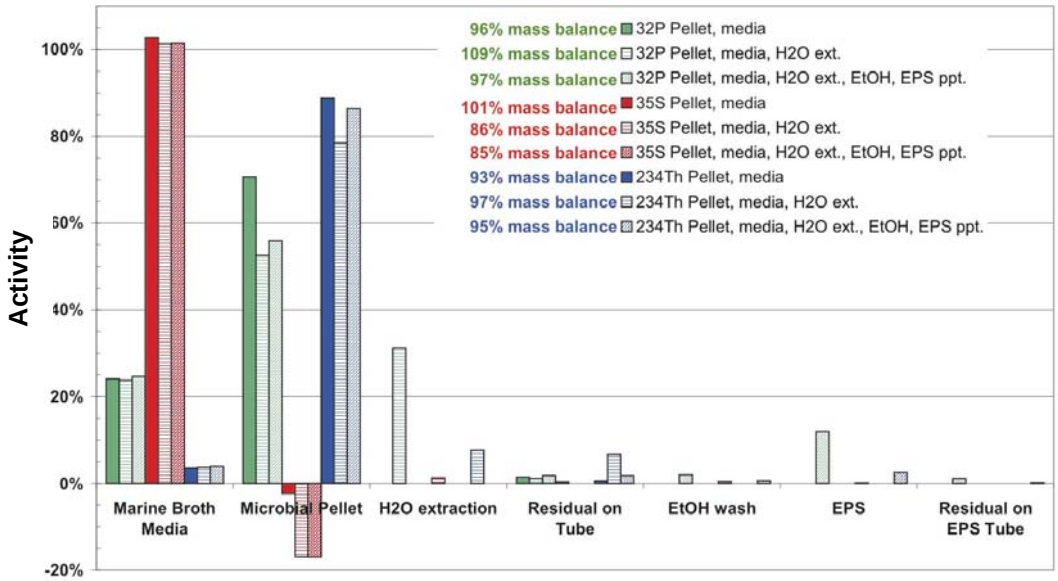

Figure 19 Partitioning experiments of ^{32}P, ^{35}S, and $^{234}Th(IV)$ of *S. stellata*.

Very little of the ^{234}Th(IV) label remained on the centrifuge tubes (ranging from 1-7% of total ^{234}Th activity). Eventually, between 0.5% and 2% of the ^{234}Th was associated with particle reactive organic matter produced by *R. gallaeciensis* and *S. stellata* at the cell surface, respectively. Thus a large portion of the ^{234}Th(IV), as is the case with $^{32}PO_4$, still remains on the cell surface, indicating that the extraction procedure worked, but did not completely remove all of the potential ligand and thorium(IV) (Figure 18 and Figure 19).

IV.1.2 Phytoplankton Incubations

In the phytoplankton samples *E. huxleyi* (CCMP374) and *S. elongatus* (CCMP1379), a greater percentage of the ^{32}P labeled PO_4 was present in the marine broth and seawater media (45-50% for *E. huxleyi* and approximately 79% for *S. elongatus*). Roughly 42% and 17% of the total ^{32}P activity was accounted for in the *E. huxleyi* and *S. elongatus* pellet fraction, respectively, for the first of the various steps. This was an indication that $^{32}PO_4$, in comparison to the bacterial samples, had lesser association with the phytoplankton pellet. As the mass balance for the subsequent steps of the extraction was obtained, it became evident that $^{32}PO_4$ was extracted successfully from the pellet in *E. huxleyi* more successfully than *S. elongatus*. Ultimately, between 20% and 5% of the $^{32}PO_4$ was incorporated by *E. huxleyi* and *S. elongatus* at the cell surface, respectively. As a result, a significant portion of the PO_4 still remained on the cell surface, but relatively less than bacterial samples. This indicates that the extraction

procedure was effective, but did not completely remove the potential ligand for thorium(IV) (Figure 20 and Figure 21).

In the case of ^{234}Th, less than 8% of total activity remained in the marine broth. 41-61% and 32-76% of the total ^{234}Th(IV) activity was associated with the microbial pellet for *E. huxleyi* and *S. elongatus*, respectively. The water extraction of the microbial pellet resulted in 33% and 17% extraction efficiency for *E. huxleyi* and *S. elongatus*, respectively. Very little of the ^{234}Th(IV) label remained on the centrifuge tubes (ranging from 2-3% of total ^{234}Th(IV) activity). Less than 10% of EPS material extracted from the bacteria was associated with ^{234}Th(IV) (9% and 11% label for *E. huxleyi* and *S. elongatus*, respectively). Thus, a large portion of the ^{234}Th(IV) as was the case with $^{32}PO_4$, still remained on the cell surface indicating that the extraction procedure was working but did not lead to a complete removal of the potential ligand and ^{234}Th(IV) (Figure 20 and Figure 21).

The purpose for conducting this radionuclide experiment was two-fold. The first was to determine the efficiency of the methodology and the second was to extract, isolate and analyze the microbial EPS product. In order to detect the isotopes, they were treated in the same manner as the raw material that was treated for isolation for chemical analysis (i.e. IEF and 2D SDS-PAGE). IEF gel electrophoresis was performed on radiolabeled EPS in order to study and compare the isoelectric (pH) profile of incubated material with that non-incubated ^{234}Th labeled EPS [see below IV.2].

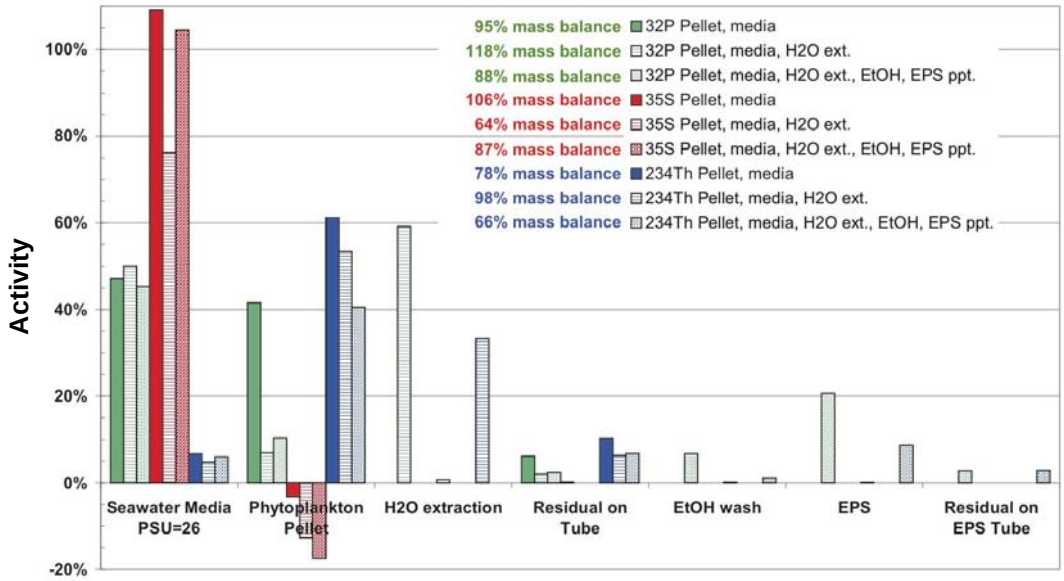

Figure 20 Partitioning experiments of ^{32}P, ^{35}S, and $^{234}Th(IV)$ of *E. huxleyi*.

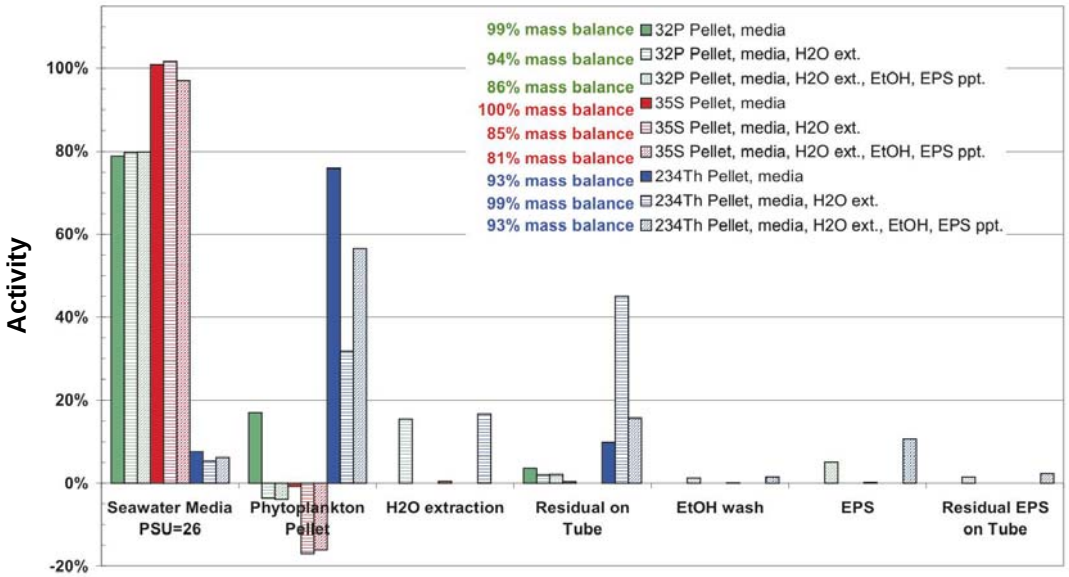

Figure 21 Partitioning experiments of ^{32}P, ^{35}S, and $^{234}Th(IV)$ of *S. elongatus*.

IV.2. Isoelectric Focusing Electrophoresis (IEF) Experiments

Isoelectric focusing (IEF) experiments were conducted as a means of primarily determining the pI (or pH_{IEF}) of $^{234}Th(IV)$ binding ligands. Two types of IEF were obtained and presented, natural IEF obtained from one dimensional IEF strip and IEF obtained from a 2D SDS-PAGE, where the sum of the molecular weight subfractions of each pH are combined to obtained a one dimensional profile (or spectrum). Pure IEF will be defined solely as IEF, and IEF obtained from 2D SDS-PAGE will be stated as such. $^{234}Th(IV)$ IEF should be compared with ^{14}C, PO_4^{3-} (from IC) and SO_4^{2-} (from IC) IEF. For all bacterial and phytoplankton isolates, a large portion (50-61%) of the $^{234}Th(IV)$ was associated with molecules in the pH range below 4 (acidic region) rather than that of ThO_2 or iron hydroxides (pH_{IEF} of 7-9, El Shafei (1996)). Marine bacteria *R. gallaeciensis* and *S. stellata* exhibited 35% of $^{234}Th(IV)$ activity at pH of 2.28, followed by 12% at a pH of 2.05 (Figure 22a, Table 23) and 24% at pH of 2.31 followed by 22% at pH 1.90 (Figure 23a, Table 24), respectively. $^{234}Th(IV)$ associated with EPS isolates from phytoplankton species *E. huxleyi* and *S. elongatus* was largely associated (~55%) with a molecule below pH of 5 (Figure 24, Table 25 and Figure 25, Table 26). Phytoplankton species *S. elongatus*, also had a significant thorium activity consisting of 30% total activity (14.8% and 16.3% at a pH of 6.22 and 6.84, respectively) (Figure 25a). This may be attributed to a) contamination of samples from airborne particulate (clay, iron oxide or silica particles) or by DNA which may have been inadvertently extracted during processing of sample. Gulf of México Station 4 72m colloidal organic

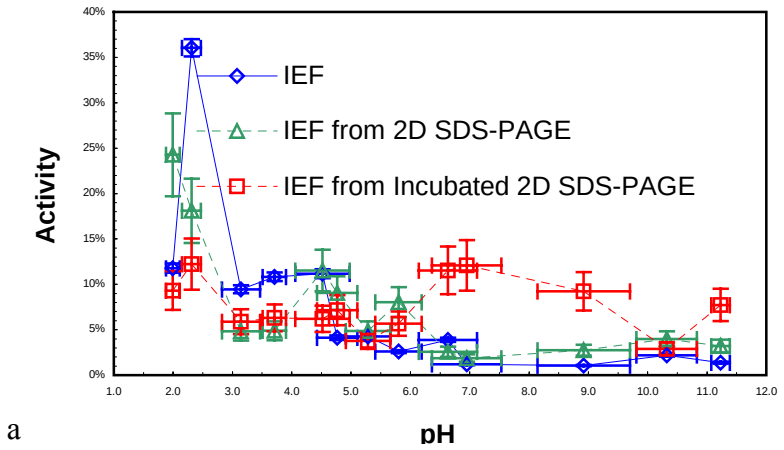

a

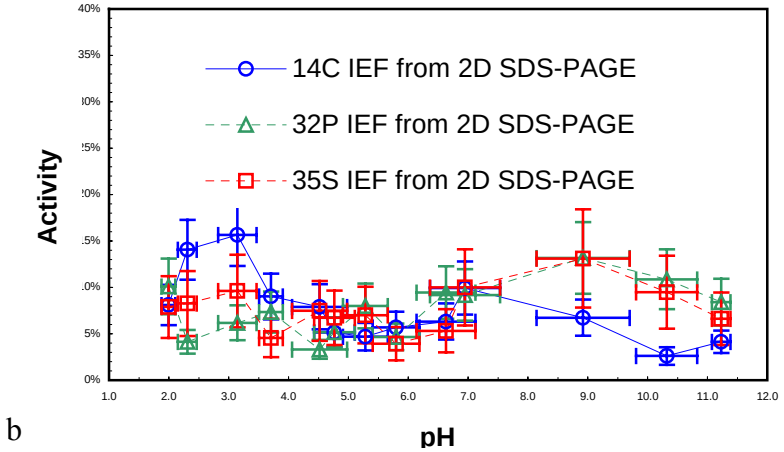

b

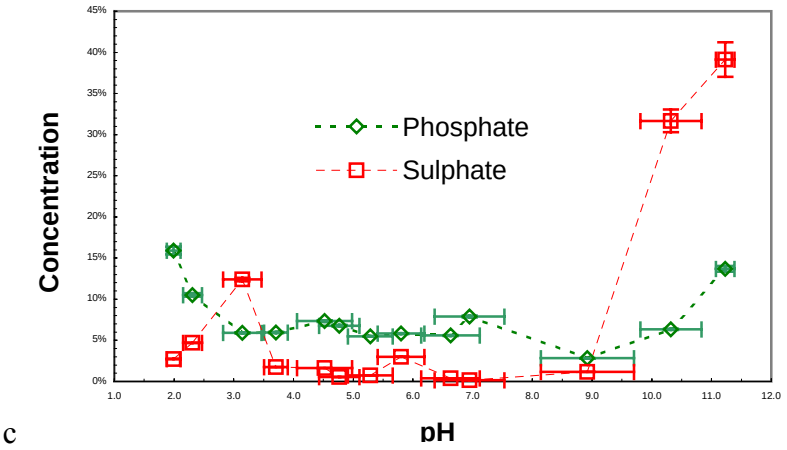

c

Figure 22 Isoelectric profile of ^{234}Th(IV) enriched PCHO labeled EPS from *R. gallaeciensis* illustrating the specific pH that is associated with the bulk of the a) thorium (IV); b) carboxylic acid (^{14}C), incubated phosphate ($^{32}PO_4$) and sulphate ($^{35}SO_4$); and c) phosphate (PO_4) and sulphate (SO_4) via ion chromatography.

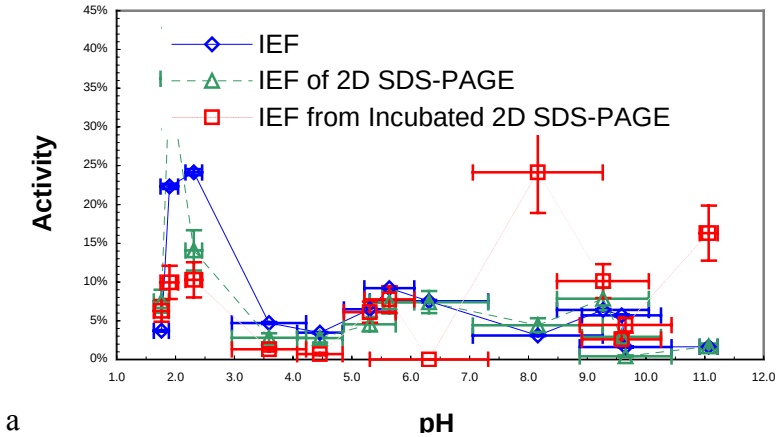

a

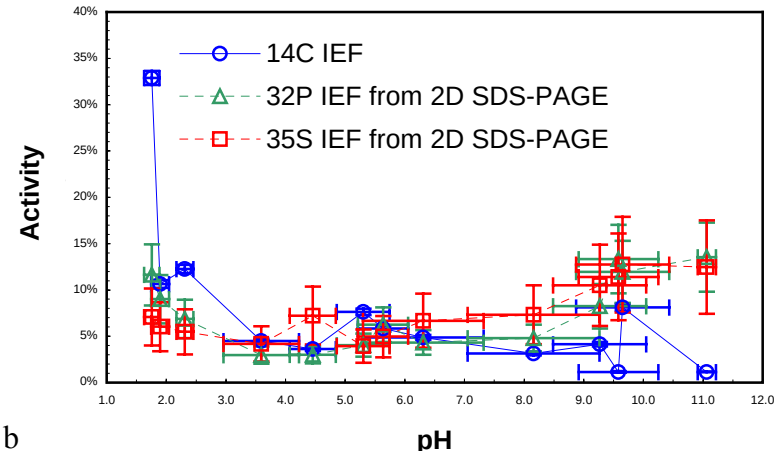

b

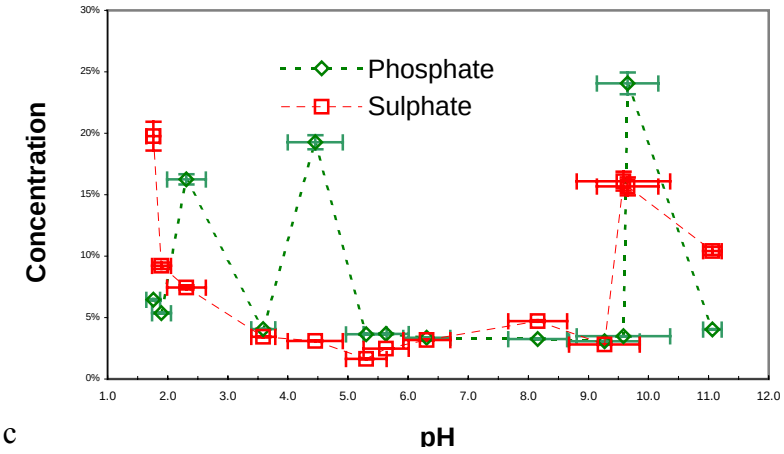

c

Figure 23 Isoelectric profile of ^{234}Th(IV) enriched PCHO labeled EPS from *S. stellata* illustrating the specific pH that is associated with the bulk of the a) thorium (IV); b) carboxylic acid (^{14}C), incubated phosphate ($^{32}PO_4$) and sulphate ($^{35}SO_4$); and c) phosphate (PO_4) and sulphate (SO_4) via ion chromatography.

sample had 54.7% total activity below pH of 4 (average pH of 2.86). Thus, 57%, 50%, 65%, 49% and 54.7% of *R. gallaeciensis*, *S. stellata*, *E. huxleyi S. elongatus*' and GOM COM activities were associated with the ^{234}Th(IV) label near pH of 2, respectively.

IEF and 2D SDS-PAGE for ^{234}Th(IV) label was conducted in parallel to corroborate the ^{234}Th(IV) affinity to acidic region. The IEF spectra obtained, from 2D SDS-PAGE of *R. gallaeciensis* and *S. stellata*, exhibited slightly different profiles from that of the simple IEF (Figure 22a and Figure 23a). IEFs obtained from 2D SDS-PAGE for *E. huxleyi* and *S. elongatus* exhibited nearly identical profiles from those of the simple IEF (Figure 24a and Figure 25a). Although there were slight variations, statistically speaking (see section IV.4.1) there was no significant difference.

The IEF spectra of incubated thorium(IV) for EPS from *R. gallaeciensis* and *S. stellata* were similar below pH of 6 (Figure 22a and Figure 23a). The incubated *E. huxleyi* ^{234}Th(IV) illustrated a peak with higher activity (27%) at pH 10.70 (Figure 24A and Figure 25a). The ^{234}Th(IV) increase was indicative of the polymeric ^{234}Th(IV) species developing during the incubations. Only the IEF obtained from incubated ^{234}Th(IV) 2D SDS-PAGE for *S. elongatus* was practically flat with activities ranging from 4-11% throughout the pH range (Figure 25a).

Labeling of the carboxylic acid functional groups of microbial species (*R. gallaeciensis*, *S. stellata*, *E. huxleyi* and *S. elongatus*) carboxylic acid functional group with dimethylamine ($[^{14}CH_3]_2NH$) reacted with about 1% of carboxylic acid functional group present, thus leaving the majority of the functional groups untouched. *R. gallaeciensis* had maxima of 16% and 14% at pH 3.14 and 2.31, respectively

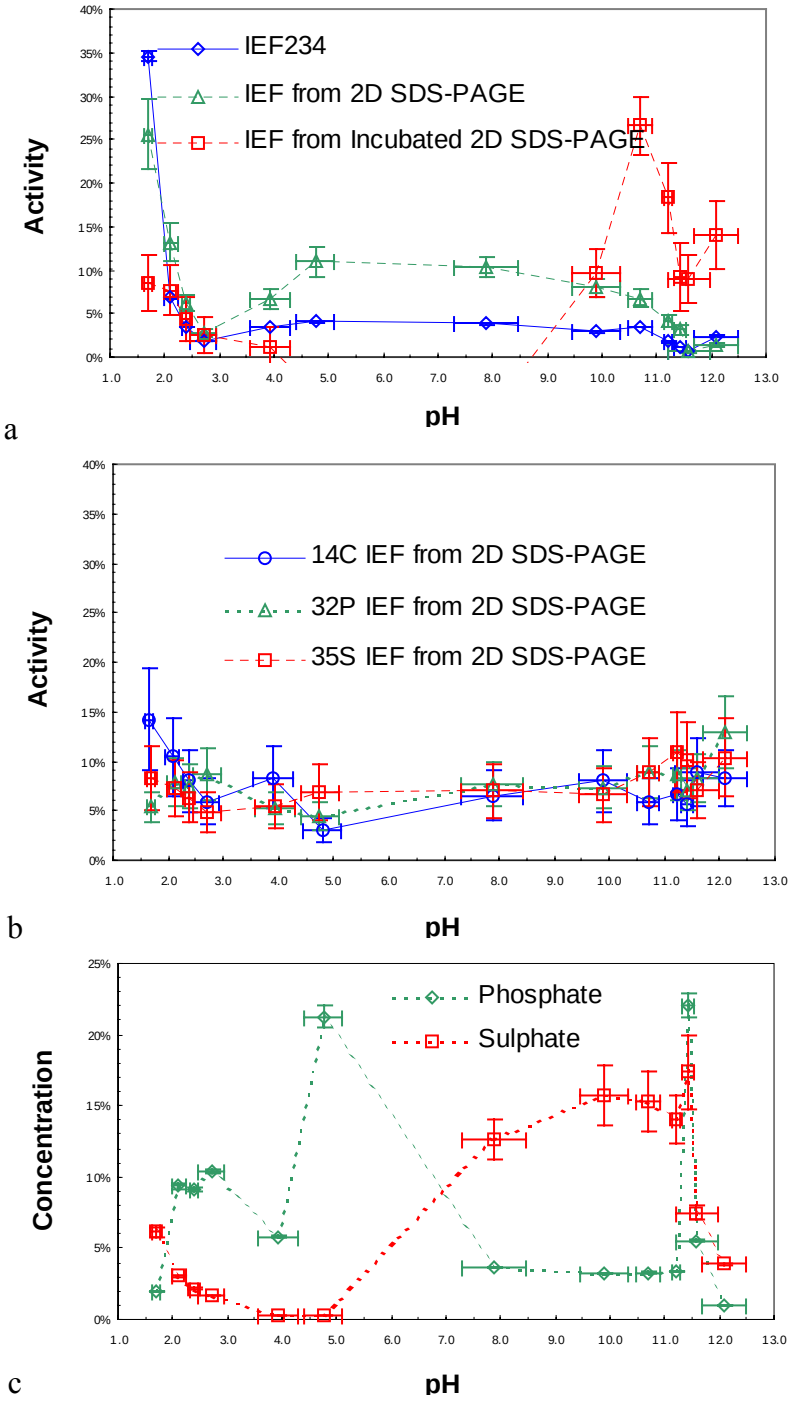

Figure 24 Isoelectric profile of ^{234}Th(IV) enriched PCHO labeled EPS from *Emiliania huxleyi* illustrating the specific pH that is associated with the bulk of the a) thorium (IV); b) carboxylic acid (^{14}C), incubated phosphate ($^{32}PO_4$) and sulphate ($^{35}SO_4$); and c) phosphate (PO_4) and sulphate (SO_4) via ion chromatography.

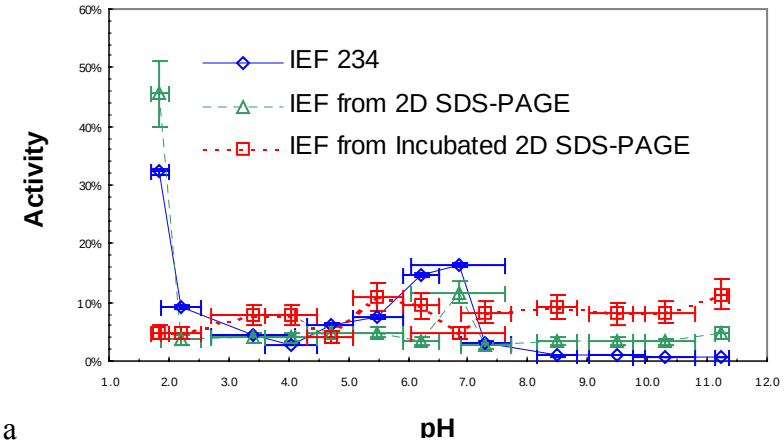

a

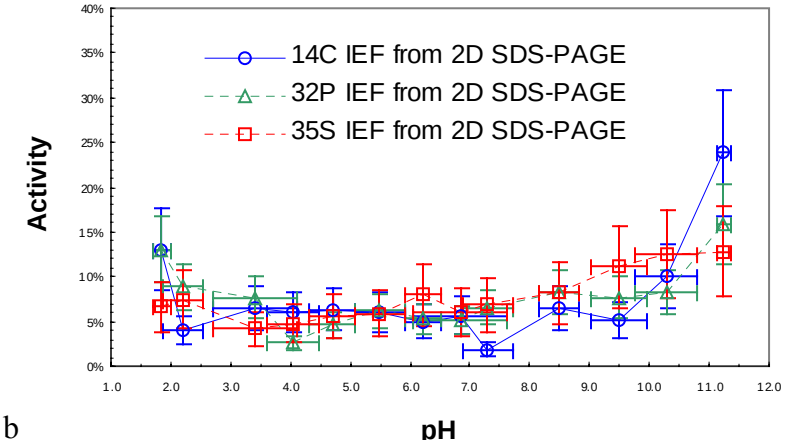

b

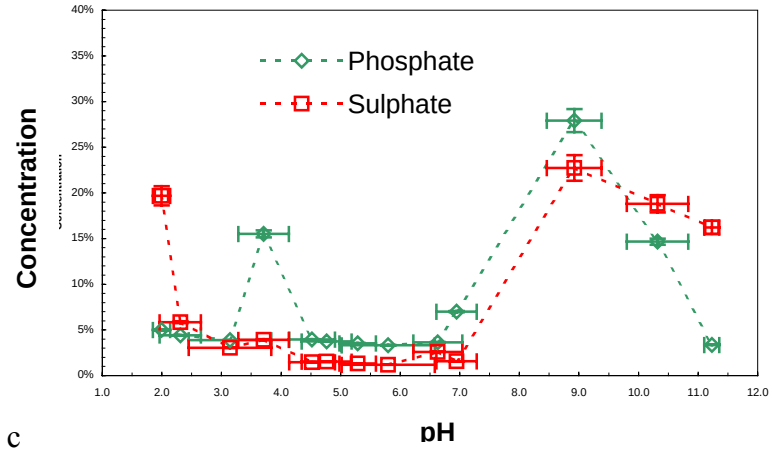

c

Figure 25 Isoelectric profile of ^{234}Th(IV) enriched PCHO labeled EPS from *S. elongatus* illustrating the specific pH that is associated with the bulk of the a) thorium (IV); b) carboxylic acid (^{14}C), incubated phosphate ($^{32}PO_4$) and sulphate ($^{35}SO_4$); and c) phosphate (PO_4) and sulphate (SO_4) via ion chromatography.

(Figure 22b). *S. stellata* had maxima of 33%, 12% and 11% at pH 1.79, 2.31 and 1.90, respectively (Figure 23b). *E. huxleyi* displayed an increase in activity towards low pH region that peaked at 14%, 10%, 8%, 6%, and 8% at pH 1.66, 2.07, 2.36, 2.69, and 3.91, respectively (Figure 24b). *S. elongatus* exhibited two major peaks at either electrode. At the low pH, the maxima occurred at 13% total activity, tapering down to 4%, 7% and 6% at pH 1.85, 2.20, 3.41 and 4.04, respectively. At the basic region, percent activity started at 7%, 5%, 10% and 24% total activity for pHs of 8.49, 9.49, 10.28 and 11.25, respectively. The general trend observed was an increase in activity at lower pH (Figure 25b).

For microbial incubations of ^{32}P and ^{35}S, the *R. gallaeciensis* (Figure 22b), *S. stellata* (Figure 23b) and *E. huxleyi* (Figure 24b) ^{32}P and ^{35}S profiled each other closely above pH 7, but behaved independently below pH 7. *S. elongatus* (Figure 25b) illustrated ^{32}P and ^{35}S activity behaving independently. The IEF profiles of the radioisotopes (i.e. $^{32}PO_4$ and $^{35}SO_4$ incubations results) must be analyzed with caution. Since such minute amounts ($^{32}PO_4$, and $^{234}Th(IV)$) or practically none ($^{35}SO_4$) was incorporated into the bacterial cultures, 2D SDS-PAGE was performed on the little extracted EPS present (1 mg). As a result, the sum of the mass fraction for each pH resulted in activity error of two standard deviations (2σ) of ~8-17%. Thus the error propagation that was carried out ranged from 12-30% and averaged approximately 22%, making the error bars on the IEF from incubated material larger than typical (Table 29, 27, 29, 31, 33 and 35).

Phosphate (PO_4^{3-}) and sulphate (SO_4^{2-}) concentrations were determined via ion chromatography (IC). There was a PO_4^{2-} increase in concentration for *R. gallaeciensis* at pH<5 (Figure 22c), three major peaks (pH 2.31, 4.46 and 9.65) for *S. stellata* (Figure 23c), three peaks (pH 2.71, 4.75 and 11.42) for *E. huxleyi* (Figure 24c) and two distinct peaks (pH 3.71 and 8.92) for *S. elongatus* (Figure 25c). The SO_4^{2-} concentration also had peaks for *R. gallaeciensis* at pH 3.14, two major peaks (pH 1.76 and 9.58) for *S. stellata*, two regions of elevated activity (pH 1.68, 7.87-11.42) for *E. huxleyi* and two distinct peaks (pH 1.99 and 8.92-11.23) for *S. elongatus*.

Gulf of México natural colloidal organic matter, collected from Station 4 warm core ring at a depth of 72 m during the R/V *Gyre* cruise of 2001, was treated exactly like the cultured samples (Figure 17). The parallel IEF and 2D SDS-PAGE were run and IEF obtained from 2D SDS-PAGE exhibited nearly identical profiles from the pure IEF (Figure 26a, Table 27). Although there were slight variations, but statistically speaking (see section IV.4.1) there was no significant difference.

The GOM Station 4 D-72m carboxylic acid IEF profile labeled with ^{14}C illustrated the same 1% of carboxylic acid functional group labeled by the $(^{14}CH_3)_2NH$. This sample had one significant peak located at the anode pH 2.21 (Figure 26b).

GOM Station 4 D-72m phosphate and sulphate concentrations (Figure 26c) showed three major PO_4 and two major SO_4 peaks. The phosphate peaks were at pH 2.21, 4.14 to 5.00 and 6.11. Sulphate peaks were at pH 2.21 and 9.25 to 10.26. Sulfate in the neutral and basic region was likely originally present as a thiol functional group in proteins.

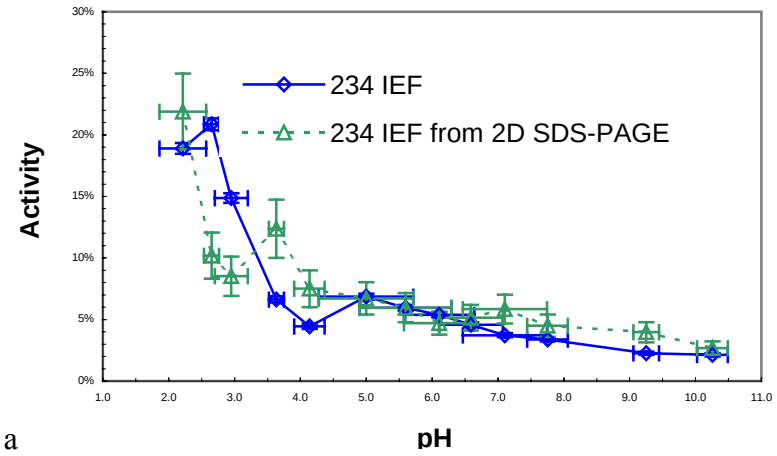

a

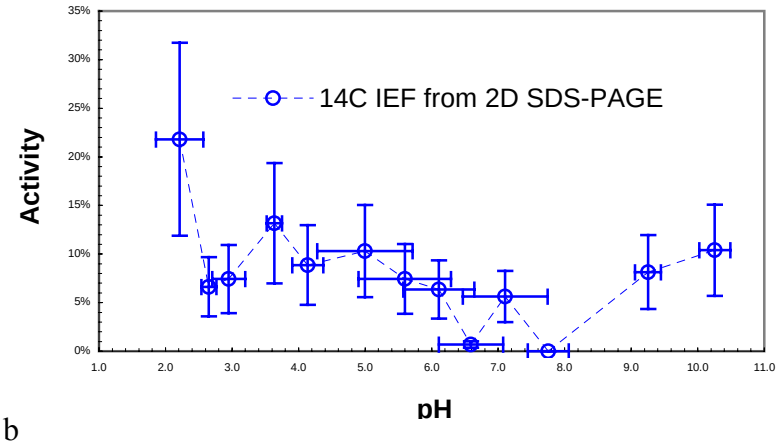

b

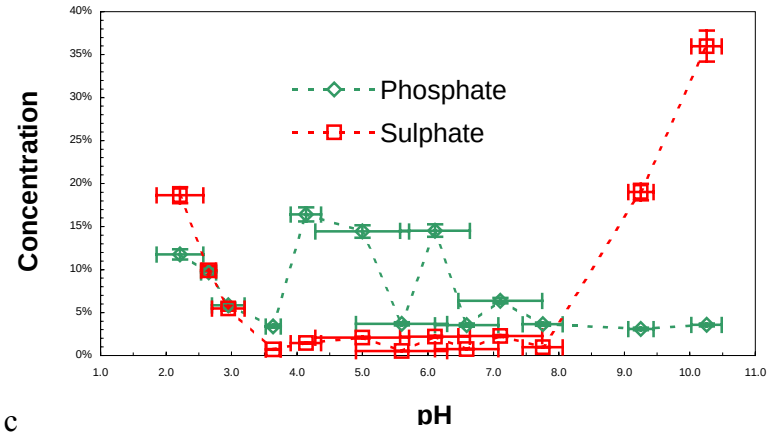

c

Figure 26 Isoelectric profile of ^{234}Th(IV) enriched PCHO labeled EPS from Gulf of México colloidal material from Station 4 (72m depth at chlorophyll A maxima) illustrating the specific pH that is associated with the bulk of the a) thorium (IV); b) carboxylic acid (^{14}C), and c) phosphate (PO_4) and sulphate (SO_4) via ion chromatography.

The concentration of PO_4 and SO_4 functional group relative to $^{234}Th(IV)$ concentration at low pH were determined via ion chromatography [III.3.4](Table 5). The PO_4 to $^{234}Th(IV)$ ratios for EPS extracted from *R. gallaeciensis* and *S. stellata*, ranged between 6.7 to 31 X 10^8 and 2.4 to 17 X 10^{14}, respectively. The SO_4 to $^{234}Th(IV)$ ratios for EPS extracted from *R. gallaeciensis* and *S. stellata*, ranged between 2.2 to 22 X 10^8 and 6.0 to 100 X 10^8, respectively. The PO_4 to $^{234}Th(IV)$ ratios for EPS extracted from *E. huxleyi* and *S. elongatus*, ranged between 1.3 to 130 X 10^7 and 7.5 to 260 X 10^7, respectively. The SO_4 to $^{234}Th(IV)$ ratios for EPS extracted from *E. huxleyi* and *S. elongatus*, ranged between 2.0 to 10 X 10^8 and 5 to 11 X 10^8, respectively. Thus, the total thorium (^{232}Th) concentration compared to the total concentration of acidic binding sites (PO_4 and SO_4) indicates that there is one thorium atom for every ~220,000,000-890,000,000 and 240,000,000-3,100,000,000 potential acidic binding sites, respectively. The remainder of such sites would be occupied by other metals in the ocean such as calcium (Table 1). This would imply that, stronger binding sites (chelating sites) could become more important. Thus, the steric environment and not necessarily the exact functional group might actually be responsible for thorium-234 complexation to macromolecular organic matter

Table 5 Ratio of PO_4^{3-} and SO_4^{2-} versus ^{234}Th(IV) for all species.

R. gallaeciensis

pH	^{234}Th(IV) (Bq)	Moles of ^{234}Th(IV) (n)	Moles of PO_4 (n)	PO_4: ^{234}Th(IV)	Moles of SO_4 (n)	SO_4: ^{234}Th(IV)
1.99	2.8	9.6E-18	3.0E-08	3.1E+09	3.8E-09	3.9E+08
2.31	8.5	8.5E-17	2.0E-08	6.7E+08	6.5E-09	2.2E+08
3.14	2.2	2.2E-18	1.1E-08	1.4E+09	1.7E-08	2.2E+09
3.71	2.6	2.6E-18	1.1E-08	1.3E+09	2.4E-09	2.8E+08

S. stellata

pH	^{234}Th(IV) (Bq)	Moles of ^{234}Th(IV) (n)	Moles of PO_4 (n)	PO_4: ^{234}Th(IV)	Moles of SO_4 (n)	SO_4: ^{234}Th(IV)
1.76	6.3	1.6E-18	9.9E-09	1.7E+09	5.9E-08	1.0E+10
1.90	38.1	9.9E-17	8.2E-09	2.4E+08	2.8E-08	8.1E+08
2.31	41.2	1.7E-17	2.5E-08	6.7E+08	2.2E-08	6.0E+08
3.59	8.0	2.1E-18	6.2E-09	8.7E+08	1.0E-08	1.4E+09

E. huxleyi

pH	^{234}Th(IV) (Bq)	Moles of ^{234}Th(IV) (n)	Moles of PO_4 (n)	PO_4: ^{234}Th(IV)	Moles of SO_4 (n)	SO_4: ^{234}Th(IV)
1.68	78.6	2.7E-16	3.5E-09	1.3E+07	5.4E-08	2.0E+08
2.11	15.6	5.4E-17	1.7E-08	3.1E+08	2.6E-08	4.9E+08
2.38	7.9	2.7E-17	1.6E-08	6.0E+08	1.9E-08	6.9E+08
2.71	4.2	1.4E-17	1.9E-08	1.3E+09	1.5E-08	1.0E+09

S. elongatus

pH	^{234}Th(IV) (Bq)	Moles of ^{234}Th(IV) (n)	Moles of PO_4 (n)	PO_4: ^{234}Th(IV)	Moles of SO_4 (n)	SO_4: ^{234}Th(IV)
1.85	30.8	1.1E-16	8.0E-09	7.5E+07	5.3E-08	5.0E+08
2.20	8.7	3.0E-17	7.1E-09	2.3E+08	1.6E-08	5.2E+08
3.41	4.4	1.5E-17	6.2E-09	4.1E+08	8.2E-09	5.4E+08
4.04	2.8	9.6E-18	2.5E-08	2.6E+09	1.1E-08	1.1E+09

IV.3. 2D SDS-PAGE (IEF+1D SDS-PAGE) of Thorium (IV) Tracking EPS – ^{234}Th

Two dimensional sodium dodecyl sulphate polyacrylamide gel electrophoresis using a 15% homogeneous gel (2D SDS-PAGE 15%) was performed on all samples to determine, and isolate the ^{234}Th(IV) binding ligand and associate it with a functional group. In the marine bacteria sample *R. gallaeciensis*, a combined 24% of ^{234}Th(IV) activity was associated exopolymeric substance (EPS) <1000 Da (1 Dalton = 1 atomic mass unit) at pH 1.99 and 2.31 (Figure 27, Table 30). This was expected from the IEF plot (Figure 22a) although the IEF plot had a combined total of 38% for same pH regions (Table 23). Upon further inspection, the sum of the ^{234}Th(IV) activity for the pH 1.99 and 2.31 (from 2D SDS-PAGE) was 42%. At an approximate pH of 2, 24% of the total ^{234}Th(IV) activity was associated with the organic matter in the molecular weight category less than 1 kDa in size range. Clearly, for *Roseobacter gallaeciensis*, the organic material associated with ^{234}Th(IV) activity is truly dissolved.

Using radiolabeled glucose, Stoderegger and Herndl (1998) determined the incorporation of glucose into intracellular and capsular pools to acquire production estimates. 55% was incorporated intracellularly and 45% percent to capsular material. Release rates of the capsular material represented circa 25% of bacterial respiration suggesting that a significant portion of the DOC pool is composed of bacterially derived semi-labile DOC (Stoderegger and Herndl, 1998). Thus, the results obtained in Figure 27 are reasonable.

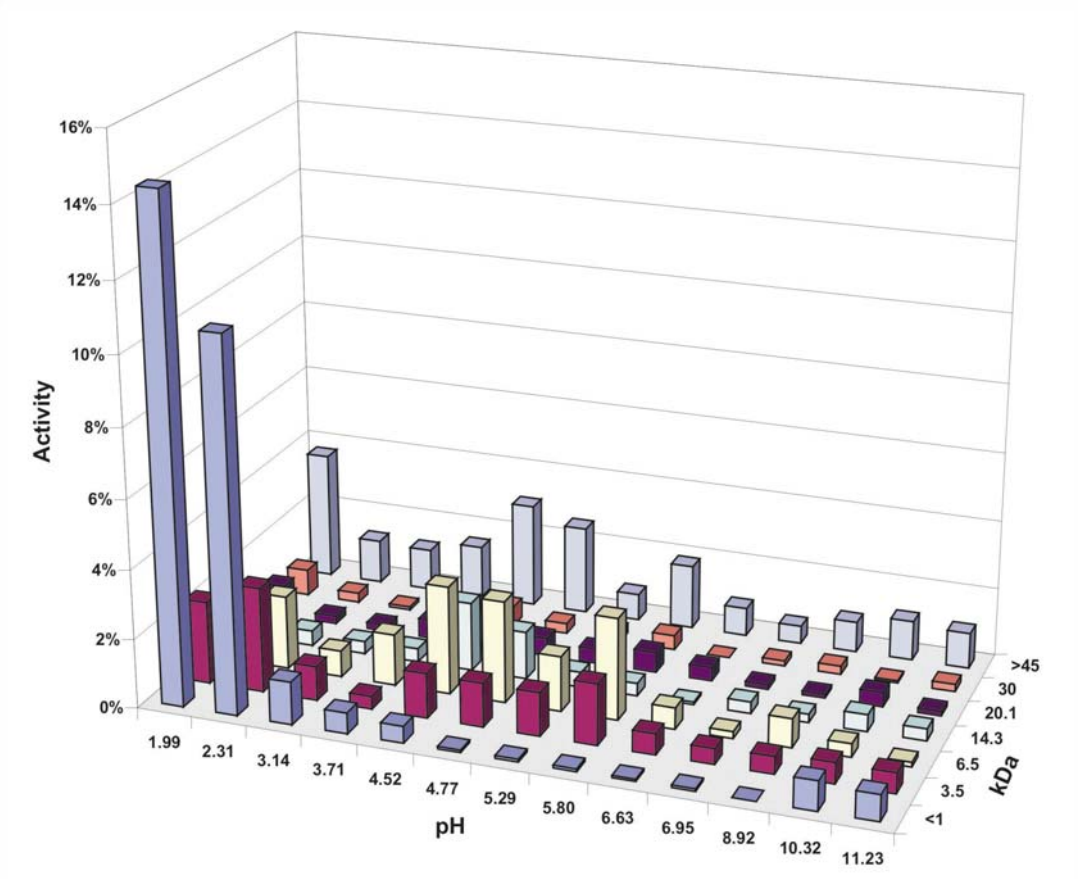

Figure 27 Plot of 15% 2D SDS-PAGE of ^{234}Th(IV) for polysaccharide enriched fraction extracted from marine bacteria *R. gallaeciensis* particulate.

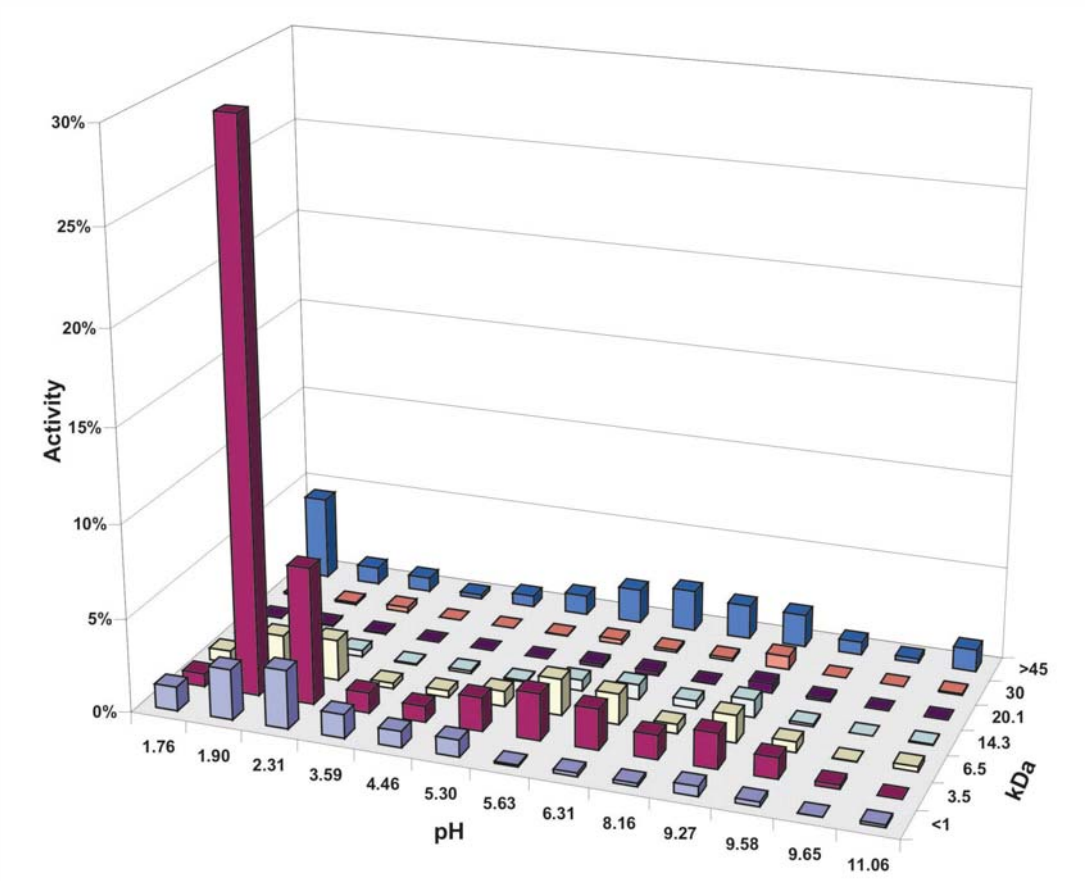

Figure 28 Plot of 15% 2D SDS-PAGE of ^{234}Th(IV) for polysaccharide enriched fraction extracted from marine bacteria *S. stellata* particulate.

For marine bacteria sample *S. stellata*, a combined 37% of total ^{234}Th(IV) activity was associated EPS around 3.5 kDa at pH 1.90 and 2.31 (Figure 28, Table 30). This was corroborated from the IEF plot (Figure 23a, Table 24), although the IEF plot had a combined total of 47% for the same pH regions. Once again, after further inspection, the sum of the ^{234}Th activity for the pH 1.99 and 2.31 (from 2D SDS-PAGE) was 50%. Evidently, for *Sagittula stellata*, at an approximate pH of 2, 37% of the total ^{234}Th(IV) activity was associated the organic matter in the molecular weight category of 3.5 kDa in size range.

For prymnesiophyte sample *E. huxleyi*, a combined 27% of total ^{234}Th(IV) activity was associated EPS around 14.3 kDa for pH between 1.68 and 3.94 averaging out to a pH of 2.56 (Figure 29, Table 32). This was corroborated from the IEF plot (Figure 24a, Table 25) although the IEF plot had a combined total of 50% for the same pH range. Once again, the sum of the ^{234}Th(IV) activity for the pH 1.99 and 2.31 (from 2D SDS-PAGE) was 50%. For phytoplankton *E. huxleyi*, at approximately pH of 2.5, 27% of the total ^{234}Th(IV) activity was associated with the organic matter in the molecular weight category of 14.3 kDa in size range.

For cyanobacteria sample *S. elongatus*, a combined 17% of total ^{234}Th(IV) activity was associated EPS ranging from 1 to 6.5 kDa (average of 3.7 kDa) for pH 1.85 (Figure 30, Table 34). This was corroborated from the IEF plot (Figure 25a, Table 26) although the IEF plot had a combined total of 32.3% for same pH range. Once again, the sum of the ^{234}Th(IV) activity for the pH 1.85 (from 2D SDS-PAGE) was 46%. For phytoplankton *S. elongatus*, at approximately pH of 1.85, 17% of the total

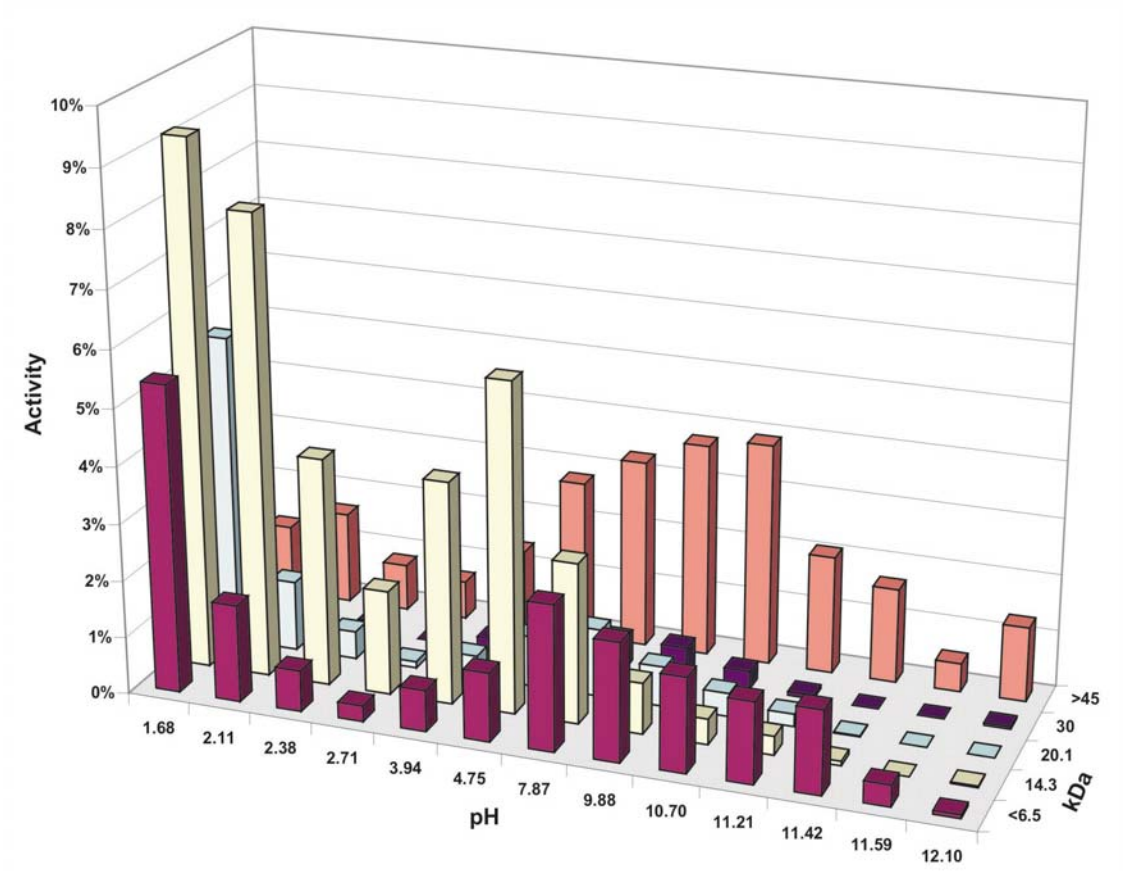

Figure 29 Plot of 15% 2D SDS-PAGE of ^{234}Th(IV) for polysaccharide enriched fraction extracted from phytoplankton *E. huxleyi* particulate.

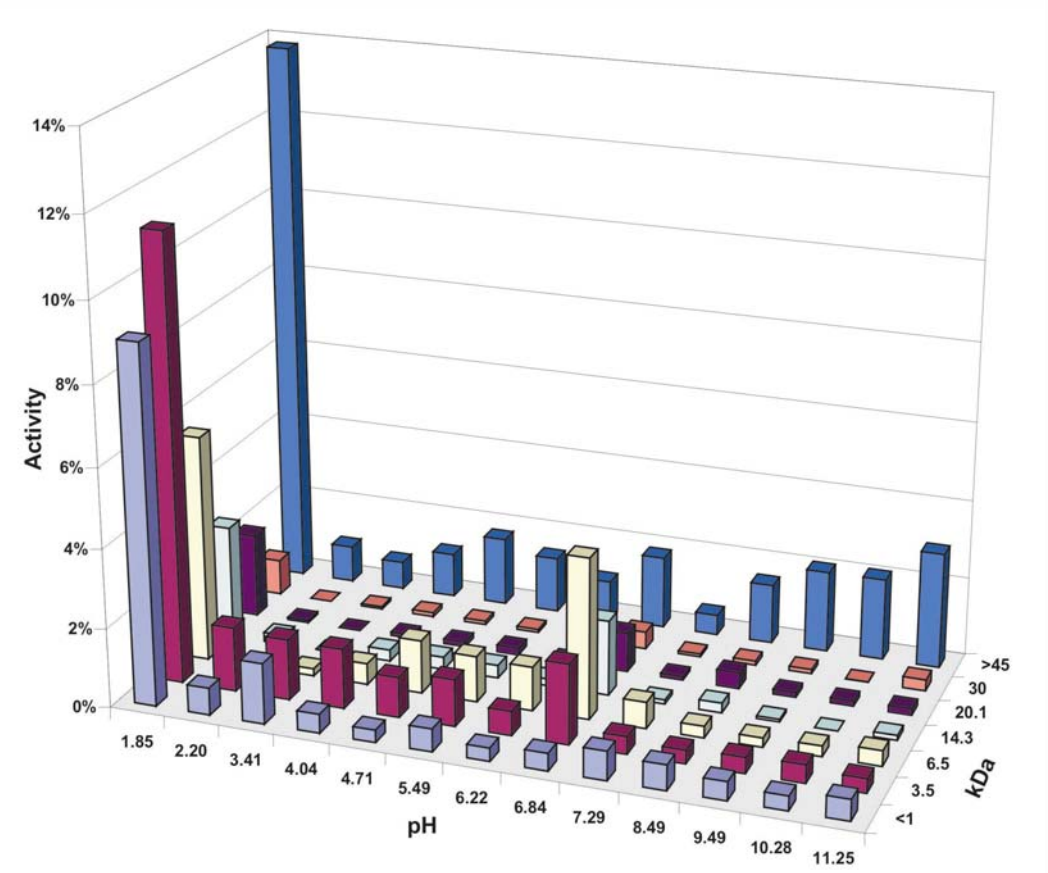

Figure 30 Plot of 15% 2D SDS-PAGE of ^{234}Th(IV) for polysaccharide enriched fraction extracted from phytoplankton *S. elongatus* particulate.

^{234}Th(IV) activity was associated with the organic matter in the molecular weight category less than 3 kDa in size range. In this case, there was another peak above 45kDa size accounting for ~14% total ^{234}Th(IV) activity. When this material was run again on a gradient (8-18%) SDS-PAGE instead of typical 15% homogenous SDS-PAGE, a large portion of the activity was associated with material above 160 kDa size range. This indicated that the material associated with ^{234}Th(IV) activity may be a breakdown products of a larger macromolecule.

IV.3.1 Carboxylic Acid Functional Group - ^{14}C

2D SDS-PAGE (15%) was performed on all samples to map out the activity associated with the methylated-^{14}C corresponding to carboxylic acid functional group (only *R. gallaeciensis* shown Figure 31, Table 38). The only reason for conducting 2D SDS-PAGE on carboxylic acid functional group for ^{14}C-dimethylated amine was to correct for the dimethylamine peak (pKa = 10.9, Mol. Weight = 33 amu). Every attempt was made to dialyze unwanted salts and unreacted dimethyl amine from organic material (III.3.2). However, there was an anomaly in initial isoelectric focusing profiles where a significant amount of ^{14}C activity was in the basic region. When the Suwannee River humic acid standard was run, there was no activity in the high pH region, primarily due to excess starting material or scarcity of radiolabel. Since the amount of marine sample was reduced 4 fold, there may have been excess reactant (radiolabel), even though the

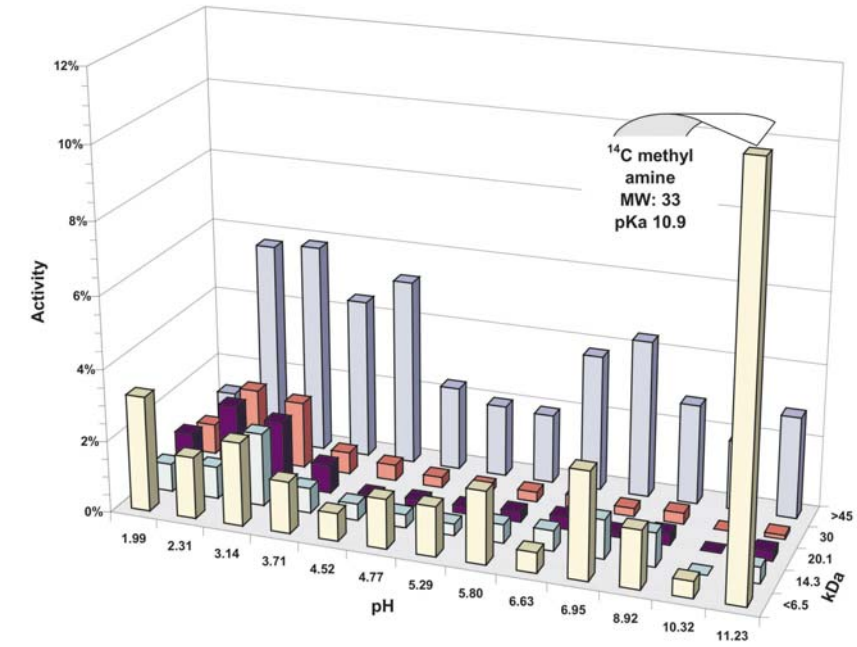

a

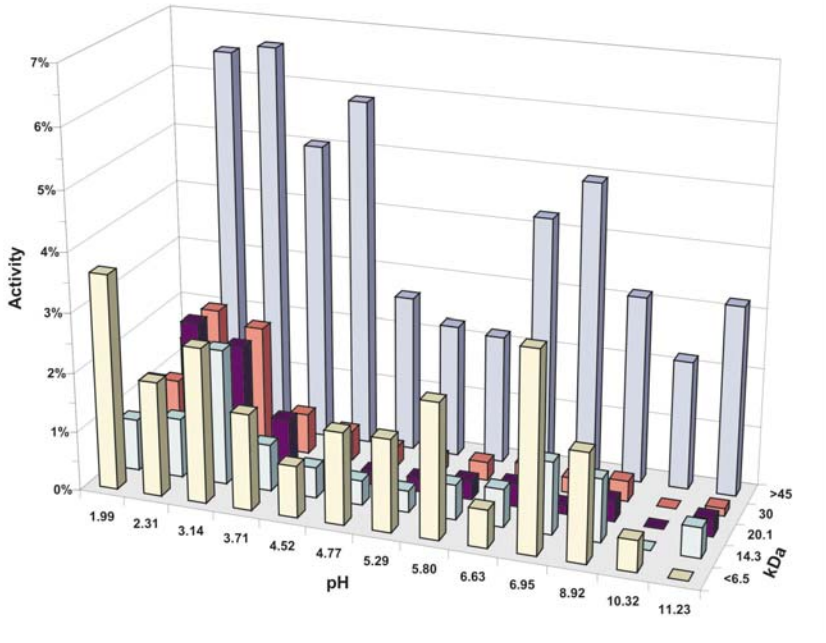

b

Figure 31 Plot of 15% 2D SDS-PAGE of ^{14}C-methylamine labeling 1% of COOH functional group a) with $^{14}CH_3NH_2$ peak and b) without $^{14}CH_3NH_2$ peak for polysaccharide enriched fraction extracted from marine bacteria *R. gallaeciensis* particulate.

procedure was scaled down accordingly. The IEF profile obtained from the 2D SDS-PAGE of carboxylic acid functional group was corrected for the peak associated with $(^{14}CH_3)_2NH$ at a pH near 10.9 less than 1kDa size.

IV.4. Statistical Analysis

Statistical analysis was conducted using SPSS software (SPSS Inc., Chicago, IL 60606) 2-tailed, bivariate correlation (α = 0.05) after testing for normality using Kolmogorov-Smirnov test. All data resulted in being parametric indicating that any correlations having a p-value at or below 0.05 were selected to be significant.

The null hypothesis (H_o) states that there is no change that occurs. Our null hypotheses were stipulated for the analysis of the IEF spectra (section I.5.1) as follows:

H_{o1} ^{234}Th(IV) will have no correlation with acidic functional groups for all samples
H_{o2} Carboxylic Acid functional group has no correlation with ^{234}Th(IV) for all samples
H_{o3} Phosphate functional group has no correlation with ^{234}Th(IV) for all samples
H_{o4} Sulphate functional group has no correlation with ^{234}Th(IV) for all samples

A p-value indicates the probability of the hypothesis being tested (usually H_o) is true (a p-value of 0.01 indicates there is a 1% chance that the hypothesis being tested is true). With critical level for rejection (α) of a hypothesis set at 0.05, the null hypothesis (H_o) is rejected with any p-value smaller than 0.05. Thus, the smaller the p-value the more confident one can be with my conclusions regarding the rejection of the null hypotheses and acceptance of alternative hypotheses (Dytham, 1999).

IV.4.1 Comparison of IEF Results

Bivariate correlation analysis was conducted for each species. All samples (*R. gallaeciensis*, *S. stellata*, *E. huxleyi*, *S. elongatus*, and GOM St4 72m, Tables 6, 7, 8, 9, and 10, respectively) displayed significant correlation between the IEF spectrum of ^{234}Th(IV) over the whole pH range for the one-dimensional isoelectric focusing (^{234}Th(IV) IEF) in addition to the IEF obtained from the sum of the parts from 2D SDS-PAGE (r=0.674, p=0.011; r=0.818, p=0.001; r=0.997, p=0.000; r=0.870, p=0.000; r=0.684, p=0.010, respectively). This allowed us to extend our range for finding correlations by allowing us to use both IEF and IEF from 2D SDS-PAGE as parameters. No significant correlation was observed for incubated ^{234}Th(IV) for all samples over the whole pH range, likely because of the presence of extraneous ligands.

The IEF spectrum of ^{234}Th(IV) of EPS from bacterial *R. gallaeciensis* (Table 6) correlated over the whole pH range with COOH and PO_4 (r=0.630, p=0.021 and r=0.634, p=0.020, respectively). In the acidic region (pH <7) *R. gallaeciensis* ^{234}Th(IV) IEF and ^{234}Th(IV) IEF from 2D SDS-PAGE correlated nicely with the incubated ^{234}Th(IV) IEF from 2D SDS-PAGE (r=0.867, p=0.005 and r=0.779, p=0.023, respectively) and PO_4 IEF (r=0.964, p=0.000 and r=0.740, p=0.036, respectively). The IEF spectrum of ^{234}Th(IV) of EPS from *S. stellata* did not correlate over the whole pH range with any of the set parameters (^{32}P, ^{35}S, COOH from 2D SDS-PAGE, PO_4, and SO_4) (all p-values >0.05, respectively).

Table 6 Bivariate correlation analysis for isoelectric focusing of radionuclides, carboxylic acid, phosphate and sulphate functional groups for *R. gallaeciensis.*

			IEF ^{234}Th(IV)	PAGE ^{234}Th(IV)	Incubation IEF ^{234}Th(IV)	Incubation IEF $^{32}PO_4$	Incubation IEF $^{35}SO_4$	COOH IEF from 2D SDS-PAGE	Ion Chromatography PO_4	Ion Chromatography SO_4	N=
	Data are normal		yes	yes	yes	yes	yes	yes	yes	yes	
whole range	**^{234}Th(IV) IEF Correlation**	r=	1.000	0.674*	0.323	*-0.495*	-0.071	0.630*	0.340	-0.193	13
		p=	-	0.011	0.281	*0.085*	0.818	0.021	0.255	0.527	
	^{234}Th(IV) IEF from 2D-SDS PAGE Correlation	r=	0.674*	1.000	0.173	-0.309	-0.108	0.270	0.634*	-0.239	13
		p=	0.011	-	0.571	0.304	0.724	0.372	0.020	0.432	
	Incubated ^{234}Th(IV) IEF from 2D-SDS PAGE correlation	r=	0.323	0.173	1.000	0.069	0.135	0.354	0.325	-0.323	13
		p=	0.281	0.571	-	0.823	0.659	0.235	0.278	0.281	
Acidic	**^{234}Th(IV) IEF Correlation**	r=	1.000	0.541	0.867**	-0.267	0.319	*0.626*	0.475	0.218	8
		p=	-	0.166	0.005	0.523	0.441	*0.097*	0.234	0.604	
	^{234}Th(IV) IEF from 2D-SDS PAGE Correlation	r=	0.541	1.000	0.779*	0.199	0.255	0.099	0.964**	-0.101	8
		p=	0.166	-	0.023	0.637	0.543	0.815	0.000	0.813	
	Incubated ^{234}Th(IV) IEF from 2D-SDS PAGE correlation	r=	0.867	0.779	1.000	-0.129	0.283	0.457	0.740*	0.145	8
		p=	0.005	0.023	-	0.762	0.496	0.255	0.036	0.732	
Basic	**^{234}Th(IV) IEF Correlation**	r=	1.000	-0.053	0.112	-0.327	-0.720	-0.320	-0.262	-0.253	5
		p=	-	0.920	0.832	0.527	0.106	0.537	0.670	0.682	
	^{234}Th(IV) IEF from 2D-SDS PAGE Correlation	r=	-0.053	1.000	-0.301	*0.766*	0.362	0.575	-0.173	0.582	5
		p=	0.920	-	0.562	*0.076*	0.481	0.233	0.781	0.303	
	Incubated ^{234}Th(IV) IEF from 2D-SDS PAGE correlation	r=	0.112	-0.301	1.000	0.019	0.009	0.489	-0.010	-0.753	5
		p=	0.832	0.562	-	0.971	0.986	0.325	0.987	0.142	

* correlation significant at the 0.05 (2-tailed)
** correlation significant at the 0.01 (2-tailed)

Table 7 Bivariate correlation analysis for isoelectric focusing of radionuclides, carboxylic acid, phosphate and sulphate functional groups for *S. stellata.*

			IEF ^{234}Th(IV)	PAGE ^{234}Th(IV)	Incubation IEF ^{234}Th(IV)	Incubation IEF $^{32}PO_4$	Incubation IEF $^{35}SO_4$	COOH IEF from 2D SDS-PAGE	Ion Chromatography PO_4	Ion Chromatography SO_4	N=
	Data are normal		yes	yes	yes	yes	yes	yes	yes	yes	
whole range	**^{234}Th(IV) IEF Correlation**	r=	1.000	0.818**	0.050	-0.083	-0.429	0.119	0.043	-0.107	13
		p=	-	0.001	0.872	0.787	0.143	0.713	0.890	0.728	
	^{234}Th(IV) IEF from 2D-SDS PAGE Correlation	r=	0.818*	1.000	0.128	0.018	-0.329	0.231	-0.140	-0.007	13
		p=	0.001	-	0.676	0.954	0.272	0.470	0.649	0.983	
	Incubated ^{234}Th(IV) IEF from 2D-SDS PAGE correlation	r=	0.050	0.128	1.000	0.186	0.106	-0.019	-0.261	-0.036	13
		p=	0.872	0.676	-	0.543	0.731	0.952	0.390	0.907	
acidic	**^{234}Th(IV) IEF Correlation**	r=	1.000	0.785*	0.743*	0.337	-0.129	-0.017	0.172	0.079	8
		p=	-	0.021	0.035	0.415	0.761	0.968	0.684	0.853	
	^{234}Th(IV) IEF from 2D-SDS PAGE Correlation	r=	0.785*	1.000	*0.652*	0.522	0.122	0.138	-0.090	0.290	8
		p=	0.021	-	*0.080*	0.185	0.774	0.745	0.832	0.485	
	Incubated ^{234}Th(IV) IEF from 2D-SDS PAGE correlation	r=	0.743*	*0.652*	1.000	*0.631*	-0.248	0.336	0.027	0.322	8
		p=	0.035	*0.080*	-	*0.094*	-0.248	0.336	0.950	0.437	
basic	**^{234}Th(IV) IEF Correlation**	r=	1.000	0.716	-0.370	-0.148	-0.233	-0.714	-0.520	-0.182	5
		p=	-	0.174	0.540	0.812	0.706	0.286	0.369	0.770	
	^{234}Th(IV) IEF from 2D-SDS PAGE Correlation	r=	0.716	1.000	0.223	-0.575	-0.556	-0.446	-0.660	*-0.809*	5
		p=	0.174	-	0.718	0.311	0.330	0.554	0.225	*0.097*	
	Incubated ^{234}Th(IV) IEF from 2D-SDS PAGE correlation	r=	-0.370	0.223	1.000	-0.617	-0.734	-0.199	-0.463	-0.699	5
		p=	0.540	0.718	-	0.267	0.158	0.801	0.432	0.189	

* Correlation significant at the 0.05 (2-tailed)

** Correlation significant at the 0.01 (2-tailed)

However, in the acidic region (pH <7), the IEF spectrum of ^{234}Th(IV) of EPS from *S. stellata* (Table 7), ^{234}Th(IV) IEF correlated nicely with that from 2D SDS-PAGE and incubated ^{234}Th(IV) IEF from 2D SDS-PAGE only (r=0.785, p=0.021 and r=0.743, p=0.035, respectively). No other correlations were apparent with any other parameters.

The IEF spectrum of ^{234}Th(IV) of EPS from phytoplankton *E. huxleyi* (Table 10) ^{234}Th(IV) and that from 2D SDS-PAGE correlated over the whole pH range with COOH from 2D SDS-PAGE only (r=0.715, p=0.003 and r=0.751, p=0.006, respectively). The IEF spectrum of ^{234}Th(IV) of EPS from *E. huxleyi* that had incubated ^{234}Th(IV) in the 2D SDS-PAGE spectrum correlated with $^{35}SO_4^{2-}$ spectrum (r=0.646, p=0.017). In the acidic region (pH <7), the IEF spectrum of ^{234}Th(IV) of EPS from *E. huxleyi* ^{234}Th(IV) and that from 2D SDS-PAGE correlated significantly with the spectrum of COOH from 2D SDS-PAGE (r=0.793, p=0.019 and r=0.772, p=0.025, respectively). The ^{234}Th(IV) IEF spectrum and that from 2D SDS-PAGE may have some association with $^{35}SO_4^{2-}$ IEF spectrum, but p-values did not make critical level cutoff of α=0.05 (r=0.629, p=0.095 and r=0.655, p=0.078, respectively). The IEF spectrum of ^{234}Th(IV) of EPS from cyanobacteria *S. elongatus* (Table 11) and that from 2D SDS-PAGE correlated over the acidic pH range with $^{32}PO_4^{2-}$ IEF spectrum (r=0.773, p=0.042 and r=0.979, p=0.032, respectively), COOH IEF spectrum from 2D SDS-PAGE (r=0.801, p=0.030 and r=0.951, p=0.001, respectively) and SO_4^{2-} IEF spectrum (r=0.863, p=0.012 and r=0.962, p=0.001, respectively).

able 8 Bivariate correlation analysis for isoelectric focusing of radionuclides, carboxylic acid, phosphate and sulphate functional groups for *E. huxleyi.*

			IEF ^{234}Th(IV)	PAGE ^{234}Th(IV)	Incubation IEF ^{234}Th(IV)	Incubation IEF $^{32}PO_4$	Incubation IEF $^{35}SO_4$	COOH IEF from 2D SDS-PAGE	Ion Chromatography IEF PO_4	Ion Chromatography IEF SO_4	N=
	Data are normal		yes	yes	yes	yes	yes	yes	yes	yes	
whole range	**^{234}Th(IV) IEF Correlation**	r=	1.000	0.997**	-0.030	-0.375	0.009	0.751**	-0.246	-0.131	13
		p=	-	0.000	0.923	0.207	0.976	0.003	0.418	0.670	
	^{234}Th(IV) IEF from 2D-SDS PAGE Correlation	r=	0.997**	1.000	-0.046	-0.414	0.014	0.715**	-0.221	-0.096	13
		p=	0.000	-	0.882	0.160	0.964	0.006	0.468	0.755	
	Incubated ^{234}Th(IV) IEF from 2D-SDS PAGE correlation	r=	-0.030	-0.046	1.000	*0.489*	0.646*	0.132	-0.389	0.473	13
		p=	0.923	0.882	-	*0.090*	0.017	0.668	0.189	0.102	
acidic	**^{234}Th(IV) IEF Correlation**	r=	1.000	0.998**	0.369	-0.363	*0.629*	0.793*	-0.383	0.044	8
		p=	-	0.000	0.369	0.377	*0.095*	0.019	0.349	0.918	
	^{234}Th(IV) IEF from 2D-SDS PAGE Correlation	r=	0.998**	1.000	0.339	-0.386	*0.655*	0.772*	-0.376	0.071	8
		p=	0.000	-	0.412	0.345	*0.078*	0.025	0.359	0.867	
	Incubated ^{234}Th(IV) IEF from 2D-SDS PAGE correlation	r=	0.369	0.339	1.000	0.097	0.200	*0.653*	-0.424	0.147	8
		p=	0.369	0.412	-	0.819	0.635	*0.079*	0.295	0.729	
basic	**^{234}Th(IV) IEF Correlation**	r=	1.000	*0.808*	0.972**	0.419	0.276	-0.413	-0.627	0.088	5
		p=	-	*0.098*	0.006	0.482	0.653	0.490	0.257	0.888	
	^{234}Th(IV) IEF from 2D-SDS PAGE Correlation	r=	*0.808*	1.000	0.894*	-0.125	0.394	*-0.817*	-0.121	0.658	5
		p=	*0.098*	-	0.041	0.841	0.511	*0.091*	0.846	0.227	
	Incubated ^{234}Th(IV) IEF from 2D-SDS PAGE correlation	r=	0.972**	0.894*	1.000	0.199	0.224	-0.496	-0.536	0.276	5
		p=	0.006	0.041	-	0.749	0.717	0.396	0.351	0.653	

* Correlation significant at the 0.05 (2-tailed)
** Correlation significant at the 0.01 (2-tailed)

Table 9 Bivariate correlation analysis for isoelectric focusing of radionuclides, carboxylic acid, phosphate and sulphate functional groups for *S. elongatus.*

			IEF ^{234}Th(IV)	PAGE ^{234}Th(IV)	Incubation IEF ^{234}Th(IV)	Incubation IEF $^{32}PO_4$	Incubation IEF $^{35}SO_4$	COOH IEF from 2D SDS-PAGE	Ion Chromatography PO_4	Ion Chromatography SO_4	N=
	Data are normal		yes	yes	yes	yes	yes	yes	yes	yes	
whole range	**^{234}Th(IV) IEF Correlation**	r=	1.000	0.870**	*-0.484*	0.153	-0.304	0.049	-0.362	0.072	13
		p=	-	0.000	*0.094*	0.617	0.313	0.874	0.225	0.816	
	^{234}Th(IV) IEF from 2D-SDS PAGE Correlation	r=	0.870**	1.000	-0.410	0.416	-0.125	0.290	-0.178	0.373	13
		p=	0.000	-	0.164	0.158	0.684	0.337	0.561	0.209	
	Incubated ^{234}Th(IV) IEF from 2D-SDS PAGE correlation	r=	*-0.484*	-0.410	1.000	0.178	0.373	0.317	0.093	0.048	13
		p=	*0.094*	0.164	-	0.560	0.209	0.291	0.762	0.877	
acidic	**^{234}Th(IV) IEF Correlation**	r=	1.000	0.914**	-0.294	0.773*	0.581	0.801*	-0.278	0.863*	8
		p=	-	0.004	0.522	0.042	0.171	0.030	0.546	0.012	
	^{234}Th(IV) IEF from 2D-SDS PAGE Correlation	r=	0.914	1.000	-0.377	0.979	0.265	0.951**	-0.089	0.962**	8
		p=	0.004	-	0.404	0.032	0.566	0.001	0.850	0.001	
	Incubated ^{234}Th(IV) IEF from 2D-SDS PAGE correlation	r=	-0.294	-0.377	1.000	-0.415	-0.153	-0.262	0.119	-0.421	8
		p=	0.522	0.404	-	0.355	0.743	0.570	0.800	0.346	
basic	**^{234}Th(IV) IEF Correlation**	r=	1.000	0.954	-0.820	-0.514	-0.664	-0.252	-0.392	-0.546	5
		p=	-	0.003	0.046	0.297	0.151	0.631	0.442	0.263	
	^{234}Th(IV) IEF from 2D-SDS PAGE Correlation	r=	0.954	1.000	-0.644	-0.286	-0.513	0.007	-0.458	-0.494	5
		p=	0.003	-	0.168	0.583	0.298	0.989	0.361	0.319	
	Incubated ^{234}Th(IV) IEF from 2D-SDS PAGE correlation	r=	-0.820	-0.644	1.000	0.882	0.698	0.687	-0.031	0.383	5
		p=	0.046	0.168	-	0.020	0.123	0.131	0.953	0.453	

* Correlation significant at the 0.05 (2-tailed)

** Correlation significant at the 0.01 (2-tailed)

Table 10 Bivariate correlation analysis for isoelectric focusing of radionuclides, carboxylic acid, phosphate and sulphate functional groups for *E. huxleyi.*

			IEF ^{234}Th(IV)	PAGE ^{234}Th(IV)	Incubation IEF ^{234}Th(IV)	Incubation IEF $^{32}PO_4$	Incubation IEF $^{35}SO_4$	COOH IEF from 2D SDS-PAGE	Ion Chromatography IEF PO_4	Ion Chromatography IEF SO_4	N=
	Data are normal		yes	yes	yes	yes	yes	yes	yes	yes	
whole range	**^{234}Th(IV) IEF Correlation**	r=	1.000	0.997**	-0.030	-0.375	0.009	0.751**	-0.246	-0.131	13
		p=	-	0.000	0.923	0.207	0.976	0.003	0.418	0.670	
	^{234}Th(IV) IEF from 2D-SDS PAGE Correlation	r=	0.997**	1.000	-0.046	-0.414	0.014	0.715**	-0.221	-0.096	13
		p=	0.000	-	0.882	0.160	0.964	0.006	0.468	0.755	
	Incubated ^{234}Th(IV) IEF from 2D-SDS PAGE correlation	r=	-0.030	-0.046	1.000	*0.489*	0.646*	0.132	-0.389	0.473	13
		p=	0.923	0.882	-	*0.090*	0.017	0.668	0.189	0.102	
acidic	**^{234}Th(IV) IEF Correlation**	r=	1.000	0.998**	0.369	-0.363	*0.629*	0.793*	-0.383	0.044	8
		p=	-	0.000	0.369	0.377	*0.095*	0.019	0.349	0.918	
	^{234}Th(IV) IEF from 2D-SDS PAGE Correlation	r=	0.998**	1.000	0.339	-0.386	*0.655*	0.772*	-0.376	0.071	8
		p=	0.000	-	0.412	0.345	*0.078*	0.025	0.359	0.867	
	Incubated ^{234}Th(IV) IEF from 2D-SDS PAGE correlation	r=	0.369	0.339	1.000	0.097	0.200	*0.653*	-0.424	0.147	8
		p=	0.369	0.412	-	0.819	0.635	*0.079*	0.295	0.729	
basic	**^{234}Th(IV) IEF Correlation**	r=	1.000	*0.808*	0.972**	0.419	0.276	-0.413	-0.627	0.088	5
		p=	-	*0.098*	0.006	0.482	0.653	0.490	0.257	0.888	
	^{234}Th(IV) IEF from 2D-SDS PAGE Correlation	r=	*0.808*	1.000	0.894*	-0.125	0.394	*-0.817*	-0.121	0.658	5
		p=	*0.098*	-	0.041	0.841	0.511	*0.091*	0.846	0.227	
	Incubated ^{234}Th(IV) IEF from 2D-SDS PAGE correlation	r=	0.972**	0.894*	1.000	0.199	0.224	-0.496	-0.536	0.276	5
		p=	0.006	0.041	-	0.749	0.717	0.396	0.351	0.653	

* Correlation significant at the 0.05 (2-tailed)

** Correlation significant at the 0.01 (2-tailed)

Table 11 Bivariate correlation analysis for isoelectric focusing of radionuclides, carboxylic acid, phosphate and sulphate functional groups for *S. elongatus.*

			IEF ^{234}Th(IV)	PAGE ^{234}Th(IV)	Incubation IEF ^{234}Th(IV)	Incubation IEF $^{32}PO_4$	Incubation IEF $^{35}SO_4$	COOH IEF from 2D SDS-PAGE	Ion Chromatography PO_4	Ion Chromatography SO_4	N=
	Data are normal		yes	yes	yes	yes	yes	yes	yes	yes	
whole range	**^{234}Th(IV) IEF Correlation**	r=	1.000	0.870**	*-0.484*	0.153	-0.304	0.049	-0.362	0.072	13
		p=	-	0.000	*0.094*	0.617	0.313	0.874	0.225	0.816	
	^{234}Th(IV) IEF from 2D-SDS PAGE Correlation	r=	0.870**	1.000	-0.410	0.416	-0.125	0.290	-0.178	0.373	13
		p=	0.000	-	0.164	0.158	0.684	0.337	0.561	0.209	
	Incubated ^{234}Th(IV) IEF from 2D-SDS PAGE correlation	r=	*-0.484*	-0.410	1.000	0.178	0.373	0.317	0.093	0.048	13
		p=	*0.094*	0.164	-	0.560	0.209	0.291	0.762	0.877	
acidic	**^{234}Th(IV) IEF Correlation**	r=	1.000	0.914**	-0.294	0.773*	0.581	0.801*	-0.278	0.863*	8
		p=	-	0.004	0.522	0.042	0.171	0.030	0.546	0.012	
	^{234}Th(IV) IEF from 2D-SDS PAGE Correlation	r=	0.914	1.000	-0.377	0.979	0.265	0.951**	-0.089	0.962**	8
		p=	0.004	-	0.404	0.032	0.566	0.001	0.850	0.001	
	Incubated ^{234}Th(IV) IEF from 2D-SDS PAGE correlation	r=	-0.294	-0.377	1.000	-0.415	-0.153	-0.262	0.119	-0.421	8
		p=	0.522	0.404	-	0.355	0.743	0.570	0.800	0.346	
basic	**^{234}Th(IV) IEF Correlation**	r=	1.000	0.954	-0.820	-0.514	-0.664	-0.252	-0.392	-0.546	5
		p=	-	0.003	0.046	0.297	0.151	0.631	0.442	0.263	
	^{234}Th(IV) IEF from 2D-SDS PAGE Correlation	r=	0.954	1.000	-0.644	-0.286	-0.513	0.007	-0.458	-0.494	5
		p=	0.003	-	0.168	0.583	0.298	0.989	0.361	0.319	
	Incubated ^{234}Th(IV) IEF from 2D-SDS PAGE correlation	r=	-0.820	-0.644	1.000	0.882	0.698	0.687	-0.031	0.383	5
		p=	0.046	0.168	-	0.020	0.123	0.131	0.953	0.453	

* Correlation significant at the 0.05 (2-tailed)

** Correlation significant at the 0.01 (2-tailed)

Table 12 Bivariate correlation analysis for isoelectric focusing of radionuclides, carboxylic acid, phosphate and sulphate functional groups for Gulf of México sample Station 6 at 72m depth (chlorophyll a maxima).

			IEF ^{234}Th(IV)	PAGE ^{234}Th(IV)	COOH IEF	COOH IEF from 2D SDS-PAGE	Ion Chromatography PO_4	Ion Chromatography SO_4	N=
	Data are normal		yes	yes	yes	yes	yes	yes	
whole range	**^{234}Th(IV) IEF Correlation**	r=	1.000	0.684**	0.356	0.405	0.310	0.162	13
		p=	-	0.010	0.233	0.169	0.303	0.597	
	^{234}Th(IV) IEF from 2D-SDS PAGE Correlation	r=	0.684**	1.000	0.511	0.717**	0.296	0.054	13
		p=	0.010	-	0.075	0.006	0.325	0.861	
	^{14}COOH IEF from 2D-SDS PAGE Correlation	r=	0.356	0.511	1.000	0.534	-0.100	0.655*	13
		p=	0.233	0.075	-	0.060	0.746	0.015	
acidic	**^{234}Th(IV) IEF Correlation**	r=	1.000	0.609	0.681*	0.391	0.118	0.851**	9
		p=	-	0.082	0.043	0.300	0.762	0.004	
	^{234}Th(IV) IEF from 2D-SDS PAGE Correlation	r=	0.609	1.000	0.967**	0.920**	0.069	0.869**	9
		p=	0.082	-	0.000	0.000	0.861	0.002	
	^{14}COOH IEF from 2D-SDS PAGE Correlation	r=	0.681*	0.967**	1.000	0.859**	0.137	0.932**	9
		p=	0.043	0.000	-	0.003	0.724	0.000	
basic	**^{234}Th(IV) IEF Correlation**	r=	1.000	0.258	-0.955*	-0.326	0.662	-0.181	4
		p=	-	0.742	0.045	0.674	0.338	0.819	
	^{234}Th(IV) IEF from 2D-SDS PAGE Correlation	r=	0.258	1.000	-0.532	-0.454	0.718	-0.936	4
		p=	0.742	-	0.468	0.546	0.282	0.064	
	^{14}COOH IEF from 2D-SDS PAGE Correlation	r=	-0.955*	-0.532	1.000	0.438	-0.792	0.451	4
		p=	0.045	0.468	-	0.562	0.208	0.549	

* Correlation significant at the 0.05 (2-tailed)

** Correlation significant at the 0.01 (2-tail)

The GOM Station 4-72m colloidal sample (Table 12) showed significant correlations over the whole pH range between ^{234}Th(IV) IEF from 2D SDS-PAGE and COOH IEF from 2D SDS-PAGE (r=0.717, p=0.006). Moreover, the COOH IEF spectrum from 2D SDS-PAGE correlated with SO_4 IEF spectrum (r=0.655, p=0.015), thus indicating there may some link between ^{234}Th(IV) and SO_4^{2-}, by association. Over the acidic region, the ^{234}Th(IV) IEF spectrum correlated with that of COOH IEF (r=0.681, p=0.043) and SO_4^{2-} IEF (r=0.851, p=0.004) providing evidence that ^{234}Th(IV) was associated with SO_4^{2-}. In addition, there were also significant correlations between ^{234}Th(IV) IEF from 2D SDS-PAGE with COOH IEF (r=0.967, p=0.000), COOH IEF from 2D SDS-PAGE (r=0.920, p=0.000) and SO_4^{2-} IEF (r=0.869, p=0.002). Also the COOH IEF spectrum from 2D SDS-PAGE correlated significantly with that of SO_4^{2-} IEF (r=0.932, p=0.000)

IV.5. Composition of Thorium Binding Organic Material

Bulk particulate organic material was extracted from the surface of marine bacteria and phytoplankton using extraction procedure developed by Staats *et al.* (1999) by minimizing cell lysis. The organic matter fraction associated with ^{234}Th(IV) was determined (via 2D SDS-PAGE) and isolated with mass yields of 2% and 1% for *S. stellata* and *S. elongatus*, respectively (Table 13). The final stage was to further characterize specific sub-fraction of colloidal organic matter. This task was performed by analyzing for dissolved organic carbon (DOC), total polysaccharide (TPCHO), uronic acid content (URA), total protein, and carbohydrate composition via gas chromatography-mass spectrometry (GC-MS).

Table 13 Mass yields of purified EPS, via 2D SDS-PAGE, of material associated with ^{234}Th(IV).

Sample	Initial Mass (mg)	Final Mass (mg)	% recovery
R. gallaeciensis	200.0	N/A	N/A
S. stellata	91.3	1.9	2.1%
E. huxleyi	231.9	N/A	N/A
S. elongatus	89.7	1.1	1.2%

IV.5.1 Determination of Total Carbohydrates, Uronic Acid,

Acidic Polysaccharides and Protein

Santschi *et al.*, (1995) conceptualized the notion of distribution of binding sites on organic matter (OM) to be about 1 meq/g-OM and determined the ratio of trace metal versus binding site. That is, for every five polysaccharide monomers, there was one functional group that will have an association with a trace metal (see Figure 7 or 8). According to Hung *et al.* (2003b), approximately 1-3% of total carbon is acid polysaccharide carbon (APS-C) in particulate or dissolved fraction, and POC and COC concentrations are 0.1μM-C and 20 μM, respectively. Thus, 1% to 3% of POC and COC yields 1 to 200 nM of APS-C in the particulate or dissolved fraction. If total thorium (^{232}Th) concentration was compared to the total concentration of acidic binding sites APS-C (i.e., 47 X 10^{-15}:1 – 200 X 10^{-9}), then this results in 1 thorium ion for every ~20,000 to 42,000,000 acidic binding sites respectively. This concept may have to be reconsidered as a result of this dissertation. The results from this dissertation indicate that for every 106 and 51 carbon atoms there is 1 phosphate functional group for *S.*

stellata and *S. elongatus*, respectively. For every 32 and 8 carbon atoms there is 1 sulphate functional group for *S. stellata* and *S. elongatus*, respectively. (Table 14). Another interpretation of this data is there are approximately 17 and 8 six carbon sugar monomers for every phosphate functional group for *S. stellata* and *S. elongatus*, respectively; and 5 and 1 six carbon sugar monomers for every sulphate functional group for *S. stellata* and *S. elongatus*, respectively. This observation provides additional evidence of steric enhancement effect or chelation.

Table 14 Carbon to phosphate and sulphate ratios for IEF.

	pH	**Mass of OM (mg)**	**% OM in ^{234}Th(IV) fraction**	**OM associated with ^{234}Th(IV) fraction (mg)**	**Moles of C (n-C)**	**C:PO_4**	**C:SO_4**
S. stellata	1.90	0.5011	2.1	0.0105	8.8E-07	106	32
S. elongatus	1.85	0.4045	1.2	0.0049	4.0E-07	51	8

The total polysaccharide content of *S. stellata* and *S. elongatus* was only 14.3% and 7.9% of total carbon content. Approximately 5.4% and 87.1% of *S. stellata* and *S. elongatus*' total polysaccharide content, respectively, was composed of uronic acids. The results for *S. elongatus* should be looked upon with caution, since the coloration of the reaction was darker than the coloration of the calibration curve. The protein concentrations accounted for 2.6% and 6.2% of total carbon for *S. stellata* and *S. elongatus*, respectively (Table 15, Figure 32).

Table 15 Dissolved organic carbon, total polysaccharide, and uronic acid content for marine bacteria and phytoplankton.

Sample	T-PCHO (% of Total DOC)	URA (% of Total DOC)	Protein (% of Total DOC)	DOC (μM-C)
S. stellata	14.3 %	0.77 %	2.6%	7647.9
S. elongatus	7.9 %	6.9 %	6.2%	7612.5

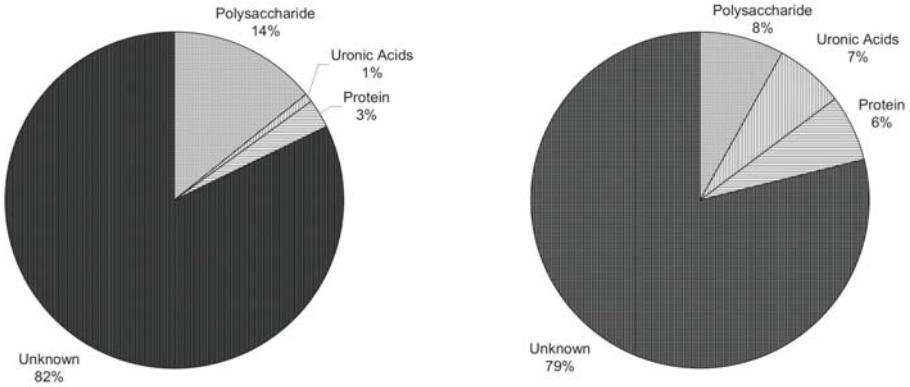

a) **b)**

Figure 32 Percent composition of uronic acids, proteins and total polysaccharides for a) *S. stellata* and b) *S. elongatus.*

Sample purity was determined by the ratio of absorption of sample solution at 260 nm and 280 nm wavelengths. If the solution does not have contamination with nucleic acids, then it would have an absorbance ratio (A_{260}:A_{280}) equal to or less than 0.6. Any value larger than this is consistent with nucleic acid contamination (Alvarado-Urbina, *person. commun.*). Thus, the amount of DNA in the *S. stellata* sample was negligible whereas the same cannot be said of *S. elongatus* (Table 16). This may be an indication that the extraction procedure used may have resulted in some cell lysis.

Table 16 DNA content for *S. stellata* and *S. elongatus.*

	Absorption [a]		Sample Purity
Sample	**280 nm**	**260 nm**	**260/280**
S. stellata	0.146	0.091	0.623
S. elongatus	0.104	0.198	1.904

[a] Absorption is blank corrected

IV.5.2 Carbohydrate Composition

The gas chromatography (GC) mass spectrometry (MS) provided secondary characterization of the organic material that was extracted from bacterial (Figure 33) and phytoplankton (Figure 34) cultures that complexed with ^{234}Th(IV). The majority of the organic material extracted from both microbial EPS samples showed galactose, glucose, mannose and xylose as the main simple sugar monomers for *S. stellata*. The principal simple sugars in *S. elongatus* are glucose, galactose, xylose and galactoglucuronic acid (Table 17). The determination of simple sugars was accomplished by comparing a collection of library of mass spectra to that of sample mass spectra at a specific retention time (Figure 35 to 51 in appendix V.7). The main difference between marine bacteria and phytoplankton gas chromatographs was the presence of galactoglucuronic acid (Figure 34b) in *S. elongatus* that was not present in *S. stellata* and the presence of mannose in *S. stellata* and not in *S. elongatus* (Figure 33b).

Table 17 Acid polysaccharides content from GC-MS of isolated EPS.

S. stellata				***S. elongatus***			
	Peak Area	**μM-C**	**% of DOC**		**Peak Area**	**μM-C**	**% of DOC**
mannose	110186	1.3	0.00018	**galactoglucuronic acid**	201146	7.0	0.09%
glucose	726211	8.9	0.00116	**glucose**	747339	26.0	0.34%
galactose	63990	0.8	0.0001	**galactose**	221659	7.7	0.10%
xylose	92451	1.1	0.00015	**xylose**	55848	1.9	0.03%
alditol	49147	0.6	7.8E-05	**alditol**	17274	0.6	0.01%
Total		12.7	0.00166	Total		43.2	0.56%

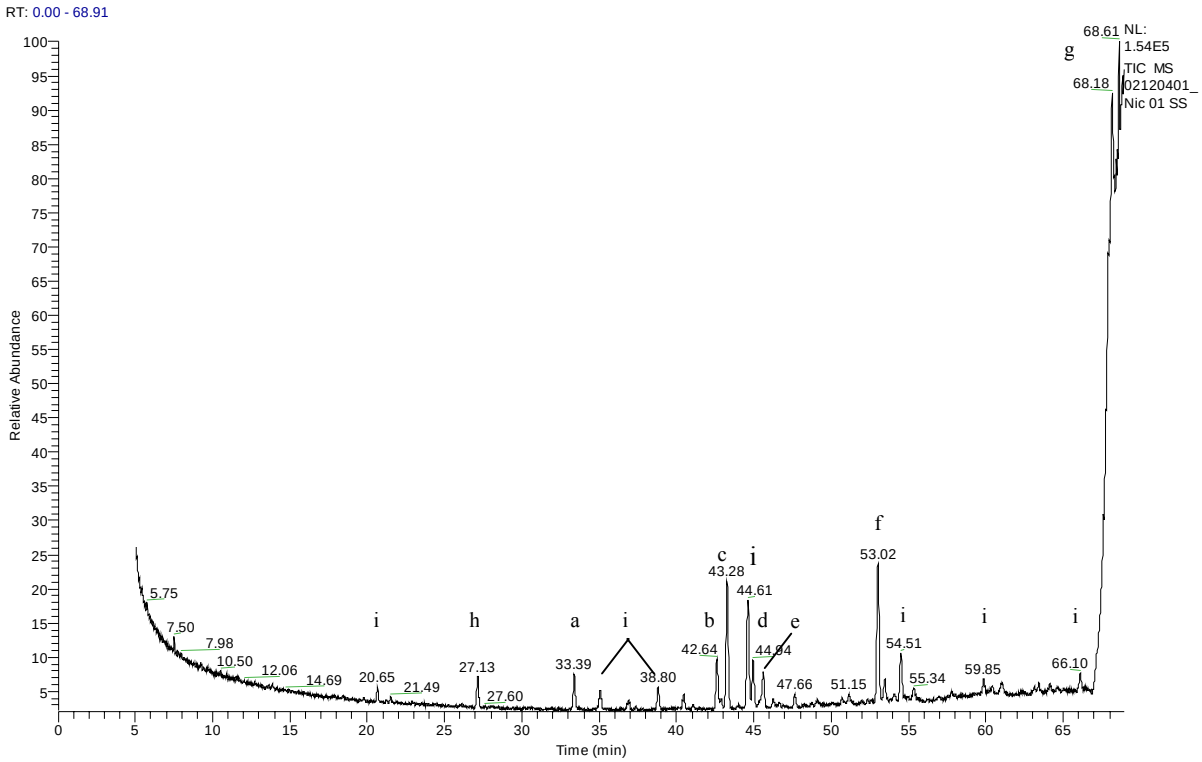

Figure 33 Gas Chromatograph of derivatized EPS from *S. stellata* where the following peaks have been identified; glucose (a, c, d, f); mannose (b); galactose (e); xylose (g); alditol (h); and unknown peaks (i).

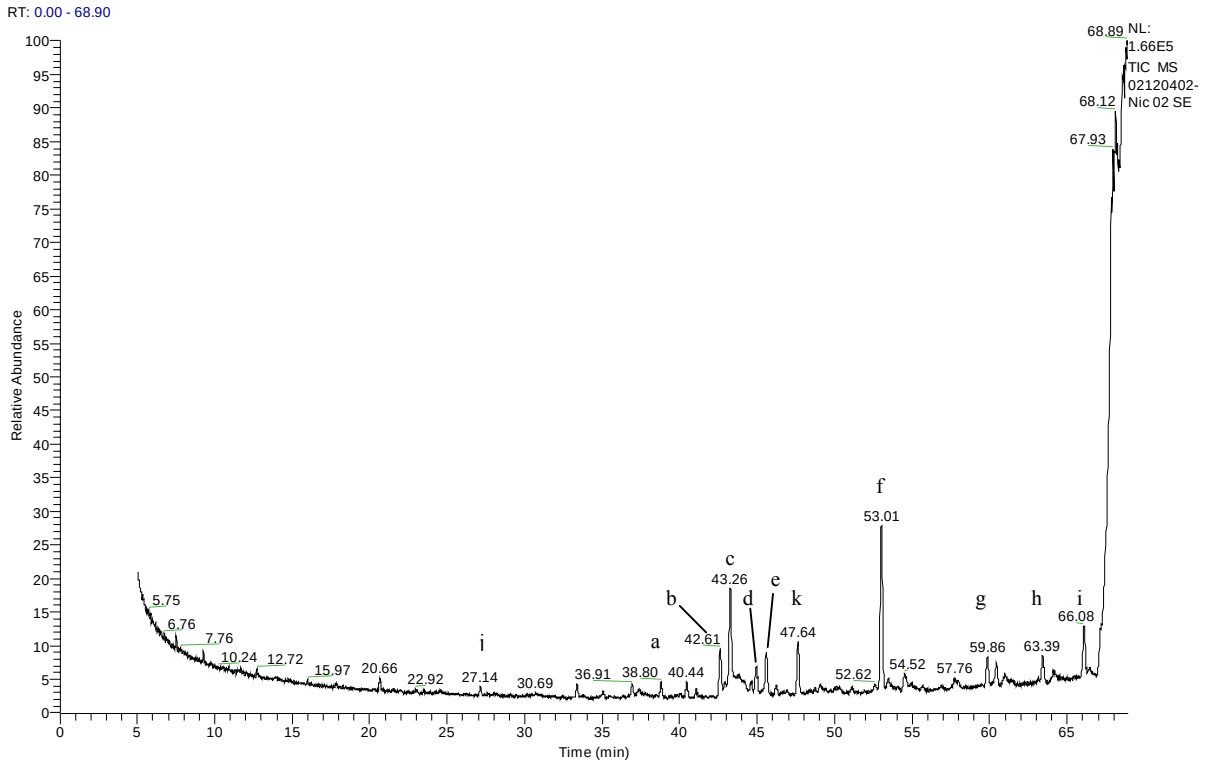

Figure 34 Gas Chromatograph of derivatized EPS from *S. elongatus* where the following peaks have been identified; galactose (a, f, h); galactoglucuronic acid (b); glucose (c, d, e, g); xylose (i); alditol (j); and unknown peaks (k).

The determination of acidic polysaccharides (APS) was achieved by the sum of individually identified monosaccharides peaks from the GC spectra (Table 17). 0.06 μMoles-C of alditol standard were spiked along with bacterial and phytoplankton samples. This allowed the ability to determine relative concentrations of monosaccharides present based on alditol peak. The APS content is approximately 0.002% and 0.56% for *S. stellata* and *S. elongatus*, respectively. Thus, APS component makes up a minute fraction of total polysaccharides for both marine bacteria and phytoplankton samples.

V. SYNTHESIS AND CONCLUSIONS

Carbon dioxide fixation by phytoplankton, through photosynthesis, results in the formation of particulate organic matter (POM). POM is subsequently decomposed by bacteria to DOM, which is subsequently used for growth and maintaining basic metabolic processes. DOM in the water is also due to release by animal excretion and phytoplankton exudation. One of the main classes of biomolecules in POM and DOM are carbohydrates, which occur as dissolved mono- and particulate or colloidal polysaccharides. Polysaccharides are produced through natural growth and metabolic processes of phytoplankton and bacteria. Phytoplankton growth and metabolic processes also maintain the cell membrane and synthesizing structural proteins, phospholipids and polysaccharides that cover the surface of the cell membrane. Exocellular polysaccharides are also responsible for cell adhesion, in response to environmental stressors (such as trace metals – possibly at toxic concentrations) or acquiring essential metal nutrients for organism's sustenance. These polysaccharides, in turn, play a vital role in the formation and occurrence of gel or 'slime' layers surrounding all living micro-organisms in the ocean. As phytoplankton fix CO_2, they grow and produce acid polysaccharide (APS) rich exopolymeric substances (EPS), in the form of mucopolysaccharides, which are part of the dissolved organic matter (DOM) pool. This DOM (which is acid polysaccharide rich, but usually contains more hydrophobic parts composed of proteins and lipids) can aggregate and form POM, settle out of water column and adsorb ^{234}Th from oceanic waters leading to a deficiency of

^{234}Th in the water column. These gel layers clearly play a significant role in the sedimentation of POM, thus affecting organic matter and metal removal rates, a role that has been overlooked by many geochemical investigations.

Total Th(IV) occurs in seawater at about 47fM (47 X 10^{-15}M) and ^{234}Th(IV) at about aM (10^{-18}M) concentrations. ^{234}Th(IV) can be removed from the water column from the dissolved state by adsorption (or surface complexation) onto marine particles. The degree of radioactive disequilibrium that occurs in the water column between ^{234}Th(IV) (particle reactive daughter) and ^{238}U (its soluble parent) is used to quantify removal rates (or flux) for ^{234}Th(IV) by adsorption to settling particles. Quantification of organic carbon export (or new production) from the euphotic zone to the deep ocean is determined by the product of the ^{234}Th export flux and the POC/^{234}Th ratio. POC/^{234}Th ratios in suspended and sinking particles are not constant, and vary with different particle sizes, water depths, and study areas. The outcome from experiments conducted from this dissertation make it apparent that interactions between ^{234}Th(IV) isotopes and macromolecular marine organic matter are ligand dependent, and thus, the variable POC/^{234}Th ratio should be a function of ligand abundance. The use of controlled laboratory experiments was used to evaluate the nature of ^{234}Th(IV) binding with different fractions of marine organic matter.

The primary objective of this research was to improve our understanding of the processes that regulate the POC/^{234}Th(IV) ratio in oceanic particles. This was accomplished through controlled laboratory experiments to chemically characterize exopolymers responsible for ^{234}Th(IV) complexation from pure cultures of

phytoplankton (*S. elongatus, E. Huxleyi*), bacteria (*R. gallaeciensis, S. stellata*) as well as colloids from the Gulf of México. Primary characterization (isoelectric point, molecular weight, carboxylic acid, phosphate and sulphate contents in isoelectric focusing profiles) was determined, and secondary characterization of isolated exopolymers responsible for ^{234}Th(IV) complexation was carried out (total polysaccharide, uronic acid content, total protein content and GC-MS).

The microbial incubation experimental results indicate that most of the ^{234}Th(IV) ended up on the surface of the cell and not on the removable EPS. *S. stellata* and *S. elongatus* yielded 2 mg (2% yield) and 1 mg (1% yield), respectively, which can be used for further characterization by NMR. The extraction procedure used to remove cell surface material did so by minimizing cell lysis. Thus, potential binding sites for ^{234}Th(IV) near the cell surface were not assessed, however, an apparently small but representative sample was successfully extracted from the procedure used in this dissertation.

For the primary characterization, isoelectric focusing profiles for potential functional groups were acquired and compared with those for ^{234}Th(IV). A set of hypotheses were stipulated as a means of testing which chemical functional groups were primarily associated with ^{234}Th(IV), using bivariate correlation analysis. Thus, hypothesis I stipulated that acidic polysaccharides (those containing acidic functional groups) are mainly responsible for surface complexation of ^{234}Th(IV) compared to neutral polysaccharides. Therefore, the null hypothesis (H_o) was ^{234}Th(IV) did not have any association with the acidic functional groups for all samples, meaning that ^{234}Th(IV)

will not be in the acidic range and will actually concentrate in the neutral pH range. Results indicate that in all samples, ^{234}Th(IV) isoelectric focusing profiles were concentrated near pH of 2 (III.2.6.1). Consequently, the alternate hypothesis, based on IEF profiles, must be accepted, which reinforced that ^{234}Th(IV) is associated with acidic functional groups. Since Th(IV) is an A-type metal (Stumm and Morgan, 1996), meaning that it prefers O over N and S containing ligands, one only needs to consider carboxyl, phosphate and sulphate functional groups. Hypothesis II was that the carboxylic acid functional group was a potential functional group candidate for ^{234}Th(IV) complexation. The null hypothesis (H_o) was that the carboxylic acid functional group has no association with ^{234}Th(IV) for all samples. Based on bivariate correlation analysis, the carboxylic acid functional group was significantly associated with ^{234}Th(IV) for *R. gallaeciensis*, *E. huxleyi*, *S. elongatus* and Gulf of México colloidal sample in the IEF spectrum. Hypothesis III, was a variation of the previous hypothesis in that the phosphate functional group was a potential functional group candidate to associate with ^{234}Th(IV) resulting in complexation. The null hypothesis (H_o) in this case was that the phosphate functional group has no association with ^{234}Th(IV) for all samples. The results from the bivariate correlation analysis clearly indicate that the phosphate functional group was associated with ^{234}Th(IV) for *R. gallaeciensis*, and *S. elongatus* sample. Hypothesis IV was yet another variation of hypothesis II where the sulphate functional group was suspected to be a potential functional group candidate for ^{234}Th complexation. Consequently, the null hypothesis (H_o) was that the sulphate functional group has no correlation with ^{234}Th for all samples.

Once again, based on bivariate correlation analysis, the sulphate functional group was most closely related with ^{234}Th(IV) for *S. elongatus* and the Gulf of México colloidal sample.

Hence, ^{234}Th(IV)-binding molecules co-occurred with carboxylic acid, phosphate and sulphate functional groups in the isoelectric focusing profiles of the different bacterial and phytoplankton EPS. The exact functional group responsible for ^{234}Th(IV) binding may be different and species dependent. Thus, the fact that different EPS with different functional group composition all strongly bind ^{234}Th(IV) may support intramolecular chelation or a steric enhancement effect. The steric enhancement effect does not depend on the exact acid functional group that is associated with ^{234}Th(IV). Recall, the alginic acid molecule (Figure 7) chelation of divalent calcium atom. The same chelating condition of the egg-box model with alginic acid polymers can exist with isolated EPS. Strong chelating environments can occur within cultured and natural EPS.

The 2D SDS-PAGE of ^{234}Th(IV) was obtained to further characterize extracted EPS from cultured and colloidal samples. The pH of the material was determined from IEF profiles indicating that the majority of the ^{234}Th(IV) label (50-61%) was associated with EPS near pH of 2. Molecular weights of organic matter associated with ^{234}Th(IV) label were subsequently determined. Marine bacteria *R. gallaeciensis* and *S. stellata* had EPS molecular weights of 1 kDa and 3.5 kDa, respectively. Phytoplankton *Emiliania huxleyi* and *Synechococcus elongatus* had EPS molecular weights of 14.3 kDa and 1-6.5 kDa, respectively. This compares to the 12 kDa molecular weight that Quigley *et al*., (2002) determined from marine colloidal Th-binding ligands.

1% of all the carboxylic acid groups were labeled using carbon-14 methylated amine reaction and thus should not have affected the chemical behavior of the bulk material even though two dimensional SDS-PAGE spectra for carboxylic acid needed to be corrected for the unreacted dimethylamine [$(^{14}CH_3)_2NH$] peak. While this method marks the presence of COOH group containing molecules, it is not a quantitative method, and thus, the actual concentration could not be calculated. The sum of each pH fraction for all molecular weights (Table 38) was plotted to illustrate the isoelectric focusing profile of the carboxylic acid functional group.

The total polysaccharide content of Th(IV)-binding EPS molecule from *S. stellata* and *S. elongatus* was only 14% and 8% of total carbon content. Approximately 5.4% and 87.1%, respectively, of the total polysaccharide content of this macromolecular ligand was composed of uronic acids. The total protein content of *S. stellata* and *S. elongatus* was 2.6% and 6.2% of total carbon content, respectively.

The GC-MS results of the organic material, extracted from microbial EPS samples that complexed with ^{234}Th(IV) provided insight into the monomers of the acidic polysaccharides that were in this fraction. The main sugar monomers consisted of galactose, glucose, mannose and xylose for *S. stellata* and galactose, glucose, galactoglucuronic acid and xylose, for *S. elongatus*.

Since the total thorium concentration in seawater is at about 47 fM (10^{-15}M) and the total organic carbon component of matter associated with ^{234}Th(IV) has been determined, the ratio of trace metal versus binding site can be assessed. The concentration of potential acidic binding sites on organic matter (OM) is about 1 meq/g-

OM (Santschi *et al*., 1995). According to Hung *et al.* (2003a), approximately 1-3% of total carbon is acid polysaccharide carbon (APS-C) in the particulate or dissolved fraction, and POC and COC concentrations are about 0.1 μM-C and 20 μM, respectively, with about 1 to 200 nM of APS-C in the particulate or dissolved fraction. If the total thorium (^{232}Th) concentration was compared to the total concentration of acidic binding sites APS-C (i.e., 47 X 10^{-15} versus 1 – 200 X 10^{-9}), this results in 1 thorium atom for every ~20,000 to 42,000,000 potential acidic binding sites in POC or COC, respectively. The remainder of such sites would be occupied by other metals in the ocean such as calcium (Table 1). The stability constants (Table 3) of Th(IV) with HPO_4^{2-} were strongest, then SO_4^{2-}, and acetic acid was most weakly bound. Given that all acidic functional groups were likely contributing candidates to the binding of Th(IV) to the EPS ligand at times, this implies this implies that the binding environment for Th(IV) is a strong chelate involving acid groups. Thus, the steric environment and not necessarily the exact functional group might actually be most important for thorium-234 complexation to macromolecular organic matter. The exact composition of organic matter (type and quantity of acid functional groups present) in EPS could influence ^{234}Th(IV) sorption to EPS and affect the POC/^{234}Th(IV) ratios as a function of water depth and particle size. One might also envision that the carbon flux of equation (Eq.1) could be modified to incorporate possible changes in concentration ratio of the Th(IV) complexing ligand to POC. However, more research would need to be undertaken before a new algorithm could be created that would be as robust as the simple eq. 1.

REFERENCES

Alberts, B., Bray, D., Lewis, J., Raff, M., Roberts, K., and Watson, J.D., 1989. Molecular Biology of the Cell (2nd Ed.) Garland Publishing Inc., New York.

Alldredge, A. M,. Passow, U., and Logan, B., 1993. The abundance and significance of a class of large, transparent organic particles in the ocean. Deep-Sea Research I, 40: 1131-1140.

Altman, S., Baer, M., Guerrier-Takada, C., and Viogue, A. 1986. Enzymatic cleavage of RNA by RNA. Trends in Biochemical Sciences, 11: 515-518.

Alvarado-Urbina, G. G., 2004. (Personal Communications, Syngen Inc., San Carlos CA.)

Anfinsen, C. B., 1973. Principles that govern the folding of proteins. Science, 181: 223-230.

Aufdenkampe, A.K., and Murray, J. W., 2002. Controls on new production: the role of iron and physical processes. Deep Sea Research II, 49: 2649-2668.

Ausebel, F. M., Brent. R., Kingston, R. E., Moore, D. D., Seidman, J. G., Smith, J. A., and Struhl, K., 1992. Analysis of proteins. In: F.M. Ausebel et al. (Editors), Short Protocols in Molecular Biology. John Wiley & Sons, New York, pp. 10.1-10.25

Bacon, M. P. and Anderson, R. F.,1982. The distribution of Thorium isotopes between dissolved and particulate forms in the deep sea. Journal of Geophysical Research, 87 (C3): 2045-2056.

Bacon, M. P., Cochran, J.K., Hirschberg, D., Hammar, T.R. and Fleer, A.P., 1996. Export flux of carbon at the equator during the EqPac time-series cruises estimated from ^{234}Th measurements. Deep-Sea Research II, 43 (4-6): 1133-1153.

Bajaj, M. and Blundell, T., 1984. Evolution and the tertiary structure of proteins. Annual Review of Biophysics and Bioengineering, 13: 453-492.

Baldwin, R. L., 1986. Seeding protein folding. Trends in Biochemical Sciences, 11: 6-9.

Baskaran, M., Santschi, P. H., Guo, L., Bianchi, T. S., and Lambert, C., 1996. ^{234}Th:^{238}U disequilibria in the Gulf of México: the importance of organic matter and particle concentration. Continental Shelf Research, 16: 353-380.

Benitez-Nelson, C., Buesseler, K. O., Karl, D. M., and Andrews, J., 2001. A time-series study of particulate matter export in the North Pacific Subtropical Gyre based on ^{234}Th:^{238}U disequilibrium. Deep-Sea Research I, 48: 2595-2611.

Berger R., Liaaen-Jensen, S., McAlister, V., and Guillard, R. R. L., 1977. Carotenoids of Prymnesiophyceae (Haptophyceae). Biochemical Systematics and Ecology, 5: 71-78.

Berkelman, T. and Stenstedt, T., 1998. 2-D Electrophoresis using immobilized pH gradients: principles and methods. Amersham Biosciences, pp. 100.

Beveridge, T. J. Forsberg, C. W., and Doyle, R. J., 1982. Major sites of metal binding in *Bacillus lincheniformis* walls. Journal of Bacteriology, 150 (3): 1438-1448.

Bhat, S., Krishnaswami, G., Lal, S., Rama, D., and Moore, W.S., 1969. $^{234}Th/^{238}U$ ratios in the ocean. Earth and Planetary Science Letters, 5: 483-491.

Biersmith, A. and Benner, R., 1998. Carbohydrates in phytoplankton and freshly produced dissolved organic matter. Marine Chemistry, 63: 131-144.

Bollag, D.M., Rozycki, M.D. and Edelstein, S.J., 1996. Protein concentration determination. In: D.M. Bollag (Editor), Protein Methods. John Wiley & Sons, New York, pp. 57-82.

Bouarab, K., Potin, P., Correa, J., and Kloareg, B., 1999. Sulphated oligosaccharides mediate the interaction between a marine red alga and its green algal pathogenic endophyte. The Plant Cell, 11: 1635-1650.

Bretscher, M. S., 1973. Membrane structure: some general principles. Science, 181: 622-629.

Brock, T.D., Madigan, M.T., Martinko, J.M. and Parker, J., 1984. Biology of Microorganisms. Prentice-Hall, Englewood Cliffs, New Jersey, pp.847.

Buesseler, K. O., 1998. The decoupling of production and particulate export in the surface ocean. Global Biogeochemical Cycles, 12: 297-310.

Buesseler, K.O., Andrews, J. A., Hartman, M. C., Belastock, R., and Chai, F., 1995. Regional estimates of the export flux of particulate organic carbon derived from thorium-234 during the JGOFS EqPac program. Deep-Sea Research II, 42 (2-3), 777-804.

Buesseler, K. O., Bacon M. P., Cochran J. K., and Livingston, H. D., 1992. Carbon and nitrogen export during the JGOFS North Atlantic bloom experiment estimated from 234Th:238U disequilibria. Deep-Sea Research, 39 (7/8): 1115–1137.

Buesseler, K.O., Ball, L., Andrews, J. A., Benitez-Nelson, C., Belastock, R., Chai, F., and Chao, Y., 1998. Upper ocean export of particulate organic carbon in the Arabian Sea derived from thorium-234. Deep-Sea Research II, 45 (10-11): 2461-2487.

Burd, A. B., Moran, S. B., and Jackson, G. A., 2000. A coupled adsorption-aggregation model of the POC/^{234}Th ratio of marine particles. Deep-Sea Research I, 47: 103-120.

Burdman, S., Jurkevitch, E., Soria-Diaz, M. E., Serrano, A. M. G., and Okon, Y., 2000. Extracellular polysaccharide composition of *Azospirillium brasilense* and its relation with cell aggregation. Federation of European Microbiological Societies - Microbiology Letters, 189: 259-264.

Caoila, M. G., Ocampo-Friedmann, R., Friedmann, E. I., 1993. Cytology of long-term dessication in the desert cyanobacterium *Chroococcidiopsis* (Chroococcales). Phycologia, 32 (5): 315-322.

Cantley, L. C., 1981. Structure and mechanism of the (Na, K)-ATPase. Current Topics in Bioenergetics, 11: 201-237.

Chisholm, S. W., Olson, R. J., Zettler, E. R., Goericke, R., Waterbury, J. B., and Welschmeyer, N. A., 1988. A novel free-living prochlorophyte abundant in the oceanic euphotic zone. Nature, 334: 340-343.

Choppin, G.R., 1988. Soluble rare-earth and actinide species in seawater. Marine Chemistry, 28 (1-3): 23-28.

Choppin, G.R., 1989. Humics and radionuclide migration. Radiochimica Acta, 44/45: 23-28.

Choppin, G.R. and Wong, P. J., 1998. The chemistry of actinide behavior in marine systems. Aquatic Geochemistry, 4: 77-101.

Chothia, C., 1984. Principles that determine the structure of proteins. Annual Review of Biochemistry, 53: 537-572.

Christensen, B. E., 1989. The role of extracellular polysaccharides in biofilms. Journal of Biotechnology, 10: 181-202.

Coale, K. H., and Bruland, K. W., 1985. $^{234}Th:^{238}U$ disequilibria within the California Current. Limnology and Oceanography, 30 (1): 22-33.

Croot, P. L., Moffett, J. W., and Brand, L. E., 2000. Production of extracellular Cu complexing ligands by eucaryotic phytoplankton in response to Cu stress. Limnology and Oceanography, 45(3): 619-627.

De Philippis, R., Sili, C., Paperi, R., and Vincenzini, M., 2001. Exopolysaccharides-producing cyanobacteria and their possible exploitation: a review. Journal of Applied Phycology, 13: 293-299.

De Philippis, R. and Vincenzini, M., 1998. Exocellular polysaccharides from cyanobacteria and their possible applications. Federation of European Microbiological Societies - Microbiology Reviews, 22: 151-175.

Dickinson, E., 2003. Hydrocolloids at interfaces and the influence on the properties of dispersed systems. Food Hydrocolloids, 17: 25-39.

Doco, T., O'Neill, M. A., and Pellerin, P., 2001. Determination of neutral and acidic glycosyl-residue compositions of plant polysaccharides by GC-EI-MS analysis of the trimethylsilyl methyl glycoside derivatives. Carbohydrate Polymers, 46: 249-259.

Doolittle, R. F., 1985. Proteins. Scientific American, 253(4): 88-99.

Dytham, C., 1999. Choosing and Using Statistics: A biologists Guide. Blackwell Science, Inc, Malden, MA, 218.

Edindin, M., 1987. The rotational and lateral diffusion of membrane proteins and lipids: phenomena and function. Current Topics in Membranes and Transport, 29: 91-127.

Edwards, R. L., Chen, J. H., Ku, T. L., and Wasserburg, G. J., 1987. Precise timing of the last interglacial period from mass spectrometric determination of thorium-230 in corals. Science, 236: 1547-1553.

Ehling-Schulz, M. and Scherer, S., 1999. UV protection in cyanobacteria. European Journal of Phycology, 34: 329-338.

El Shafei, G. M. S., 1996. The polarizing power of metal cations in (Hydr)oxides. Journal of Colloid and Interface Science, 182: 249-253.

Fajon, C., Cauwet, G., Lebaron, P., Terzic, S., Ahel, M., Malej, A., Mozetic, P. and Turk, V., 1999. The accumulation and release of polysaccharides by planktonic cells and the subsequent bacterial response during a controlled experiment. Federation of European Microbiological Societies - Microbiology Ecology, 29: 351-363.

Falchini, L., Sparvoli, E., and Tomaselli, L., 1996. Effect of *Nostoc* (Cyanobacteria) inoculation on the structure and stability of clay soils. Biology and Fertility of Soils, 23: 346-352.

Filisetti-Cozzi, T.M., and Carpita, N.C., 1991. Measurement of uronic acids without interference from neutral sugars. Analytical Biochemistry, 197 (1):157-162.

Fox, K. F., Wunschel, D. S., Fox, A., and Stewart, G. C., 1998. Complementarity of GC-MS and LC-MS analysis for determination of carbohydrate profiles of vegetative cells and spores of bacilli. Journal of Microbiological Methods, 33: 1-11.

Franklin, L. A., and Forster, R. M., 1997. Review-the changing irradiance environment: consequence for marine macrophyte physiology, productivity and ecology. European Journal of Phycology, 32: 207-232.

Geesey, G. G., 1982. Microbial exopolymers: Ecological and economic considerations. ASM News, 48 (1): 9-14.

Geesey, G.G., and Jang, L., 1989. Interactions Between Metal Ions and Capsular Polymers. In: T.J. Beveridge and R.J. Doyle (Editors), Metal Ions and Bacteria. John Wiley & Sons, Toronto.

Gilbeaut, D. M., 2000. Nucleotide sugars and glycosyltransferases for synthesis of cell wall matrix polysaccharides. Plant Physiology and Biochemistry, 38: 69-80.

Goldthwait, S. A. and Alldredge, A. L., 2004. Transparent Exopolymer Particles (TEP) degrade slowly in laboratory incubations. In Special Session 5.14 The Aquatic Gel Phase: Its Role in Biogeochemical Cycles. American Society of Limnology and Oceanography and The Oceanography Society Ocean Research Conference, Hawaii.

Gonzalez, J. M., Mayer, F., Moran, M. A., Hodson, R. E. and Whitman, W. B., 1997. *Sagittula stellata* gen. Nov., sp. Nov., a lignin-transforming bacterium from coastal environment. International Journal of Systematic Bacteriology, 47 (3): 773-780.

Grasshoff, K., Kremling, K. and Ehrhardt, M., 1999. Methods of Seawater Analysis. Wiley-VCH Verlag, New York.

Gröniger, A., Sinha, R. P., Klisch, M., and Häder, D.-P., 2000. Photoprotective compounds in cyanobacteria, phytoplankton and macroalgae - a database. Journal of Photochemistry and Photobiology B: Biology, 58: 115-122.

Grotjan, Jr., H. E., Padrnos-Hicks, P. A., and Keel, B. A., 1986. Ion chromatographic method for the analysis of sulphate in complex carbohydrates. Journal of Chromatography, 367: 367-375.

Guo, L., and Santschi, P.H., 1997. Isotopic and elemental characterization of colloidal organic matter from the Chesapeake Bay and Galveston Bay. Marine Chemistry, 59: 1-15.

Guo, L.-D., Coleman, C. H., Santschi, P. H., 1994. The distribution of colloidal and dissolved organic carbon in the Gulf of México. Marine Chemistry, 45: 105-119.

Guo, L.-D., Hung, C.-C., Santschi, P. H. and Walsh, I. D., 2002. ^{234}Th scavenging and its relationship to acid polysaccharide abundance in the Gulf of México. Marine Chemistry, 78 (2-3): 103-119.

Guo, L., Santschi, P. H., Cifuentes, L., Trumbore, S. E., and Southon, J., 1996. Cycling of high-molecular-weight dissolved organic matter in the Middle Atlantic Bight as revealed by carbon isotopic (^{13}C and ^{14}C) signatures. Limnology and Oceanography 41(6): 1242-1252.

Guo, L., Santschi, P. H., and Warnken, K. W., 2000a. Trace metal composition of colloidal material in estuarine and marine environments. Marine Chemistry, 70: 257-275.

Guo, L., Wen, L.-S., Tang, D., and Santschi, P. H., 2000b. Re-examination of cross-flow ultrafiltration for sampling aquatic colloids: evidence from molecular probes. Marine Chemistry, 69: 75-90.

Gustaffson, Ö., Gschwend, P. M., Buesseler, K. O., 1997. Using ^{234}Th disequilibria to estimate the vertical removal rates of polycyclic aromatic hydrocarbons from the surface ocean. Marine Chemistry, 57: 11-23.

Harris, D.C., 1991. Quantitative Chemical Analysis. W. H. Freeman and Company, New York.

Hill, D. R., Keenan, T. W., Helm, R. F., Potts, M., Crowe, L. M., and Crowe, J. H., 1997. Extracellular polysaccharide of Nostoc commune (Cyanobacteria) inhibits fusion of membrane vesicles during desiccation. Journal of Applied Phycology, 9: 237-248.

Hirose, K., and Tanoue, E., 2001. Strong ligand for thorium complexation in marine bacteria. Marine Environmental Research, 51: 95-121.

Hirst, E. L., Percival, E., and Wold, J. K., 1964. The structure of alginic acid. Part V. Partial hydrolysis of the reduced polysaccharide. Journal of the Chemical Society, 1493-1498.

Hirst, E. L. and Rees, D. A., 1965. The structure of alginic acid. Part V. Isolation and unambiguous characterization of some hydrolysis products of the methylated polysaccharide. Journal of the Chemical Society, 1182-1188.

Hokin, L. E., 1976. The molecular machine for driving the coupled transport of Na^+ and K^+ ion ($Na^+ + K^+$)-activated ATPase. Trends in Biochemical Sciences, 1: 233-237.

Holden, M. T. G., Chhabra, S. R., de Nys, R., Stead, P., Bainton, N. J., Hill, P. J., Manefield, M., Kumar, N., Labatte, M., England, D., Rice, S., Givskov, M., Salmond, G. P. C., Steward, G. S. A. B., Bycroft, B. W., Kejelleberg, S., and Williams, P. 1999. Quorum-sensing cross talk isolation and chemical characterization of cyclic dipeptides from *Pseudomonas aureginosa* and other Gram-negative bacteria. Molecular Microbiology, 33 (6): 1254-1266.

Hopkins, C. R., 1986. Membrane boundaries involved in the uptake and intracellular processing of cell surface receptors. Trends in Biochemical Sciences, 11 (11): 473-477.

Hung, C.-C., 2004. (Personal Communications, Texas A&M University at Galveston, Department of Oceanography, TX)

Hung, C.-C. and Santschi, P. H., 2001. Spectrophotometric determination of total uronic acids in seawater using cation-exchange separation and pre-concentration by lyophilization. Analytica Chimica Acta, 42 (7): 111-117.

Hung, C.-C., Guo, L., Santschi, P. H., Alvarado Quiroz, N. G., and Haye, J. M., 2003a. Distribution of carbohydrate species in the Gulf of México. Marine Chemistry, 81: 119-135.

Hung, C.-C., Guo, L., Schultz, G., Pinckney, J. L., and Santschi, P. H., 2003b. Production and fluxes of carbohydrate species in the Gulf of México. Global Biogeochemical Cycles 17(2): 1055, doi10.1029/2002GB001988.

Islam, T., and Lindhardt, R.J., 2003. Chemistry, biochemistry and pharmaceutical potentials of glycosaminoglycans and related saccharides. In: C.-H. Wong (Editor), Carbohydrate-based Drug Delivery. Wiley-VCH, Weinheim, pp. 407-433.

Keeling, C.D., and Whorf, T.P., 1994. Atmospheric CO_2 records from sites in the SIO sampling network. In: T.A. Boden, D.P. Kaiser, R.J. Sepanski and F.W. Stoss (Editors), Trends '93: A Compendium of Data on Global Change. Oak Ridge National Laboratory, Oak Ridge, Tennessee.

Kleinfeld, A. M., 1987. Current views of membrane structure. Current Topics in Membranes and Transport, 29: 1-25.

Koblizek, M., Komenda, J., Masojidek, J., and Pechar, L., 2000. Cell aggregation of cyanobacterium *Synechococcus elongatus*: role of electron transport chain. Journal of Phycology, 36: 662-668.

Kornfeld, R. and Kornfeld, S., 1980. Structure of glycoproteins and their oligosaccharide units. In: W.J. Lenarz (Editor), The Biochemistry of Glycoproteins and Proteoglycans. Plenum, New York.

Koshland, Jr. D. E., 1984. Control of enzyme activity and metabolic pathways. Trends in Biochemical Sciences, 9: 155-159.

Ku, T. L., Knauss, K. G., Matthieu, G. G., 1977. Uranium in the open ocean: concentration and isotopic composition. Deep-Sea Research, 24: 1005-1017.

Lambert, J., and Mazzola, E. P., 2004. Nuclear Magnetic Resonance Spectroscopy: An Introduction to Principles, Applications, and Experimental Methods. Prentice Hall, Upper Saddle River, New Jersey.

Lambert, J. B., Shurvell, H. F., Lightner, D. A., and Cooks, R. G., 1987. Introduction to Organic Spectroscopy. MacMillan Publishing Company, New York.

Langmuir, D., and Herman, J., 1980. The mobility of thorium in natural waters at low temperatures. Geochimica et Cosmochimica Acta, 44: 1753-1766.

Larsen, B., and Haug, A., 1971. Biosynthesis of alginate. Carbohydrate Research, 17: 287-296.

Leppard, G.G., 1995. The characterization of algal and microbial mucilage and their aggregates in aquatic ecosystems. The Science of the Total Environment, 165: 103-131.

Leppard, G. G., 1997. Colloidal organic fibrils of acid polysaccharides in surface waters: electron-optical characteristics, activities and chemical estimates of abundance. Colloids and Surfaces A: Physicochemical and Engineering Aspects, 120: 1-15.

Leustek, T., Martin, M. N., Bick, J.-A., and Davies, J. P., 2000. Pathways and regulation of sulfur metabolism revealed through molecular and genetic studies. Annual Review of Plant Physiology and Plant Molecular Biology, 51: 141-165.

Liu, H., and Buskey, E. J., 2000. Hypersalinity enhances the production of extracellular polymeric substances (EPS) in the Texas Brown Tide Alga, Aureoumbra lagunensis (Pelagophyceae) Journal of Phycology, 36: 71-77.

Lohrenz, S. E., Fahnenstiel, G. L., Redalje, D. G., Lang, G. A., Dagg, M. J., Whitledge, T. E., and Dortch, Q., 1999. Nutrients, irradiance, and mixing as factors regulating primary production in coastal waters impacted by the Mississippi River Plume. Continental Shelf Research, 19: 1113-1141.

Lohrenz, S. E., Redalje, D. G., Verity, P. G., Flagg, C. N., and Matulewski, K. V., 2002. Primary production on the continental shelf off Cape Hatteras, North Carolina. Deep-Sea Research II, 49: 4479-4509.

Lombardi, A.T., Vieira, A.A.H., and Sartori, L.A., 2002. Mucilaginous capsule adsorption and intracellular uptake of copper by *Kirchneriella aperta* (Chlorococcales). Journal of Phycology, 38 (2): 332-337.

McDonald, J. A., 1988. Extracellular matrix assembly. Annual Review of Cell Biology, 4: 183-207.

McDougald, D., Srinivasan, S., Rice, S. A., and Kjelleberg, S., 2003. Signal-mediated cross-talk regulates stress adaptation in Vibrio species. Microbiology, 149: 1923–1933.

Marketon, M. M., Glenn, S. A., Eberhard, A., and González, J. E., 2003. Quorum sensing controls exopolysaccharide production in *Sinorhizobium meliloti*. Journal of Bacteriology, 185 (1): 325-331.

Martel, A.E. and Smith, R.M. 1990. Critical Stability Constants. Plenum Press, New York.

Marx, R. B., and Aitken, M. D., 2000. A material-balance approach for modeling bacterial chemotaxis to a consumable substrate in the capillary assay. Biotechnology and Bioengineering, 68 (3): 308-315.

Matijevic, E., Abramson, M.B., Schulz, K.F., and Kerker, M., 1960. Detection of metal ion hydrolysis by coagulation: II. Thorium. Journal of Physical Chemistry, 64: 1157-1161.

Matsumoto, E ., 1975. Th-234-U-238 Radioactive disequilibrium in surface layer of Ocean. Geochimica et Cosmochimica Acta, 39 (2): 205-212.

Meunier, F., and Wilkinson, K. J., 2002. Nonperturbing fluorescent labeling of polysaccharides. Biomacromolecules, 3: 857-864

Milner-White, E. J. and Poet, R., 1987. Loops, bulges, turns and hairpins in proteins. Trends in Biochemical Sciences, 12: 189-192.

Moe, S. T., Draget, K. I., Skjåk-Bræk, G., and Smidrød, O., 1995. Alginates. In: A. M. Stephen (Editor), Food Polysaccharides and Their Application. Dekker, Inc., New York, pp. 245-286.

Montreuil, J., Bouquelet, S., Debray, H., Lemoine, J., Michalski, J.-C., Spik, G., and Strecker, G.., 1994. Glycoproteins. In: M.F. Chaplin and J.F. Kennedy (Editors), Carbohydrate Analysis: A Practical Approach. The Practical Approach Series. Oxford University Press, New York.

Moran, S. B. and Buesseler, K. O., 1992. Short residence. time of colloids in the upper ocean estimated from ^{238}U-^{234}Th disequilibria. Nature, 359, 17 September: 221-223.

Moran, S. B., Charette, M. A., Hoff, J. A., Edwards, R.L., and Landing, W.M., 1997. Distribution of Th-230 in the Labrador Sea and its relation to ventilation. Earth and Planetary Science Letters, 150 (1-2): 151-160.

Moran, S. B., Weinstein, S. E., Edmonds, H. N., Smith, J. N., Kelly, R. P., Pilson, M. E. Q., and Harrison, W. G., 2003. Does 234Th/238U disequilibrium provide an accurate record of the export flux of particulate organic carbon from the upper ocean. Limnology and Oceanography, 48 (3): 1018-1029.

Murray, J. W., Downs, J. N., Strom, S., Wei, C.-L., and Jannasch, H. W., 1989. Nutrient assimilation, export production and ^{234}Th scavenging in the eastern equatorial pacific. Deep-Sea Research, 36 (10): 1471-1489.

Murray, J. W., Young, J., Newton, J., Dunne, J., Chappin, T., Paul, B., and McCarthy, J., 1996. Export flux of particulate organic carbon from the central equatorial Pacific determined using a combined drifting trap-^{234}Th approach. Deep-Sea Research II, 43 (4-6): 1095-1132.

Myklestad, S. M., 1995. Release of extracellular products by phytoplankton with special emphasis on polysaccharides. The Science of the Total Environment, 165: 155-164.

Myklestad, S. M., Skånøy, E., and Hestmann, S., 1997. A sensitive and rapid method for analysis of dissolved mono- and polysaccharides in seawater. Marine Chemistry, 56 (3-4): 279-286.

Nash, K. L., and Choppin, G. R. 1980. Interaction of humic and fulvic acids with Th(IV). Journal of Inorganic Nuclear Chemistry, 42: 1045-1050.

Nishizuka, Y., 1984. Protein kinase in signal transduction. Trends in Biochemical Sciences, 9: 163-166.

Olden, K., Bernard, B. A., Humphries, M. J., Yeo, T.-K., Yeo, K.-T., White, S. L., Newton, S. A., Bauer, H. C., and Parent, J. B., 1985. Function of glycoprotein glycans. Trends in Biochemical Sciences, 10: 78-82.

Pariente, V., 2004. Personal Collection, College Station, Texas.

Passow, U., 2002. Transparent exopolymer particles (TEP) in aquatic environments. Progress in Oceanography, 55: 287-333.

Pilson, M. E. Q., 1998. An Introduction to the Chemistry of the Sea. Prentice Hall, Upper Saddle River, New Jersey.

Pistocchi, R., Mormile, A. M., Guerrini, F., Isani, G., and Boni, L., 2000. Increased production of extra- and intracellular metal-ligands in phytoplankton exposed to copper and cadmium. Journal of Applied Phycology, 12: 469-477.

Plaxton, W.C. and Carswell, M.C., 1999. Metabolic aspects of the phosphate starvation response in plants. In: H. R. Lerner (Editor), Plant Responses to Environmental Stresses: From Phytohormones to Genome Reorganization. Dekker, Inc., New York, pp. 349-372.

Potin, P., Bouarab, K., Küpper, F., and Kloareg, B., 1999. Oligosaccharide recognition signals and defense reactions in marine plant-microbe interactions. Current Opinion in Microbiology, 2: 276-283.

Potts, M., 1999. Minireview-Mechanisms of desiccation tolerance in cyanobacteria. European Journal of Phycology, 34: 319-328.

Provasoli-Guillard Center for Culture of Marine Phytoplankton - CCMP 374

Quigley, M. S., 2000. Tracing colloid-colloid and colloid-particle interactions using thorium. Ph.D. Dissertation, Texas A&M University; College Station.

Quigley, M. S., Honeyman, B. D., and Santschi, P. H., 1996. Thorium sorption in the marine environment: equilibrium partitioning at the hematite/water interface, sorption/desorption kinetics and particle tracing. Aquatic Geochemistry, 1: 277-301.

Quigley, M. S., Santschi, P.H., Guo, L.-D. and Honeyman, B. D., 2001. Sorption irreversibility and coagulation behavior of 234Th with marine NOM. Marine Chemistry, 76: 27-45.

Raghothama, K. G., 1999. Phosphate acquisition**.** Annual Review of Plant Physiology and Plant Molecular Biology, 50: 665-693.

Raghothama, K. G., 2000. Phosphate transport and signaling. Current Opinion in Plant Biology, 3 (3): 182–187.

Reddi, A. H., 1984. Chapter 10 - Extracellular matrix and development. In: K.A. Piez and A.H. Reddi (Editors), Extracellular Matrix Biochemistry. Elsevier, New York, pp. 375-412.

Reichle, D., Houghton, J., Kane, B., Ekmann, J., Benson, S., Clarke, J., Dahlman, R., Hendrey, G., Herzog, H., Hunter-Cevera, J., Jacobs, G., Judkins, R., Ogden, J., Palmisano, A., Socolow, R., Stringer, J., Surles, T., Wolsky, A., Woodward, N., and York, M. 1999. Carbon Sequestration Research and Development. U. S. Department of Energy: Washington, D.C.

Reinhardt, A., 2003. (Personal Communications, CABE, Geneva).

Robyt, J.F., 1997. Essentials of Carbohydrate Chemistry. Springer Advanced Texts in Chemistry. Springer-Verlag, New York.

Ruiz-Ponte, C., Cilia, V., Lambert, C., and Nicolas, J.L., 1998. *Roseobacter gallaeciensis* sp. Nov., a new marine bacterium isolated from rearing sand collectors of the scallop Pecten maximus. International Journal of Systematic Bacteriology, 48: 537-542.

Samuelsen, A. B., Cohen, E. H., Paulsen, B. S., Brüll, L. P., and Thomas-Oates, J. E., 1999. Structural studies of a heteroxylan from Plantago major L. seeds by partial hydrolysis, HPAEC-PD, methylation and GC-MS, ESMS and ESMS/MS. Carbohydrate Research, 315: 312-318.

Santschi, P. H., Balnois, E., Wilkinson, K. J., Zhang J., Buffle, J., and Guo, L., 1998. Fibrillar polysaccharides in marine macromolecular organic matter as imaged by atomic force microscopy and transmission electron microscopy. Limnology and Oceanography, 43 (5): 896-908.

Santschi, P. H., Guo, L., Baskaran, M., Trumbore, S., Southon, J., Bianchi, T. S., Honeyman, B., and Cifuentes, L., 1995. Isotopic evidence for the contemporary origin of high-molecular weight organic matter in oceanic environments. Geochimica et Cosmochimica Acta, 59 (3): 625-631.

Santschi, P. H., Guo, L.-D. Walsh, I. D., Quigley, M. S. and Baskaran, M., 1999. Boundary exchange and scavenging of radionuclides in continental margin water of the Middle Atlantic Bight: implications for organic carbon fluxes. Continental Shelf Research, 19: 609-636.

Santschi, P.H., Hung, C.-C., Schultz, G., Alvarado-Quiroz, N., Guo, L., Pinckney, J., Walsh, I., 2003. Control of acid polysaccharide production and 234Th and POC export fluxes by marine organisms. Geophysical Research Letters, 30, dio, 10.1029/2002GL016046.

Schuster, B. and Sleyter, U. B., 2000. S-layer-supported lipid membrane. Reviews in Molecular Biotechnology, 74 233-254.

Sciorra, V. A., and Morris, A. J., 2002. Roles for lipid phosphate phosphatases in regulation of cellular signaling. Biochimica et Biophysica Acta, 1582 45– 51.

Scott, D. M., 1987. Sodium cotransport systems: cellular, molecular and regulatory aspects. Bioessays, 7: 71-78.

Silvestri, L. J., Hurst, R. E., Simpson, L., and Settine, J. M., 1982. Analysis of sulphate in complex carbohydrates. Analytical Biochemistry, 123: 303-309.

Singer, S. J. and Nicolson, G. L., 1972. The fluid mosaic model of the structure of the cell membranes. Science, 175: 720-731.

Sinha, R. P., Klisch, M., Gröniger, A., and Häder, D.-P., 1998. Ultraviolet-absorbing/screening substances in cyanobacteria, phytoplankton and macroalgae. Journal of Photochemistry and Photobiology B: Biology, 47: 83-94.

Smith, P. K., Krohn R.I., Hermanson, G. T., Mallia A. K., Gartner F. H., Provenzano M. D., Fujimoto E. K., Goeke N. M., Olson B. J., and Klenk D. C., 1985. Measurement of protein using Bicinchoninic acid. Analytical Biochemistry, 150 (1): 76-85.

Smith, D. C., Steward, G. F., Long, R. A., and Azam, F., 1995. Bacterial mediation of carbon fluxes during diatom bloom in mesocosm. Deep-Sea Research II, 42 (1): 75-97.

Staats, N., De Winder, B., Stal, L. J., and Mur, L. R., 1999. Isolation and characterization of extracellular polysaccharides from the epipelic diatoms *Cylindrotheca closterium* and *Navicula salinarum*. European Journal of Phycology, 34: 161-169.

Sternström, T. A., 1989. Bacterial hydrophobicity, an overall parameter for the measurement of adhesion potential to soil particles. Applied and Environmental Microbiology, 55(1): 142-147.

Stoderegger, K., and Herndl, G. J., 1998. Production and release of bacterial capsular material and its subsequent utilization by marine bacterioplankton. Limnology and Oceanography, 43(5): 877-884.

Storch, J. and Kleinfeld, A. M., 1985. The lipid structure of biological membranes. Trends in Biochemical Sciences, 10: 418-421.

Stumm, W. and Morgan, J. J., 1996. Aquatic Chemistry: Chemical Equilibria and Rates in Natural Waters. John Wiley & Sons, Inc., New York, 1022 pp.

Sun, S.F., 1994. High-Performance Liquid Chromatography and Electrophoresis, Physical Chemistry of Macromolecules: Basic Principles and Issues. John Wiley & Sons, Inc., New York, pp. 417-453.

Suzumura, M., and Ingall, E. D., 2001. Concentrations of lipid phosphorus and its abundance in dissolved and particulate organic phosphorus in coastal seawater. Marine Chemistry, 75: 141-149.

Sweadner, K. J. and Goldin, S., M., 1980. Active transport of sodium and potassium ions: mechanism, function and regulation. The New England Journal of Medicine, 302 (14): 777-783.

Tanford, C., 1983. Mechanism of free energy coupling in active transport. Annual Review of Biochemistry, 53: 379-409.

Tipper, D. J., Ghuysen, J.-M., and Strominger, J. L., 1965. Structure of the cell wall of *Staphylococcus aureus*, strain Copenhagen III. Further studies of the disaccharides. Biochemistry, 4 (3): 468-473.

Trubetskoj, O. A., Trubetskaya, O. E., and Khomutova, T. E., 1992. Isolation, purification and some physico-chemical properties of soil humic substances fractions obtained by polyacrylamide gel electrophoresis. Soil Biology & Biochemistry, 24: 893-896.

Tsuneda, S., Aikawa, H., Hayashi, H., Yuasa, A., and Hirata, A., 2003. Extracellular polymeric substances responsible for adhesion onto solid surface. Federation of European Microbiological Societies - Microbiology Letters, 223: 287-292.

Walters, J. S. and Hedges, J. I., 1988. Simultaneous determination of uronic acids and aldoses in plankton, plant tissues and sediment by capillary gas chromatography of N-hexylaldonamide and alditol acetates. Analytical Chemistry, 60: 988-994.

Wang, Y., Chen, Y., Lavin, C., and Gretz, M. R., 2000. Extracellular matrix assembly in diatoms (Bacillariophyceae). IV.[1] Ultrastructure of *Achnanthes longipes* and *Cymberlla cistula* as revealed by high-pressure freezing/freeze substitution and cryo-field emissions Scanning Electron Microscopy. Journal of Phycology, 36: 367-378.

Warwick, P., Carlsen, L., Randall, A., Yhao, R., and Lassen, P., 1993. ^{14}C and ^{125}I labelling of humic material for use in environmental studies. Chem. And Ecol., 8: 65-80.

Waterbury, J. B., Watson, S. B., Guillard, R. R. L., and Brand, L. E., 1979. Widespread occurrence of a unicellular, marine, planktonic, cyanobacterium. Nature, 277: 293-294.

Watt, F. M., 1986. The extracellular matrix and cell shape. Trends in Biochemical Sciences, 11: 482-485.

Wen, L-S., Santschi, P. H., Gill, G., and Paternostro, C., 1999. Estuarine trace metal distribution in Galveston Bay: importance of colloidal forms in the speciation of the dissolved phase. Marine Chemistry, 63: 185-212.

West, I. C., 1983. The biochemistry of membrane transport. Chapman and Hall, New York, 80 pp.

Westermeier, R., 1997. Electrophoresis in Practice. VCH Wiley Company, Weinheim, 331 pp.

Wingender, J., Neu, T.R. and Flemming, H.-C., 1999. What are bacterial extracellular polymeric substances. In: J. Wingender, T.R. Neu and H.-C. Flemming (Editors), Microbial Extracellular Polymeric Substances. Springer, New York, 1-19.

Wolfe, G. V., 2000. The chemical defense ecology of marine unicellular plankton: constraints, mechanisms and impacts. Biological Bulletin, 198: 225-244.

Zimmer, R. K. and Butman, C. A., 2000. Chemical signaling processes in the marine environment. Biological Bulletin, 198: 168-187.

APPENDIX

V.1. Appendix I Multiphor II Gel Electrophoresis System (IEF and SDS-PAGE)

Taken from Immobiline DryStrip Kit for 2-D Electrophoresis Instruction manual (Pharmacia Biotech/Amersham Biosciences, 18-1038-63).

Isoelectric focusing with an immobilized pH gradient (IPG) was used to focus acidic and basic macromolecules to obtain distinct spots. Immobiline DryStrip precast polyacrylamide gels (T=4%, C=3%) of pH 3-10 are cast on plastic support film and contain an immobilized pH gradient.

V.1.1 Isoelectric Focusing Electrophoresis

100μl sample capacity was mixed in 100 μl with the rehydration solution. Using a current profile below (Table 18).

Table 18 Current profile of 19701 Volt-hours (V_h) for Isoelectric Focusing

Phase	Voltage	mA	W	Time (hr)	V_h
1	300	1	5	0.01	1
2	300	1	5	6.5	1,950
3	2000	1	5	5	5,750
4	2000	1	5	6	12,000
			Total	17.5	19,700

Rehydration Solution

12.0	g	Urea
50	mg	DTT (PlusOne, Lot No.: K25839753 908)
0.13	ml	Pharmalyte 3-10 (Pharmacia Biotech, Lot No.: 249419)
0.13	ml	Triton X-100 (PlusOne, Lot No.: K1994782545)
few grains of bromophenol blue (BPB)		

make up to 25ml with d.d.H_2O. Make fresh everyday.

Equilibration Stock Solution – Tris-HCl pH 6.8

61 g	Tris
460-490 ml	1.0 M HCl

make up to 1000 ml with d.d.H_2O

V.1.2 Appendix I.1 0.1mm 2D SDS-PAGE

To perform a 2D SDS-PAGE, the IEF strip from V.1.1 is placed in Petri dish with equilibration solution #1 for ten minutes. The IEF strip is then subsequently treated with equilibration solution #2 for another ten minutes. After the IEF strip is allowed to dry on long edge, as per instruction manual, the IEF strip is cut into 1 cm long pieces. These pieces are then placed on 15% homogenous SDS-PAGE gel in order. Five microliters of rainbow colored protein weight markers (Amersham Biosciences, Low molecular weight range RPN 755 Batch No.: 73) was added in order to visualize molecular mass sections ranging from less than 1.0 kDa (bromophenol blue), 3.5 kDa (insulin (b) chain), 6.5 kDa (aprotinin), 14.3 kDa (lysozyme), 20.1 kDa (trypsin inhibitor), 30 kDa (carbonic anhydrase) and 45 kDa (ovalbumin). The gel was then run for 2 hours at 600V.

Equilibration Solution

20	ml	Equilibration Stock solution – Tris-HCl pH 6.8
72	g	Urea (Fisher, Lot No.:015206)
60	ml	glycerol (USB, Lot No.:113569)
2.0	g	SDS (USB, Lot No.:113071)

Add 67 ml of d.d.H_2O for final volume of 200 ml.
Divide the total solution in two.
To equilibration solution #1 add 600 mg of DTT.
To equilibration solution #2 add 4.5 g of iodoacetamide (Sigma, Lot No.:033K5320)).

V.2. Appendix I.2 3mm thick 15% SDS-PAGE

Taken from Ausebel *et al.* (1992) Analysis of Proteins in *Short Protocols in Molecular Biology.*

Reagents

4x Tris-Cl/SDS, pH 6.8

6.05 g Tris base (0.5 M Tris-Cl, final)
0.4 g SDS (0.4% SDS, final)
Adjust to pH 6.8 with 1N HCl
Add H_2O to 100 ml

Filter solution though a 0.45μm filter and store at 4°C

4x Tris-Cl/SDS, pH 8.8

91 g Tris base (1.5 M Tris-Cl, final)
2 g SDS (0.4% SDS, final)
Adjust to pH 8.8 with 1N HCl
Add d.d.H_2O to 500 ml

Filter solution though a 0.45μm filter and store at 4°C

2x SDS/sample buffer

25 ml 4xTris-Cl/SDS, pH 6.8
20 ml glycerol
4 g SDS
2 ml 2-ME or 3.1 g DTT
1 mg bromophenol blue
Prepared with distilled deionized water and made up to 100 ml and mix
Stored in 1 ml aliquots at –70°C

5x SDS/electrophoresis buffer

15.1 g Tris base
72.0 g glycine
5.0 g SDS
Prepared with distilled deionized water and made up to 1000 ml and mix

30% Acrylamide/bisacrylamide solution

300 g Acrylamide (USB, Lot No.:112951)
8 g Bisacrylamide (USB, Lot No.:113421)
Dissolved into 1000 ml

Casting of Gel

Preparation of PAGE gel was undertaken by assembling glass plates by sandwiching two glass pates with corresponding spacers according to P10DS owner's manual (Owl separations systems). 20 milliliters of 2% solution was prepared by microwaving agarose for approximately 1 minute. The agarose solution was pipetted into the trough below the glass, located at the base of the lower buffer chamber.

The 15% polyacrylamide gel was prepared by;

60.0 ml 30% acrylamide/0.8%bisacrylamide
30.0 ml 4X Tris-Cl/HCl, pH 8.8
30.0 ml H_2O
200 μl 10% ammonium persulphate (Fisher, Lot No.:947443)
160 μl TEMED (Fisher Biotech, Lot No.:036774)

V.3. Appendix II Bicinchoninic Acid (BCA) Protein Assay

Taken from Bollag *et al.* (1996) Protein determination in *Protein Methods.*

Reagents

BCA (Bicinchoninic acid)
$Na_2CO_3 \cdot H_2O$
$Na_2C_4H_4O_6 \cdot 2H_2O$
NaOH
$NaHCO_3$
$CuSO_4 \cdot 5H_2O$

Solutions

Reagent 1

10.0 g	BCA (1%)
20.0 g	$Na_2CO_3 \cdot H_2O$ (2%)
1.6 g	$Na_2C_4H_4O_6 \cdot 2H_2O$ (0.16%)
4.0 g	NaOH (0.4%)
9.5 g	$NaHCO_3$ (0.95%)

Dissolve to 1000 ml volume of d.d.H_2O and adjust pH to 11.25.

Reagent 2

2.0 g	$CuSO_4 \cdot 5H_2O$ (4%)

Dissolve to 50 ml volume of d.d.H_2O.

Standard Working Reagent (SWR)

50 volumes Reagent 1
1 volume Reagent 2
Stable for 1 week

1. Mix 1 volume of sample with 20 volumes of SWR (100 μl and 2 ml of SWR)
2. Incubate at room temperature for 2 hours
3. Read A_{562}

V.4. Appendix III Radionuclide partitioning results

Table 19 Radionuclide Partitioning Data for *R. gallaeciensis*

^{234}Th(IV) (cpm[a])	Step 1[1]	Mass Balance	Step 2[2]	Mass Balance	Step 3[3]	Mass Balance
Total	9419.4	100%	9419.4	100%	8466.0	100%
Marine Broth	249.6	3%	258.6	3%	170.4	2%
Bacterial Pellet	5287.9	56%	6326.9	67%	6346.9	75%
H_2O extraction	N/A		47.2	1%	N/A	
Residual on Tube	104.1	1%	370.2	4%	308.1	4%
EtOH wash	N/A	0%	N/A	0%	108.6	1%
EPS	N/A		N/A		29.6	0%
Residual EPS on Tube	N/A		N/A		8	0%
Yield		60%		74%		82%
^{32}P (cpm[a])	**Step 1[1]**	**Mass Balance**	**Step 2[2]**	**Mass Balance**	**Step 3[3]**	**Mass Balance**
Total	14980.3	100%	14980.3	100%	13716.7	100%
Marine Broth	1911.6	13%	2346.6	16%	1787.4	13%
Bacterial Pellet	8444.0	56%	6854.4	46%	6718.4	49%
H_2O extraction	N/A		6744.4	45%	N/A	
Residual on Tube	316.0	2%	364	2%	285	2%
EtOH wash	N/A		N/A		16.6	0%
EPS	N/A		N/A		2609.7	19%
Residual EPS on Tube	N/A		N/A		158.3	1%
Yield		71%		109%		84%
^{35}S (cpm[a])	**Step 1[1]**	**Mass Balance**	**Step 2[2]**	**Mass Balance**	**Step 3[3]**	**Mass Balance**
Total	1313037.6	100%	1313037.6	100%	1221618.0	100%
Marine Broth	1830837.6	139%	1831437.6	139%	1640658.0	134%
Bacterial Pellet	-268614.3	-20%	-303410.0	-23%	-271435.0	-22%
H_2O extraction	N/A		23521.5	2%	N/A	
Residual on Tube	6171.7	0.47%	229.3	0.02%	237.7	0.02%
EtOH wash	N/A	0%	N/A		2754.7	0.23%
EPS	N/A		N/A		2507.4	0.21%
Residual EPS on Tube	N/A		N/A		96.8	0.01%
Yield		119%		118%		113%

[a] All activity is background corrected

[1] Ultracentrifugation separation between microbial pellet and ambient media (seawater or marine broth)

[2] Ultracentrifugation separation between microbial pellet and ambient media, with H_2O wash of microbial pellet.

[3] Ultracentrifugation separation between microbial pellet and ambient media with H_2O wash of microbial pellet and subsequent Ethanol precipitation of microbial EPS.

Table 20 Radionuclide Partitioning Data for *S. stellata*

^{234}Th(IV) (cpm[a])	Step 1[1]	Mass Balance	Step 2[2]	Mass Balance	Step 3[3]	Mass Balance
Total	11123.0	100%	11123.0	100%	10624.0	100%
Marine Broth	392.3	4%	410.4	4%	417.6	4%
Bacterial Pellet	9886.4	89%	8734.1	79%	9175.4	86%
H_2O extraction	N/A		847.6	8%	N/A	
Residual on Tube	67.6	1%	744.1	7%	185.2	2%
EtOH wash	N/A		N/A		67.2	1%
EPS	N/A		N/A		262.7	2%
Residual EPS on Tube	N/A		N/A		13.8	0.13%
Yield		93%		97%		95%
^{32}P (cpm[a])	**Step 1[1]**	**Mass Balance**	**Step 2[2]**	**Mass Balance**	**Step 3[3]**	**Mass Balance**
Total	16772.6	100%	16772.6	100%	15731.3	100%
Marine Broth	4040.4	24%	3994.8	24%	3872.4	25%
Bacterial Pellet	11850.6	71%	8820.8	53%	8790.6	56%
H_2O extraction	N/A		5235.9	31%	N/A	
Residual on Tube	240.2	1%	190.4	1%	281.9	2%
EtOH wash	N/A	0%	N/A	0%	309.2	2%
EPS	N/A		N/A		1873.2	12%
Residual EPS on Tube	N/A		N/A		179.2	1%
Yield		96%		109%		97%
^{35}S (cpm[a])	**Step 1[1]**	**Mass Balance**	**Step 2[2]**	**Mass Balance**	**Step 3[3]**	**Mass Balance**
Total	1916037.6	100%	1916037.6	100%	1884408.0	100%
Marine Broth	1970337.6	103%	1941537.6	101%	1912608.0	101%
Bacterial Pellet	-45775	-2%	-323485.4	-17%	-318666.6	-17%
H_2O extraction	N/A		24618.2	1%	N/A	
Residual on Tube	7335.2	0.38%	29.5	0%	13.7	0%
EtOH wash	N/A		N/A		8580.7	0%
EPS	N/A		N/A		1544.4	0%
Residual EPS on Tube	N/A		N/A		60	0%
Yield		101%		86%		85%

[a] All activity is background corrected

[1] Ultracentrifugation separation between microbial pellet and ambient media (seawater or marine broth)

[2] Ultracentrifugation separation between microbial pellet and ambient media, with H_2O wash of microbial pellet.

[3] Ultracentrifugation separation between microbial pellet and ambient media with H_2O wash of microbial pellet and subsequent Ethanol precipitation of microbial EPS.

Table 21 Radionuclide Partitioning Data for *E. huxleyi*

^{234}Th(IV) (cpm[a])	Step 1[1]	Mass Balance	Step 2[2]	Mass Balance	Step 3[3]	Mass Balance
Total	8771.4	100%	8771.4	100%	8398.2	100%
Seawater Media PSU=26	585.6	7%	2517	5%	502.8	6%
Phytoplankton Pellet	5364.5	61%	4688.5	53%	3404.8	41%
H_2O extraction	N/A		2916.2	33%	N/A	
Residual on Tube	905.7	10%	554.2	6%	565.5	7%
EtOH wash	N/A		N/A		98.0	1%
EPS	N/A		N/A		730.5	9%
Residual EPS on Tube	N/A		N/A		235.4	3%
Yield		78%		98%		66%
^{32}P (cpm[a])	**Step 1[1]**	**Mass Balance**	**Step 2[2]**	**Mass Balance**	**Step 3[3]**	**Mass Balance**
Total	14110.8	100%	12875.3	100%	12875.3	100%
Seawater Media PSU=26	6645.6	47%	7060.2	50%	5839.2	45%
Phytoplankton Pellet	5861.7	42%	974.72	7%	1337.9	10%
H_2O extraction	N/A		8348.14	59%	N/A	
Residual on Tube	867.5	6%	276.1	2%	299.2	2%
EtOH wash	N/A		N/A		862.8	7%
EPS	N/A		N/A		2657.1	21%
Residual EPS on Tube	N/A		N/A		348.8	3%
Yield		95%		118%		88%
^{35}S (cpm[a])	**Step 1[1]**	**Mass Balance**	**Step 2[2]**	**Mass Balance**	**Step 3[3]**	**Mass Balance**
Total	1805355.0	100%	1805355.0	100%	1804155.0	100%
Seawater Media PSU=26	1969605.0	109%	1376727.5	76%	1884705.0	104%
Phytoplankton Pellet	-57050.0	-3%	-229187.4	-13%	-313831.7	-17%
H_2O extraction	N/A		13431.3	1%	N/A	
Residual on Tube	3944.1	0.22%	82.6	0.0046%	64.5	0.004%
EtOH wash	N/A		N/A		3003.2	0.166%
EPS	N/A		N/A		2366.2	0.131%
Residual EPS on Tube	N/A		N/A		108.4	0.006%
Yield		106%		64%		87%

[a] All activity is background corrected

[1] Ultracentrifugation separation between microbial pellet and ambient media (seawater or marine broth)

[2] Ultracentrifugation separation between microbial pellet and ambient media, with H_2O wash of microbial pellet.

[3] Ultracentrifugation separation between microbial pellet and ambient media with H_2O wash of microbial pellet and subsequent Ethanol precipitation of microbial EPS.

Table 22 Radionuclide Partitioning Data for *S. elongatus*

^{234}Th(IV) (cpm[a])	Step 1[1]	Mass Balance	Step 2[2]	Mass Balance	Step 3[3]	Mass Balance
Total	9115.2	100%	9115.2	100%	8937.0	100%
Seawater Media PSU=26	684.6	8%	486.6	5%	555.0	6%
Phytoplankton Pellet	6917.1	76%	2901.0	32%	5058.1	57%
H_2O extraction	N/A		1516.6	17%	N/A	
Residual on Tube	900.4	10%	4105.2	45%	1400.0	16%
EtOH wash	N/A	0%	N/A	0%	138.0	2%
EPS	N/A	0%	N/A	0%	954.8	11%
Residual EPS on Tube	N/A	0%	N/A	0%	198.3	2%
Yield		93%		99%		93%
^{32}P (cpm[a])	**Step 1[1]**	**Mass Balance**	**Step 2[2]**	**Mass Balance**	**Step 3[3]**	**Mass Balance**
Total	14382.5	100%	14382.5	100%	14125.3	100%
Seawater Media PSU=26	11343.5	79%	11473.8	80%	11286.6	80%
Phytoplankton Pellet	2435.7	17%	-519.2	-4%	-548.2	-4%
H_2O extraction	N/A		2229.0	15%	N/A	
Residual on Tube	512.4	4%	282.3	2%	284.1	2%
EtOH wash	N/A		N/A		179.2	1%
EPS	N/A		N/A		716.8	5%
Residual EPS on Tube	N/A		N/A		210.4	1%
Yield		99%		94%		86%
^{35}S (cpm[a])	**Step 1[1]**	**Mass Balance**	**Step 2[2]**	**Mass Balance**	**Step 3[3]**	**Mass Balance**
Total	1847509.2	100%	1847509.2	100.00%	1879453.8	100.00%
Seawater Media PSU=26	1864009.2	100.89%	1879159.2	101.71%	1824103.8	97.05%
Phytoplankton Pellet	-14900	-0.81%	-313045.9	-16.94%	-303865.8	-16.17%
H_2O extraction	N/A		8414.7	0.46%	N/A	
Residual on Tube	7457.4	0.40%	56.3	0.00%	60.7	0.003%
EtOH wash	N/A		N/A		982.0	0.052%
EPS	N/A		N/A		3308.6	0.176%
Residual EPS on Tube	N/A		N/A		58.6	0.003%
Yield		100%		85%		81%

[a] All activity is background corrected

[1] Ultracentrifugation separation between microbial pellet and ambient media (seawater or marine broth)

[2] Ultracentrifugation separation between microbial pellet and ambient media, with H_2O wash of microbial pellet.

[3] Ultracentrifugation separation between microbial pellet and ambient media with H_2O wash of microbial pellet and subsequent Ethanol precipitation of microbial EPS.

V.5. Appendix IV Isoelectric focusing Data

Table 23 Isoelectric focusing data of *R. gallaeciensis*

PH	Error	^{234}Th(IV) Activity of EtOH precipitated EPS (cpm[a])	2σ	Percent Yield	2σ	^{32}P Activity of Incubated EPS (cpm[a])	Percent Yield	2σ	^{35}S Activity of Incubated EPS (cpm[a])	Yield	2σ	PO_4 (nM)	Yield	Error	SO_4 (nM)	Yield	Error
1.99	0.12	93.3	4.3	11.8%	0.5%	28.64	10.1%	3.0%	28.83	7.9%	3.3%	29.86	15.9%	0.5%	3.78	2.74%	0.01%
2.31	0.16	285.5	2.7	36.1%	1.0%	11.74	4.1%	1.3%	30.23	8.3%	3.5%	19.75	10.5%	0.2%	6.48	4.70%	0.03%
3.14	0.32	74.8	4.6	9.5%	0.4%	17.54	6.2%	1.9%	35.13	9.6%	3.9%	11.07	5.9%	0.1%	17.12	12.40%	0.21%
3.71	0.20	85.7	4.4	10.8%	0.5%	20.84	7.3%	2.2%	16.63	4.6%	2.1%	11.17	5.9%	0.1%	2.43	1.76%	0.00%
4.52	0.46	88.5	4.4	11.2%	0.5%	9.44	3.3%	1.0%	27.33	7.5%	3.2%	13.78	7.3%	0.1%	2.24	1.62%	0.00%
4.77	0.34	32.7	6.0	4.1%	0.2%	14.64	5.2%	1.6%	24.53	6.7%	2.9%	12.73	6.8%	0.1%	0.75	0.54%	0.00%
5.29	0.38	33.7	6.0	4.3%	0.3%	22.74	8.0%	2.4%	25.63	7.0%	3.0%	10.30	5.5%	0.1%	1.04	0.75%	0.00%
5.80	0.39	20.5	6.7	2.6%	0.2%	13.24	4.7%	1.4%	14.33	3.9%	1.8%	10.93	5.8%	0.1%	4.15	3.01%	0.01%
6.63	0.49	30.8	6.1	3.9%	0.2%	26.84	9.5%	2.8%	19.43	5.3%	2.3%	10.49	5.6%	0.1%	0.51	0.37%	0.00%
6.95	0.59	9.4	7.6	1.2%	0.1%	26.04	9.2%	2.8%	36.53	10.0%	4.1%	14.81	7.9%	0.1%	0.19	0.14%	0.00%
8.92	0.78	8.4	7.7	1.1%	0.1%	37.34	13.2%	3.9%	47.93	13.1%	5.3%	5.30	2.8%	0.0%	1.63	1.18%	0.00%
10.32	0.51	17.4	6.9	2.2%	0.2%	30.84	10.9%	3.2%	34.63	9.5%	3.9%	11.87	6.3%	0.1%	43.72	31.67%	1.38%
11.23	0.16	10.9	7.5	1.4%	0.1%	23.84	8.4%	2.5%	24.23	6.6%	2.8%	25.68	13.7%	0.4%	54.02	39.13%	2.11%

[a] All activity is background corrected

Table 24 Isoelectric focusing data of *S. stellata*

PH	Error	^{234}Th(IV) Activity of EtOH precipitated EPS (cpm[a])	2σ	Percent Yield	2σ	^{32}P Activity of Incubated EPS (cpm[a])	Percent Yield	2σ	^{35}S Activity of Incubated EPS (cpm[a])	Yield	2σ	PO_4 (nM)	Yield	Error	SO_4 (nM)	Yield	Error
1.76	0.13	212.1	3.1	3.7%	0.1%	59.10	11.6%	3.3%	21.85	7.1%	3.1%	9.89	6.4%	0.1%	59.26	19.8%	1.2%
1.90	0.15	1282.4	1.5	22.3%	0.3%	45.80	9.0%	2.6%	18.63	6.0%	2.6%	8.25	5.4%	0.0%	27.66	9.2%	0.3%
2.31	0.14	1386.8	1.6	24.2%	0.4%	34.90	6.9%	2.1%	16.93	5.5%	2.4%	24.93	16.3%	0.4%	22.37	7.5%	0.2%
3.59	0.63	269.3	2.8	4.7%	0.1%	15.10	3.0%	0.9%	12.95	4.2%	1.9%	6.25	4.1%	0.0%	10.28	3.4%	0.0%
4.46	0.39	198.5	3.2	3.5%	0.1%	15.30	3.0%	0.9%	22.33	7.2%	3.1%	29.56	19.3%	0.6%	9.31	3.1%	0.0%
5.30	0.44	371.0	2.4	6.5%	0.2%	20.60	4.1%	1.2%	12.15	3.9%	1.8%	5.60	3.7%	0.0%	4.90	1.6%	0.0%
5.63	0.42	528.3	2.0	9.2%	0.2%	31.80	6.3%	1.9%	15.33	5.0%	2.2%	5.63	3.7%	0.0%	7.45	2.5%	0.0%
6.31	1.01	432.1	2.2	7.5%	0.2%	22.00	4.3%	1.3%	20.63	6.7%	2.9%	5.16	3.4%	0.0%	9.57	3.2%	0.0%
8.16	1.10	177.9	3.3	3.1%	0.1%	24.40	4.8%	1.5%	22.63	7.3%	3.2%	5.01	3.3%	0.0%	14.17	4.7%	0.1%
9.27	0.78	366.7	2.4	6.4%	0.2%	41.90	8.2%	2.4%	32.43	10.5%	4.4%	4.72	3.1%	0.0%	8.40	2.8%	0.0%
9.58	0.67	325.9	2.5	5.7%	0.1%	67.70	13.3%	3.7%	35.23	11.4%	4.7%	5.34	3.5%	0.0%	48.31	16.1%	0.8%
9.65	0.78	92.6	4.4	1.6%	0.1%	60.80	12.0%	3.4%	39.33	12.7%	5.2%	36.90	24.1%	0.9%	47.02	15.7%	0.7%
11.06	0.15	94.5	4.3	1.6%	0.1%	68.80	13.5%	3.7%	38.53	12.5%	5.0%	6.18	4.0%	0.0%	31.28	10.4%	0.3%

[a] All activity is background corrected

Table 25 Isoelectric focusing data of *E. huxleyi*

PH	Error	^{234}Th(IV) Activity of EtOH precipitated EPS (cpm[a])	2σ	Percent Yield	2σ	^{32}P Activity of Incubated EPS (cpm[a])	Percent Yield	2σ	^{35}S Activity of Incubated EPS (cpm[a])	Yield	2σ	PO_4 (nM)	Yield	Error	SO_4 (nM)	Yield	Error
1.68	0.07	2643.8	1.7	34.5%	0.6%	20.84	5.4%	1.5%	47.93	8.3%	3.2%	3.54	2.0%	0.0%	53.58	6.1%	0.3%
2.11	0.12	524.2	2.0	6.8%	0.1%	30.64	7.9%	2.3%	42.03	7.3%	2.9%	16.69	9.4%	0.2%	26.45	3.0%	0.1%
2.38	0.08	265.2	2.7	3.5%	0.1%	29.14	7.5%	2.2%	36.53	6.3%	2.6%	16.33	9.1%	0.1%	18.88	2.2%	0.0%
2.71	0.24	140.8	3.6	1.8%	0.1%	33.94	8.7%	2.6%	27.83	4.8%	2.0%	18.57	10.4%	0.2%	14.62	1.7%	0.0%
3.94	0.37	264.9	2.8	3.5%	0.1%	20.34	5.2%	1.6%	31.33	5.4%	2.3%	10.35	5.8%	0.1%	1.86	0.2%	0.0%
4.75	0.35	316.0	2.5	4.1%	0.1%	17.34	4.5%	1.4%	40.03	6.9%	2.8%	37.98	21.3%	0.8%	2.24	0.3%	0.0%
7.87	0.58	296.9	2.6	3.9%	0.1%	29.94	7.7%	2.3%	40.33	7.0%	2.8%	6.45	3.6%	0.0%	110.76	12.7%	1.4%
9.88	0.44	222.3	2.9	2.9%	0.1%	28.64	7.4%	2.2%	38.03	6.6%	2.7%	5.68	3.2%	0.0%	137.20	15.7%	2.2%
10.70	0.21	265.2	2.7	3.5%	0.1%	34.54	8.9%	2.6%	51.03	8.8%	3.4%	5.87	3.3%	0.0%	133.66	15.3%	2.0%
11.21	0.07	133.3	3.7	1.7%	0.1%	33.44	8.6%	2.5%	63.13	10.9%	4.0%	6.03	3.4%	0.0%	122.81	14.1%	1.7%
11.42	0.11	90.9	4.3	1.2%	0.1%	27.84	7.2%	2.1%	58.73	10.2%	3.8%	39.39	22.1%	0.9%	151.52	17.4%	2.6%
11.59	0.39	47.8	5.3	0.6%	0.0%	32.44	8.3%	2.5%	41.23	7.1%	2.9%	9.86	5.5%	0.1%	65.49	7.5%	0.5%
12.10	0.41	183.3	3.2	2.4%	0.1%	50.14	12.9%	3.7%	59.83	10.4%	4.0%	1.79	1.0%	0.0%	33.76	3.9%	0.1%

[a] All activity is background corrected

Table 26 Isoelectric focusing data of *S. elongatus*

PH	Error	^{234}Th(IV) Activity of EtOH precipitated EPS (cpm[a])	2σ	Percent Yield	2σ	^{32}P Activity of Incubated EPS (cpm[a])	Percent Yield	2σ	^{35}S Activity of Incubated EPS (cpm[a])	Yield	2σ	PO_4 (nM)	Yield	Error	SO_4 (nM)	Yield	Error
1.85	0.15	1037.0	1.6	32.3%	0.5%	48.34	13.0%	3.7%	21.83	6.6%	2.9%	8.00	5.0%	0.0%	53.25	19.7%	1.0%
2.20	0.35	293.7	2.7	9.1%	0.2%	32.94	8.8%	2.6%	24.63	7.5%	3.2%	7.09	4.4%	0.0%	15.80	5.8%	0.1%
3.41	0.69	147.4	3.6	4.6%	0.2%	28.64	7.7%	2.3%	13.93	4.2%	1.9%	6.21	3.9%	0.0%	8.25	3.1%	0.0%
4.04	0.43	93.1	4.4	2.9%	0.1%	9.64	2.6%	0.8%	15.83	4.8%	2.1%	24.85	15.5%	0.4%	10.64	3.9%	0.0%
4.71	0.38	197.1	3.2	6.1%	0.2%	17.24	4.6%	1.4%	18.43	5.6%	2.5%	6.37	4.0%	0.0%	3.97	1.5%	0.0%
5.49	0.42	240.5	2.9	7.5%	0.2%	23.14	6.2%	1.9%	19.43	5.9%	2.6%	5.99	3.7%	0.0%	4.18	1.5%	0.0%
6.22	0.31	474.9	2.1	14.8%	0.3%	19.74	5.3%	1.6%	26.33	8.0%	3.4%	5.68	3.5%	0.0%	3.59	1.3%	0.0%
6.84	0.78	522.7	2.0	16.3%	0.3%	18.94	5.1%	1.5%	20.23	6.1%	2.7%	5.34	3.3%	0.0%	3.25	1.2%	0.0%
7.29	0.41	100.5	4.2	3.1%	0.1%	24.44	6.6%	2.0%	22.53	6.8%	3.0%	5.86	3.7%	0.0%	7.04	2.6%	0.0%
8.49	0.34	28.5	6.5	0.9%	0.1%	30.74	8.3%	2.4%	27.03	8.2%	3.5%	11.22	7.0%	0.1%	4.23	1.6%	0.0%
9.49	0.46	30.8	6.4	1.0%	0.1%	28.54	7.7%	2.3%	36.53	11.1%	4.5%	44.73	27.9%	1.2%	61.43	22.7%	1.4%
10.28	0.52	22.9	6.8	0.7%	0.0%	30.94	8.3%	2.5%	41.23	12.5%	5.0%	23.49	14.7%	0.3%	50.86	18.8%	1.0%
11.25	0.13	24.7	6.7	0.8%	0.1%	59.04	15.9%	4.4%	42.23	12.8%	5.1%	5.40	3.4%	0.0%	43.87	16.2%	0.7%

[a] All activity is background corrected

Table 27 Isoelectric focusing data of Gulf of México Station 4 72m depth sample

pH	Error	^{234}Th(IV) Activity of EtOH precipitated EPS (cpm[a])	2σ	Yield	2σ	PO_4 (nM)	Yield	Error	SO_4 (nM)	Yield	Error
2.21	0.35	375.5	2.4	18.9%	0.4%	32.28	11.8%	0.4%	44.93	18.7%	0.8%
2.65	0.11	414.5	2.3	20.9%	0.5%	26.52	9.7%	0.3%	23.82	9.9%	0.2%
2.95	0.25	295.2	2.6	14.9%	0.4%	16.02	5.8%	0.1%	13.22	5.5%	0.1%
3.64	0.11	131.8	3.8	6.6%	0.3%	9.34	3.4%	0.0%	1.69	0.7%	0.0%
4.14	0.23	88.3	4.4	4.4%	0.2%	45.09	16.4%	0.7%	3.46	1.4%	0.0%
5.00	0.72	136.1	3.7	6.9%	0.3%	39.61	14.4%	0.6%	5.03	2.1%	0.0%
5.60	0.70	118.4	4.0	6.0%	0.2%	10.14	3.7%	0.0%	1.27	0.5%	0.0%
6.11	0.53	107.1	4.1	5.4%	0.2%	39.89	14.5%	0.6%	5.31	2.2%	0.0%
6.59	0.48	90.8	4.4	4.6%	0.2%	9.72	3.5%	0.0%	1.78	0.7%	0.0%
7.11	0.64	74.1	4.8	3.7%	0.2%	17.52	6.4%	0.1%	5.43	2.3%	0.0%
7.75	0.31	67.4	4.9	3.4%	0.2%	9.99	3.6%	0.0%	2.34	1.0%	0.0%
9.25	0.19	45.1	5.6	2.3%	0.1%	8.48	3.1%	0.0%	45.80	19.0%	0.9%
10.26	0.23	42.3	5.8	2.1%	0.1%	9.77	3.6%	0.0%	86.63	36.0%	3.1%

[a] All activity is background corrected

V.6. Appendix V 2D SDS-PAGE (15%) Data

Table 28 ^{234}Th(IV) activity for 2D SDS-PAGE for *R. gallaeciensis*

Mol. Wt.	Activity [a] (cpm) pH													
KDa	**1.99**	**2.31**	**3.14**	**3.71**	**4.52**	**4.77**	**5.29**	**5.80**	**6.63**	**6.95**	**8.92**	**10.32**	**11.23**	
<1	167.4	124.8	14.4	7.1	5.7	0.9	0.9	0.9	0.8	0.9	-0.9	10.0	8.8	
3.5	27.7	35.2	11.5	4.3	15.1	14.8	14.7	20.6	7.1	5.3	5.9	7.1	6.9	
6.5	14.0	24.7	8.9	17.3	36.4	34.2	18.6	34.3	7.3	2.4	9.7	4.6	1.6	
14.3	10.4	5.1	4.3	4.6	23.2	16.1	5.2	4.3	0.9	4.0	2.9	5.8	4.1	
20.1	10.6	2.6	2.2	6.4	12.0	6.1	5.0	6.9	4.6	1.7	1.3	4.9	1.6	
30	8.9	3.3	1.1	-0.6	6.7	3.5	3.5	4.9	0.0	1.8	2.9	0.8	2.5	
>45	43.2	14.9	14.2	17.9	35.1	29.8	9.0	21.7	9.6	6.1	10.3	13.4	12.1	Total
Sub total	281.9	210.3	56.3	56.8	133.9	105.1	56.7	93.4	30.1	21.9	32.0	46.3	37.3	1161.4
Mol. Wt	**Percent of total Activity pH**													
KDa	**1.99**	**2.31**	**3.14**	**3.71**	**4.52**	**4.77**	**5.29**	**5.80**	**6.63**	**6.95**	**8.92**	**10.32**	**11.23**	
<1	14.4%	10.7%	1.2%	0.6%	0.5%	0.1%	0.1%	0.1%	0.1%	0.1%	-0.1%	0.9%	0.8%	
3.5	2.4%	3.0%	1.0%	0.4%	1.3%	1.3%	1.3%	1.8%	0.6%	0.5%	0.5%	0.6%	0.6%	
6.5	1.2%	2.1%	0.8%	1.5%	3.1%	2.9%	1.6%	2.9%	0.6%	0.2%	0.8%	0.4%	0.1%	
14.3	0.9%	0.4%	0.4%	0.4%	2.0%	1.4%	0.4%	0.4%	0.1%	0.3%	0.2%	0.5%	0.3%	
20.1	0.9%	0.2%	0.2%	0.5%	1.0%	0.5%	0.4%	0.6%	0.4%	0.1%	0.1%	0.4%	0.1%	
30	0.8%	0.3%	0.1%	0.0%	0.6%	0.3%	0.3%	0.4%	0.0%	0.2%	0.2%	0.1%	0.2%	
>45	3.7%	1.3%	1.2%	1.5%	3.0%	2.6%	0.8%	1.9%	0.8%	0.5%	0.9%	1.1%	1.0%	Total
Sub total	24.3%	18.1%	4.8%	4.9%	11.5%	9.0%	4.9%	8.0%	2.6%	1.9%	2.8%	4.0%	3.2%	100%

[a] All activity was background corrected

Table 29 Propagation of errors for ^{234}Th(IV) activity for 2D SDS-PAGE for *R..gallaeciensis*

	2 σ values for ^{234}Th(IV) activity (%)												
	pH												
kDa	**1.99**	**2.31**	**3.14**	**3.71**	**4.52**	**4.77**	**5.29**	**5.80**	**6.63**	**6.95**	**8.92**	**10.32**	**11.23**
<1	4.2	4.7	7.6	8.1	8.2	8.5	8.5	8.5	8.5	8.5	8.6	7.9	7.9
3.5	6.9	6.7	7.8	8.3	7.6	7.6	7.6	7.3	8.1	8.2	8.1	8.1	8.1
6.5	7.7	7.1	7.9	7.5	6.6	6.7	7.4	6.7	8.1	8.4	7.9	8.2	8.5
14.3	7.9	8.2	8.3	8.2	7.2	7.5	8.2	8.3	8.5	8.3	8.4	8.2	8.3
20.1	7.8	8.4	8.4	8.1	7.8	8.1	8.2	8.1	8.2	8.5	8.5	8.2	8.5
30	7.9	8.3	8.5	8.6	8.1	8.3	8.3	8.2	8.6	8.4	8.4	8.5	8.4
>45	6.40	7.60	7.8	7.4	6.7	6.9	7.9	7.3	7.9	8.1	7.9	7.7	7.8
	18.8%	19.5%	21.3%	21.3%	19.7%	20.4%	21.2%	20.6%	21.9%	22.1%	21.8%	21.5%	21.7%

Table 30 ^{234}Th(IV) activity for 2D SDS-PAGE for *S. stellata*

Mol. Wt.	Activity [a] (cpm) pH													
kDa	**1.76**	**1.90**	**2.31**	**3.59**	**4.46**	**5.30**	**5.63**	**6.31**	**8.16**	**9.27**	**9.58**	**9.65**	**11.06**	
<1	32.5	68.1	79.2	32.2	22.1	23.1	2.5	5.0	4.4	13.6	6.4	0.2	3.6	
3.5	17.5	756.6	184.9	27.4	21.6	45.3	63.0	55.0	32.8	48.0	28.6	5.7	-0.4	
6.5	16.7	49.7	55.0	7.7	9.2	20.6	49.3	41.5	12.8	37.4	14.2	0.7	6.8	
14.3	6.9	12.6	8.8	1.8	3.8	1.7	14.8	20.6	10.8	24.1	3.5	-0.7	1.5	
20.1	0.9	2.0	1.4	-2.8	-2.6	-3.1	4.3	5.7	0.9	12.4	3.2	0.0	-1.2	
30	2.6	2.9	6.9	-1.7	0.0	1.0	6.3	3.5	3.7	18.1	0.1	-1.0	1.9	
>45	112.9	23.2	19.3	5.8	15.3	26.5	46.2	55.6	46.0	44.2	17.5	5.9	30.3	
Sub total	190.0	915.1	355.5	70.4	69.4	115.1	186.4	186.9	111.4	197.8	73.5	10.8	42.5	2524.8
Mol. Wt	**Percent of total Activity** pH													
kDa	**1.76**	**1.90**	**2.31**	**3.59**	**4.46**	**5.30**	**5.63**	**6.31**	**8.16**	**9.27**	**9.58**	**9.65**	**11.06**	
<1	1%	3%	3%	1%	1%	1%	0%	0%	0%	1%	0%	0%	0%	
3.5	1%	30%	7%	1%	1%	2%	2%	2%	1%	2%	1%	0%	0%	
6.5	1%	2%	2%	0%	0%	1%	2%	2%	1%	1%	1%	0%	0%	
14.3	0%	0%	0%	0%	0%	0%	1%	1%	0%	1%	0%	0%	0%	
20.1	0%	0%	0%	0%	0%	0%	0%	0%	0%	0%	0%	0%	0%	
30	0%	0%	0%	0%	0%	0%	0%	0%	0%	1%	0%	0%	0%	
>45	4%	1%	1%	0%	1%	1%	2%	2%	2%	2%	1%	0%	1%	
Sub total	8%	36%	14%	3%	3%	5%	7%	7%	4%	8%	3%	0%	2%	100%

[a] All activity was background corrected

Table 31 Propagation of errors for ^{234}Th(IV) activity for 2D SDS-PAGE for *S. stellata*

	2 σ values for ^{234}Th(IV) activity (%)												
	pH												
kDa	**1.76**	**1.90**	**2.31**	**3.59**	**4.46**	**5.30**	**5.63**	**6.31**	**8.16**	**9.27**	**9.58**	**9.65**	**11.06**
<1	6.8	5.7	5.5	6.8	7.2	7.2	8.4	8.2	8.2	7.7	8.2	8.5	8.3
3.5	7.5	2.2	4.1	7.0	7.2	6.3	5.8	6.0	6.8	6.2	6.9	8.1	8.6
6.5	7.5	6.2	6.0	8.0	7.9	7.3	6.2	6.5	7.7	6.6	7.6	8.5	8.1
14.3	8.1	7.7	7.9	8.4	8.3	8.4	7.6	7.3	7.8	7.1	8.3	8.6	8.5
20.1	8.5	8.4	8.5	8.8	8.8	8.8	8.2	8.1	8.5	7.7	8.3	8.6	8.7
30	8.4	8.3	8.1	8.8	8.6	8.5	8.1	8.3	8.3	7.4	8.6	8.6	8.4
>45	4.9	7.2	7.4	8.1	7.6	7.0	6.3	6.0	6.3	6.5	7.5	8.1	6.9
	19.7%	18.1%	18.4%	21.2%	21.1%	20.4%	19.3%	19.2%	20.4%	18.7%	21.0%	22.4%	21.7%

Table 32 ^{234}Th(IV) activity for 2D SDS-PAGE for *E. huxleyi*

Mol. Wt.	Activity [a] (cpm) pH													
Kda	**1.68**	**2.11**	**2.38**	**2.71**	**3.94**	**4.75**	**7.87**	**9.88**	**10.70**	**11.21**	**11.42**	**11.59**	**12.10**	
<6.5	210.5	66.7	28.2	10.8	28.4	47.2	99.7	81.3	64.9	55.6	57.2	14.8	2.6	
14.3	359.5	315.0	156.3	71.6	152.4	225.0	109.7	35.1	17.6	12.9	3.2	-4.2	1.0	
20.1	213.1	48.0	19.1	4.3	15.0	34.6	46.7	27.4	16.0	8.7	0.6	-2.8	-2.7	
30	168.2	22.3	7.9	-1.6	8.2	13.4	21.7	22.5	12.6	2.6	-2.0	-3.9	1.6	
>45	48.0	63.3	32.1	26.2	54.2	109.1	129.6	146.9	152.8	81.2	65.1	19.7	51.4	Total
Sub total	999.3	515.3	243.6	111.3	258.2	429.3	407.4	313.2	263.9	161.0	124.1	23.6	53.9	3904.1
Mol. Wt	**Percent of total Activity** pH													
kDa	**1.68**	**2.11**	**2.38**	**2.71**	**3.94**	**4.75**	**7.87**	**9.88**	**10.70**	**11.21**	**11.42**	**11.59**	**12.10**	
<6.5	5%	2%	1%	0%	1%	1%	3%	2%	2%	1%	1%	0%	0%	
14.3	9%	8%	4%	2%	4%	6%	3%	1%	0%	0%	0%	0%	0%	
20.1	5%	1%	0%	0%	0%	1%	1%	1%	0%	0%	0%	0%	0%	
30	4%	1%	0%	0%	0%	0%	1%	1%	0%	0%	0%	0%	0%	
>45	1%	2%	1%	1%	1%	3%	3%	4%	4%	2%	2%	1%	1%	
	26%	13%	6%	3%	7%	11%	10%	8%	7%	4%	3%	1%	1%	100%

[a] All activity was background corrected

Table 33 Propagation of errors for ^{234}Th(IV) activity for 2D SDS-PAGE for *E. huxleyi*

	2 σ values for ^{234}Th(IV) activity (%)												
	pH												
kDa	**1.66**	**2.07**	**2.36**	**2.69**	**3.91**	**4.79**	**7.87**	**9.88**	**10.70**	**11.21**	**11.42**	**11.59**	**12.10**
<6.5	4.7	2.9	2.4	3.6	4.1	4.1	3.4	3.7	4.1	4.8	5.5	6.1	8.4
14.3	6.2	7.2	6.5	7.5	6.9	6.2	5.0	5.3	5.9	7.0	7.8	6.8	8.9
20.1	6.6	7.8	7.5	7.2	7.4	6.5	3.3	4.5	5.2	6.4	7.4	6.5	8.9
30	8.4	7.8	8.4	7.8	7.9	7.0	3.3	6.0	7.0	7.9	8.2	6.6	8.8
>45	5.3	7.8	6.3	6.4	6.0	4.8	3.4	4.7	5.5	6.7	7.2	5.0	7.0
	16%	17%	16%	17%	17%	15%	11%	13%	15%	17%	18%	15%	21%

Table 34 ^{234}Th(IV) activity for 2D SDS-PAGE for *S. elongatus*

Mol. Wt.	Activity [a] (cpm) pH													
kDa	**1.85**	**2.20**	**3.41**	**4.04**	**4.71**	**5.49**	**6.22**	**6.84**	**7.29**	**8.49**	**9.49**	**10.28**	**11.25**	
<1	277.0	21.1	47.2	14.8	9.7	17.8	10.4	13.7	22.6	19.7	14.5	11.3	16.4	
3.5	344.9	49.8	47.1	46.4	31.2	36.4	18.8	62.1	13.7	10.5	12.4	14.1	11.1	
6.5	176.0	2.1	5.5	16.4	41.4	35.7	34.2	125.0	20.6	9.1	7.3	8.3	12.0	
14.3	88.3	7.4	0.5	8.9	9.8	10.0	5.4	58.6	3.2	7.7	2.1	-2.0	3.8	
20.1	65.5	1.8	-0.1	2.7	3.7	5.4	1.7	30.7	2.8	12.6	3.8	4.1	4.9	
30	27.9	-0.1	1.9	3.3	2.8	2.5	2.2	13.5	2.3	3.4	3.4	0.2	8.7	
>45	425.6	28.7	21.8	34.6	53.3	43.5	30.6	56.4	15.8	46.7	63.4	63.8	90.6	Total
Sub total	1405.2	110.8	123.9	127.1	151.9	151.3	103.3	360.0	81.0	109.7	106.9	99.8	147.5	3078.4
Mol. Wt	**Percent of total Activity** pH													
kDa	**1.85**	**2.20**	**3.41**	**4.04**	**4.71**	**5.49**	**6.22**	**6.84**	**7.29**	**8.49**	**9.49**	**10.28**	**11.25**	
<1	9%	1%	2%	0%	0%	1%	0%	0%	1%	1%	0%	0%	1%	
3.5	11%	2%	2%	2%	1%	1%	1%	2%	0%	0%	0%	0%	0%	
6.5	6%	0%	0%	1%	1%	1%	1%	4%	1%	0%	0%	0%	0%	
14.3	3%	0%	0%	0%	0%	0%	0%	2%	0%	0%	0%	0%	0%	
20.1	2%	0%	0%	0%	0%	0%	0%	1%	0%	0%	0%	0%	0%	
30	1%	0%	0%	0%	0%	0%	0%	0%	0%	0%	0%	0%	0%	
>45	14%	1%	1%	1%	2%	1%	1%	2%	1%	2%	2%	2%	3%	
	46%	4%	4%	4%	5%	5%	3%	12%	3%	4%	3%	3%	5%	100%

[a] All activity was background corrected

Table 35 Propagation of errors for ^{234}Th(IV) activity for 2D SDS-PAGE for *S. elongatus*

	2 σ values for ^{234}Th(IV) activity (%)												
	pH												
kDa	**1.85**	**2.20**	**3.41**	**4.04**	**4.71**	**5.49**	**6.22**	**6.84**	**7.29**	**8.49**	**9.49**	**10.28**	**11.25**
<1	3.5	7.1	6.1	7.4	7.6	7.2	7.6	7.4	7.0	7.1	7.4	7.6	7.3
3.5	3.1	6.1	6.1	6.2	6.7	6.5	7.2	5.8	7.4	7.6	7.5	7.4	7.6
6.5	4.1	8.1	7.9	7.3	6.3	6.5	6.6	4.7	7.1	7.7	7.8	7.7	7.5
14.3	5.2	7.8	8.2	7.7	7.6	7.6	7.9	5.8	8.0	7.8	8.1	8.4	8.0
20.1	5.7	8.1	8.3	8.1	8.0	7.9	8.1	6.7	8.1	7.5	8.0	8.0	7.9
30	6.8	8.3	8.1	8.0	8.1	8.1	8.1	7.4	8.1	8.0	8.0	8.2	7.7
>45	2.9	6.8	7.0	6.5	6.0	6.3	6.7	5.9	7.3	6.2	5.7	5.7	5.2
	12.3%	19.8%	19.7%	19.4%	19.1%	19.0%	19.8%	16.7%	20.1%	19.6%	19.9%	20.1%	19.5%

Table 36 ^{234}Th(IV) activity for 2D SDS-PAGE for Gulf of México Sample St. 4 72m

Mol. Wt.	Activity [a] (cpm) pH													
kDa	**2.21**	**2.65**	**2.95**	**3.64**	**4.14**	**5.00**	**5.60**	**6.11**	**6.59**	**7.11**	**7.75**	**9.25**	**10.26**	
<1	30.9	10.0	6.1	3.7	-0.9	-1.3	0.4	2.3	-0.5	4.9	2.4	-0.8	3.9	
3.5	22.2	9.8	8.3	7.5	8.6	7.6	6.6	9.7	8.1	12.5	14.0	15.0	7.9	
6.5	316.3	252.9	137.6	104.7	98.5	114.6	120.0	63.0	50.6	64.9	39.2	27.1	20.0	
14.3	104.9	29.7	15.5	13.5	6.4	8.7	8.3	8.3	6.7	1.7	1.3	2.8	3.6	
20.1	98.6	7.6	11.8	12.3	1.2	5.5	5.8	9.9	7.7	5.6	2.6	5.7	10.7	
30	101.6	11.1	11.4	4.6	3.3	6.7	3.6	4.7	0.6	5.6	6.1	6.3	6.3	
>45	467.2	210.2	253.8	498.8	274.3	208.7	166.4	147.1	195.6	210.1	169.5	150.9	87.4	Total
Sub total	1141.5	531.1	444.3	644.9	391.2	350.3	310.9	244.8	268.6	305.1	234.9	206.8	139.6	5213.6
Mol. Wt	**Percent of total Activity** pH													
kDa	**2.21**	**2.65**	**2.95**	**3.64**	**4.14**	**5.00**	**5.60**	**6.11**	**6.59**	**7.11**	**7.75**	**9.25**	**10.26**	
<1	1%	0%	0%	0%	0%	0%	0%	0%	0%	0%	0%	0%	0%	
3.5	0%	0%	0%	0%	0%	0%	0%	0%	0%	0%	0%	0%	0%	
6.5	6%	5%	3%	2%	2%	2%	2%	1%	1%	1%	1%	1%	0%	
14.3	2%	1%	0%	0%	0%	0%	0%	0%	0%	0%	0%	0%	0%	
20.1	2%	0%	0%	0%	0%	0%	0%	0%	0%	0%	0%	0%	0%	
30	2%	0%	0%	0%	0%	0%	0%	0%	0%	0%	0%	0%	0%	
>45	9%	4%	5%	10%	5%	4%	3%	3%	4%	4%	3%	3%	2%	Total
Sub total	22%	10%	9%	12%	8%	7%	6%	5%	5%	6%	5%	4%	3%	100%

[a] All activity was background corrected

Table 37 Propagation of errors for ^{234}Th(IV) activity for 2D SDS-PAGE for Gulf of México Sample St. 4 72m

	2 σ values for ^{234}Th(IV) activity (%) pH												
kDa	**2.21**	**2.65**	**2.95**	**3.64**	**4.14**	**5.00**	**5.60**	**6.11**	**6.59**	**7.11**	**7.75**	**9.25**	**10.26**
<1	6.9	8.0	8.3	8.5	8.8	8.9	8.7	8.6	8.8	8.4	8.5	8.8	8.4
3.5	7.3	8.0	8.1	8.2	8.1	8.2	8.2	8.0	8.1	7.9	7.8	7.7	8.1
6.5	3.3	3.6	4.6	5.0	5.1	4.9	4.8	5.9	6.2	5.8	6.6	7.1	7.4
14.3	5.0	7.0	7.7	7.8	8.3	8.1	8.1	8.1	8.2	8.6	8.6	8.5	8.5
20.1	5.1	8.2	7.9	7.9	8.6	8.3	8.3	8.0	8.2	8.3	8.5	8.3	8.0
30	5.1	7.9	7.9	8.4	8.5	8.2	8.5	8.4	8.7	8.3	8.3	8.3	8.3
>45	2.8	3.9	3.6	2.7	3.5	3.9	4.3	4.5	4.0	3.9	4.2	4.4	5.4
	14.1%	18.3%	18.8%	19.1%	19.9%	19.7%	19.8%	19.8%	20.2%	19.8%	20.3%	20.4%	20.6%

Table 38 ^{14}C activity for 2D SDS-PAGE of $(^{14}CH_3)_2NH$ labeling of COOH functional group for *R. gallaeciensis*

Mol. Wt.	**Activity [a] (cpm) pH**													
kDa	**1.99**	**2.31**	**3.14**	**3.71**	**4.52**	**4.77**	**5.29**	**5.80**	**6.63**	**6.95**	**8.92**	**10.32**	**11.23**	
<6.5	41.9	22.4	30.3	18.8	10.1	18.0	18.1	26.4	7.4	38.8	21.1	6.1	147.9[B]	
14.3	10.1	11.6	26.5	9.1	6.0	4.8	4.2	6.8	7.4	14.1	12.3	-0.7	5.9	
20.1	14.4	27.3	23.8	10.4	1.8	2.6	2.7	3.7	4.5	1.8	4.2	-0.2	3.5	
30	11.0	26.5	24.2	7.9	5.8	3.8	3.1	3.6	4.5	3.0	4.0	-0.1	1.5	
>45	16.3	74.7	76.4	58.2	67.7	30.4	26.0	25.1	49.3	57.1	36.3	25.1	36.9	Total
Sub total	93.7	162.5	181.2	104.4	91.4	59.6	54.1	65.6	73.1	114.8	77.9	30.2	195.7	1,304.2
Mol. Wt	**Percent of total Activity with $(^{14}CH_3)_2NH$ pH**													
kDa	**1.99**	**2.31**	**3.14**	**3.71**	**4.52**	**4.77**	**5.29**	**5.80**	**6.63**	**6.95**	**8.92**	**10.32**	**11.23**	
6.5	3%	2%	2%	1%	1%	1%	1%	2%	1%	3%	2%	0%	11%	
14.3	1%	1%	2%	1%	0%	0%	0%	1%	1%	1%	1%	0%	0%	
20.1	1%	2%	2%	1%	0%	0%	0%	0%	0%	0%	0%	0%	0%	
30	1%	2%	2%	1%	0%	0%	0%	0%	0%	0%	0%	0%	0%	
>45	1%	6%	6%	4%	5%	2%	2%	2%	4%	4%	3%	2%	3%	Total
Sub total	7%	12%	14%	8%	7%	5%	4%	5%	6%	9%	6%	2%	15%	100%
Mol. Wt	**Percent of total Activity without $(^{14}CH_3)_2NH$ pH**													
kDa	**1.99**	**2.31**	**3.14**	**3.71**	**4.52**	**4.77**	**5.29**	**5.80**	**6.63**	**6.95**	**8.92**	**10.32**	**11.23**	
6.5	4%	2%	3%	2%	1%	2%	2%	2%	1%	3%	2%	1%	0%	
14.3	1%	1%	2%	1%	1%	0%	0%	1%	1%	1%	1%	0%	1%	
20.1	1%	2%	2%	1%	0%	0%	0%	0%	0%	0%	0%	0%	0%	
30	1%	2%	2%	1%	1%	0%	0%	0%	0%	0%	0%	0%	0%	
>45	1%	6%	7%	5%	6%	3%	2%	2%	4%	5%	3%	2%	3%	Total
Sub total	8%	14%	16%	9%	8%	5%	5%	6%	6%	10%	7%	3%	4%	100%

[a] All activity was background corrected
[b] ^{14}C activity associated with $(^{14}CH_3)_2NH$

Table 39 Propagation of errors for ^{14}C activity for 2D SDS-PAGE labeling of COOH group for *R. gallaeciensis*

	2 σ values for ^{234}Th(IV) activity (%)												
	pH												
kDa	**1.99**	**2.31**	**3.14**	**3.71**	**4.52**	**4.77**	**5.29**	**5.80**	**6.63**	**6.95**	**8.92**	**10.32**	**11.23**
<6.5	8.6	10.7	9.7	11.3	13.3	11.5	11.4	10.1	14.2	8.8	10.9	14.7	5.0
14.3	13.3	12.9	10.1	13.6	14.7	15.2	15.5	14.4	14.2	12.3	12.7	18.5	14.8
20.1	12.2	10.0	10.5	13.2	16.8	16.3	16.3	15.8	15.4	16.8	15.5	18.1	15.9
30	13.1	10.1	10.5	14.0	14.8	15.7	16.1	15.8	15.4	16.1	15.6	18.0	17.0
>45	11.8	6.8	6.7	7.5	7.1	9.7	10.3	10.3	8.1	7.6	9.1	10.3	9.0
	27%	23%	21%	27%	31%	31%	32%	30%	31%	29%	29%	36%	29%

V.7. Appendix VI Gas Chromatography Mass Spectra

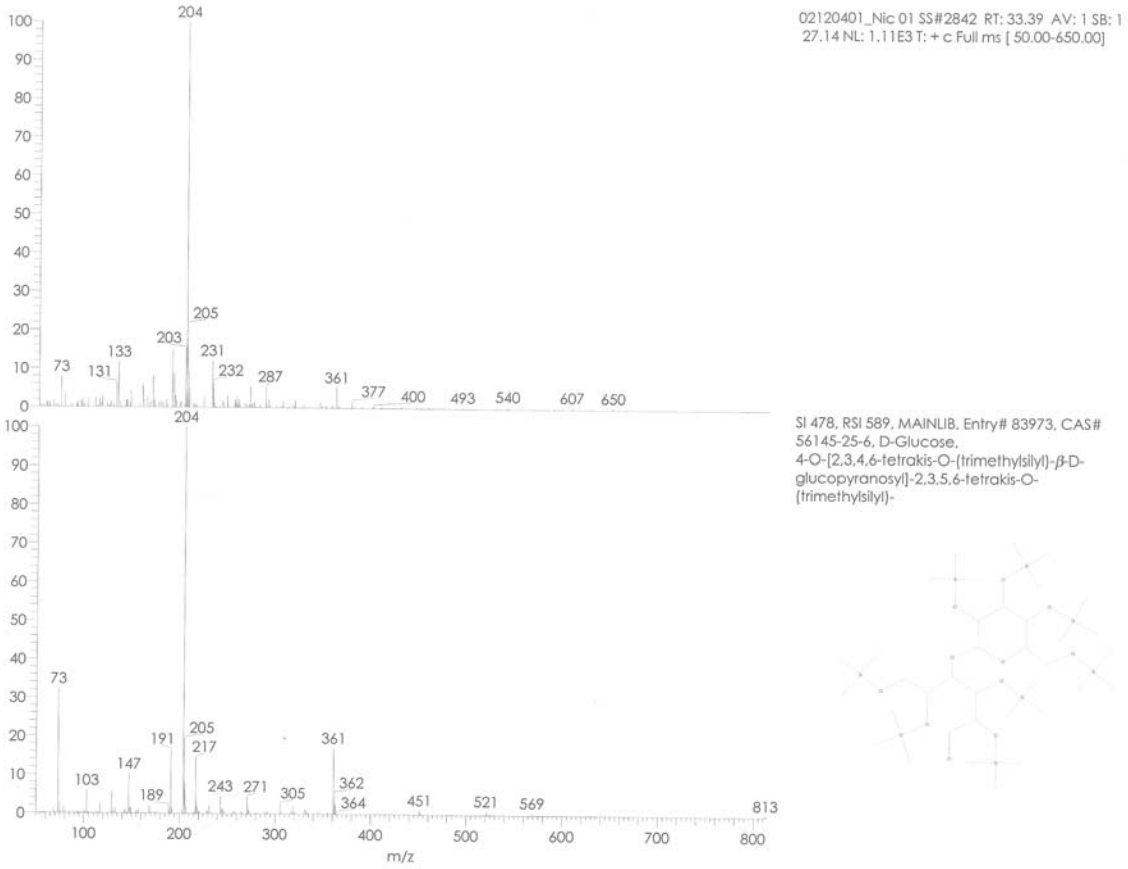

Figure 35 Mass Spectra of EPS from *S. stellata* at for gas chromatography peak at 33.39 minutes

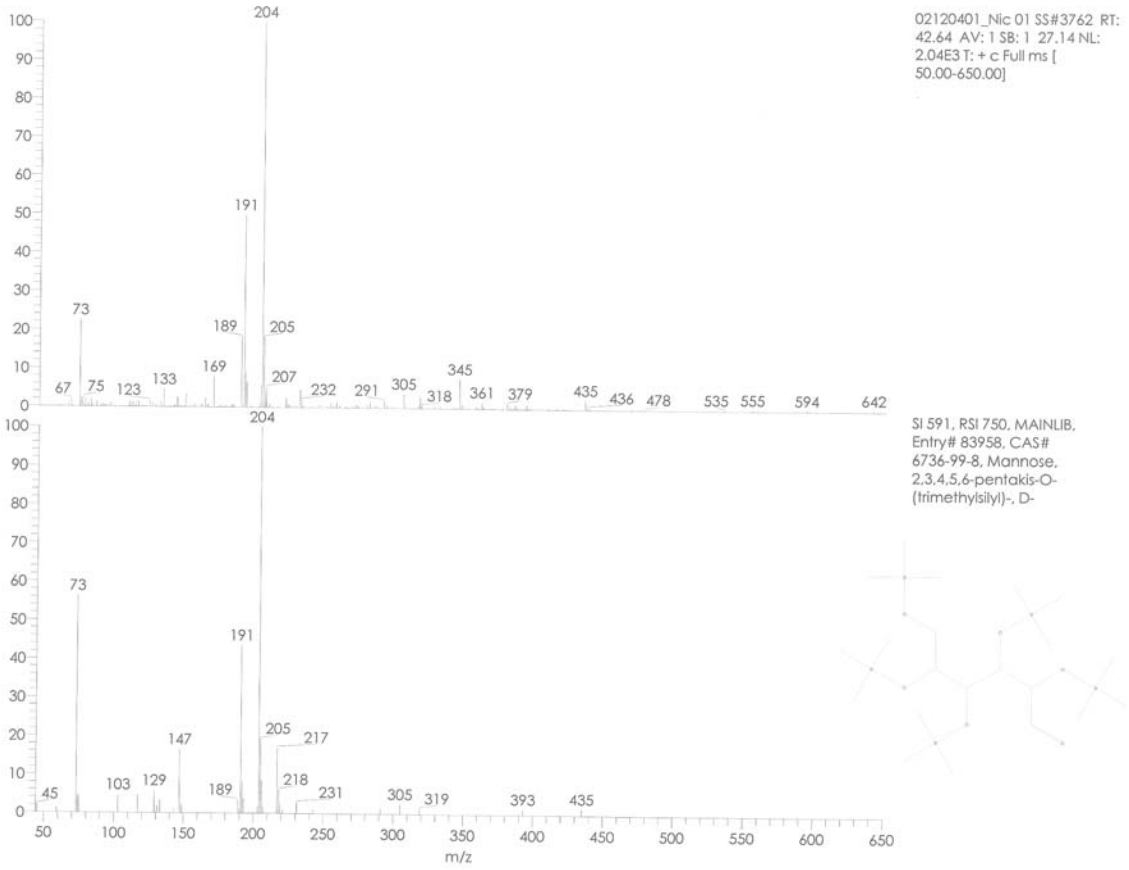

Figure 36 Mass Spectra of EPS from *S. stellata* at for gas chromatography peak at 42.64 minutes

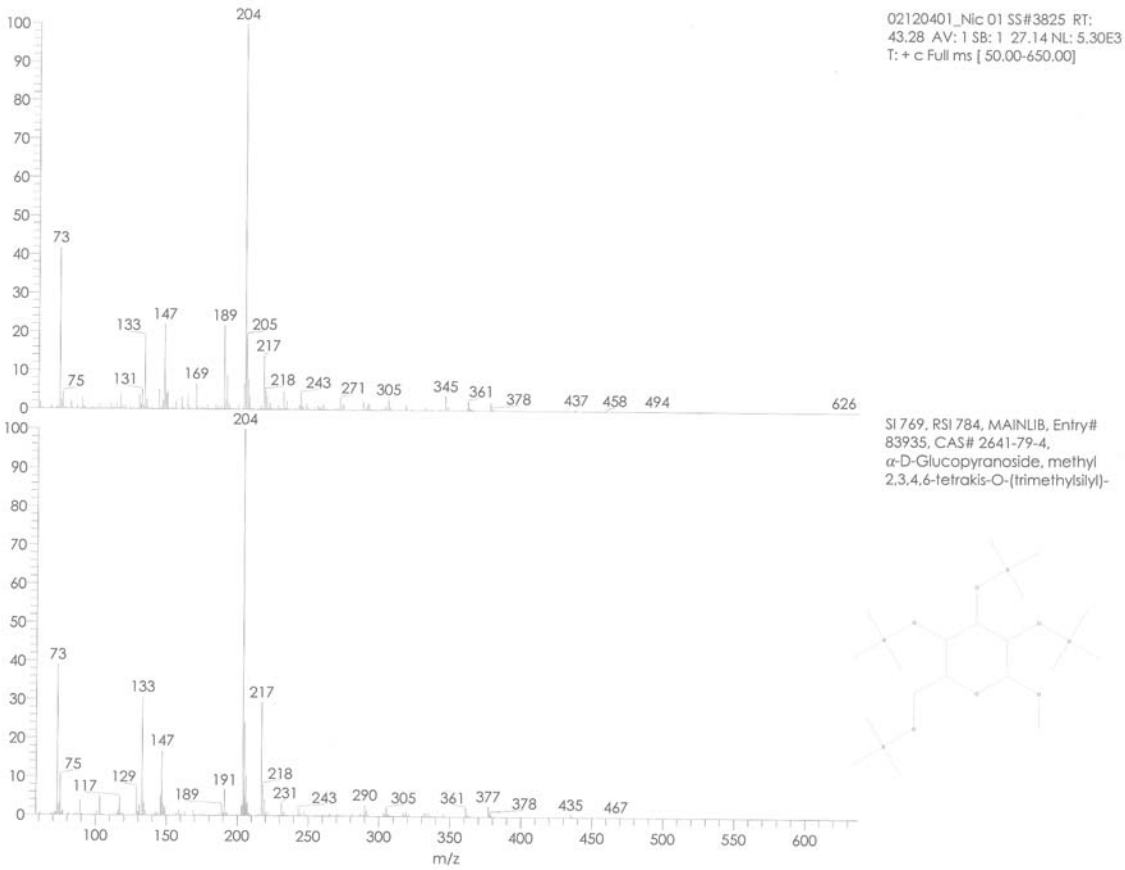

Figure 37 Mass Spectra of EPS from *S. stellata* at for gas chromatography peak at 43.28 minutes

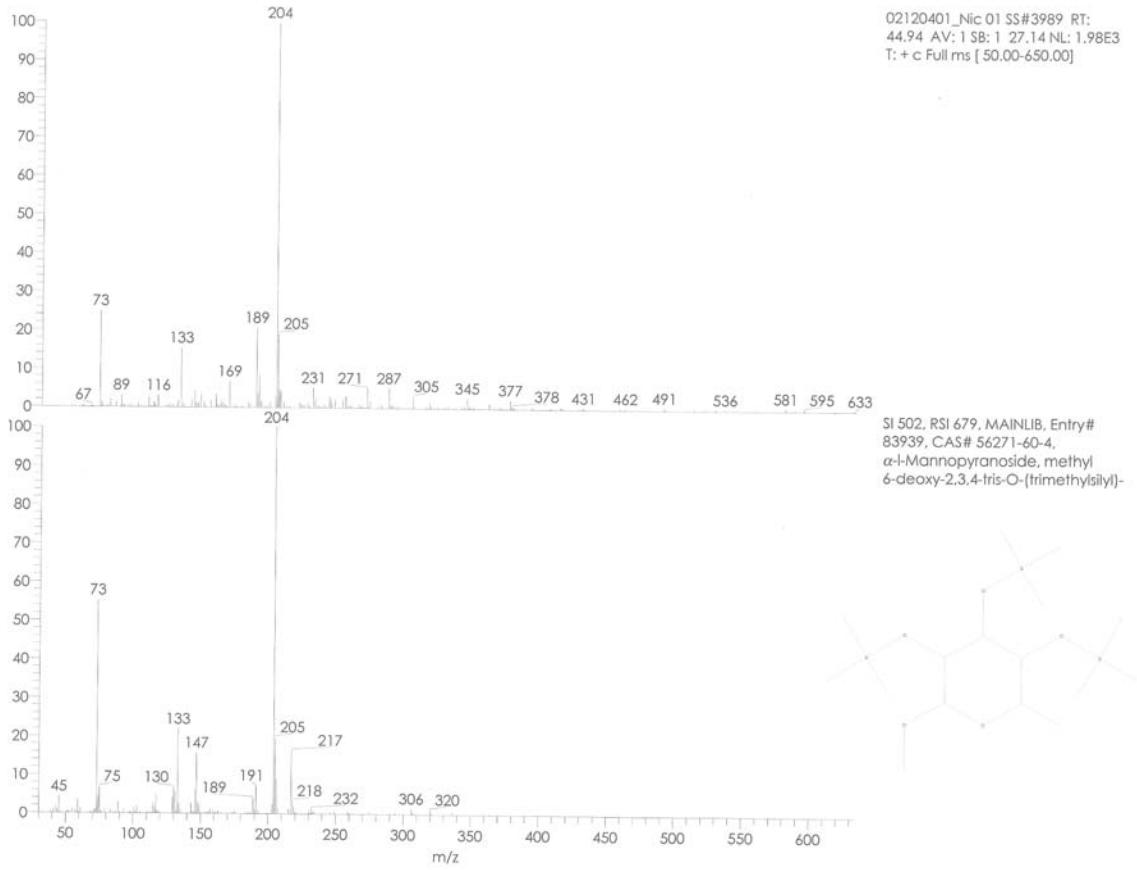

Figure 38 Mass Spectra of EPS from *S. stellata* at for gas chromatography peak at 44.94 minutes

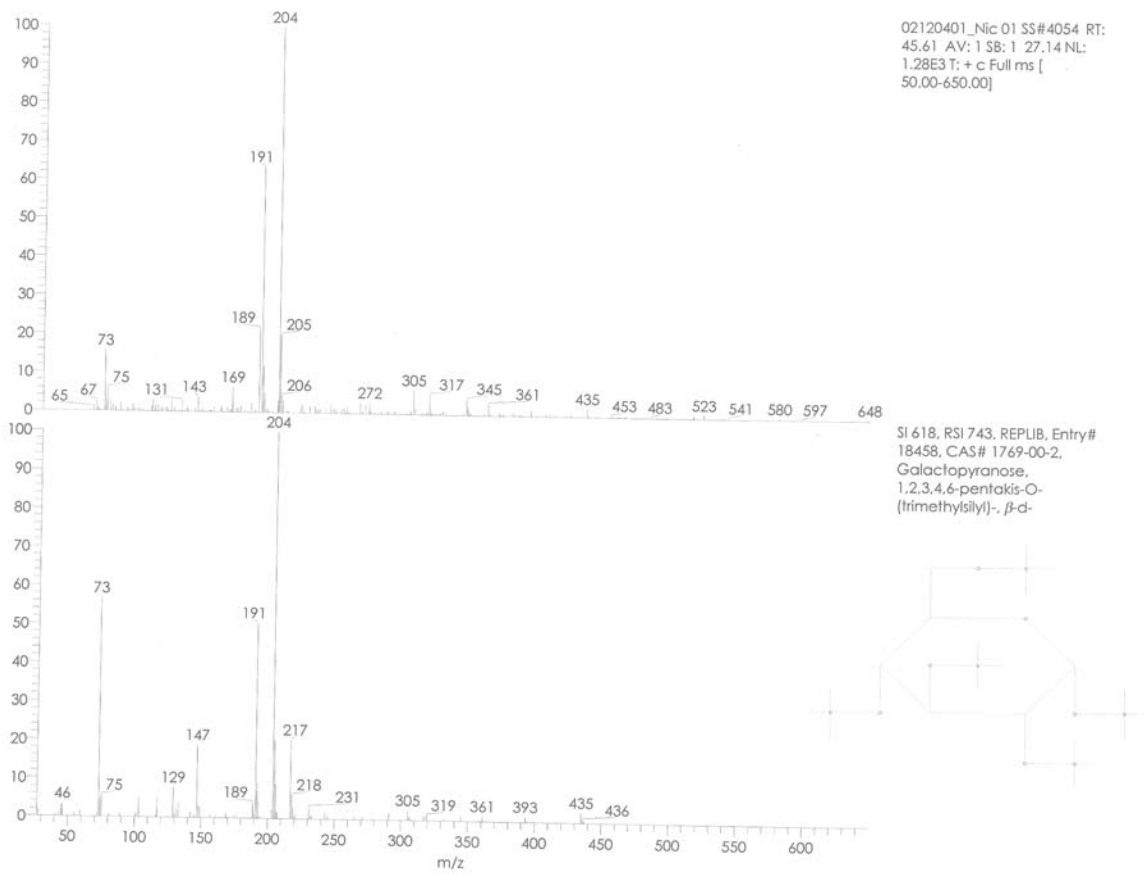

Figure 39 Mass Spectra of EPS from *S. stellata* at for gas chromatography peak at 45.61 minutes

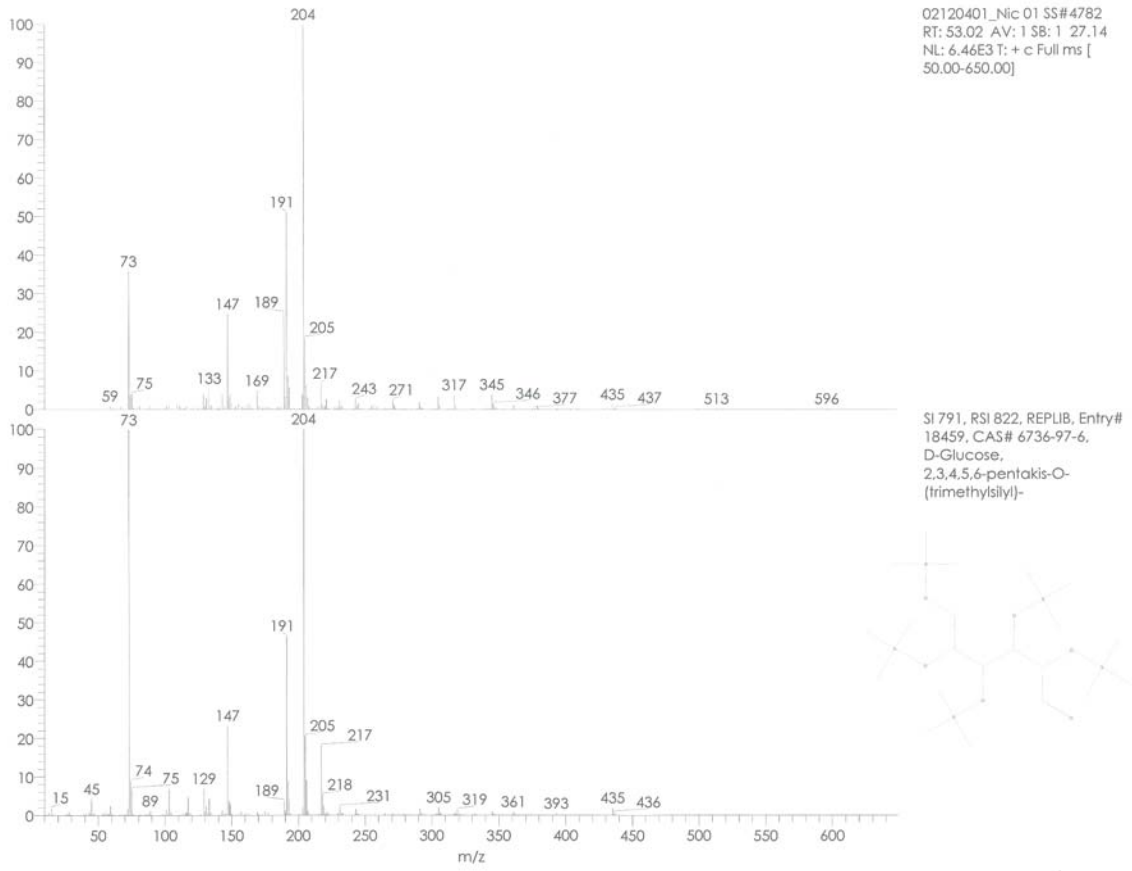

Figure 40 Mass Spectra of EPS from *S. stellata* at for gas chromatography peak at 53.02 minutes

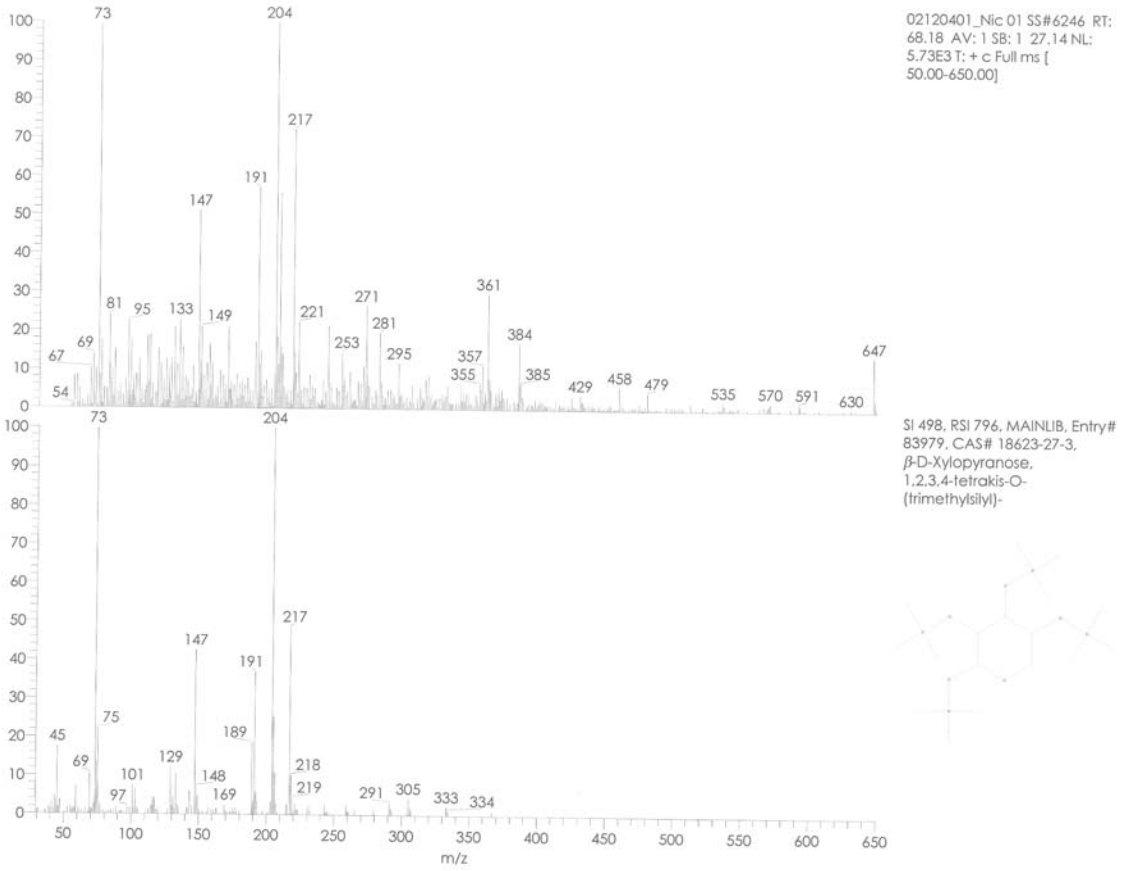

Figure 41 Mass Spectra of EPS from *S. stellata* at for gas chromatography peak at 68.18 minutes

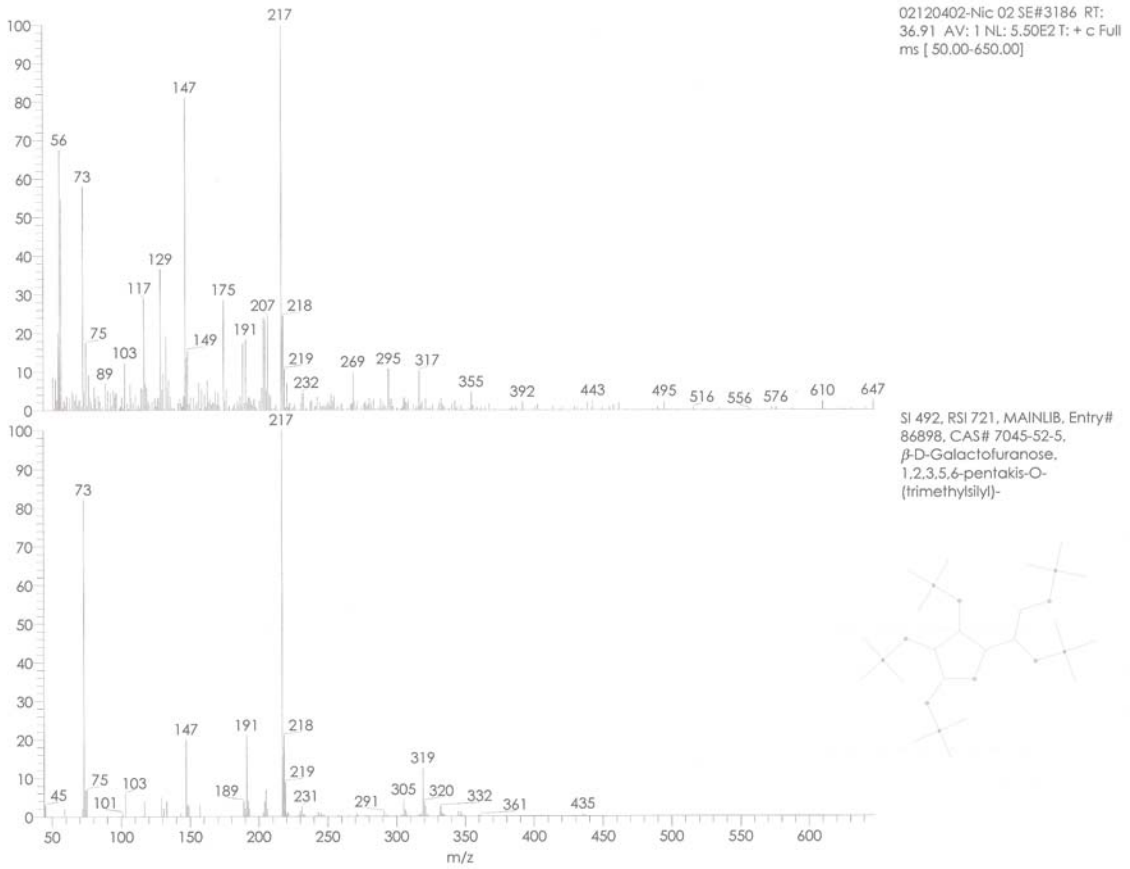

Figure 42 Mass Spectra of EPS from *S. elongatus* at for gas chromatography peak at 36.91 minutes

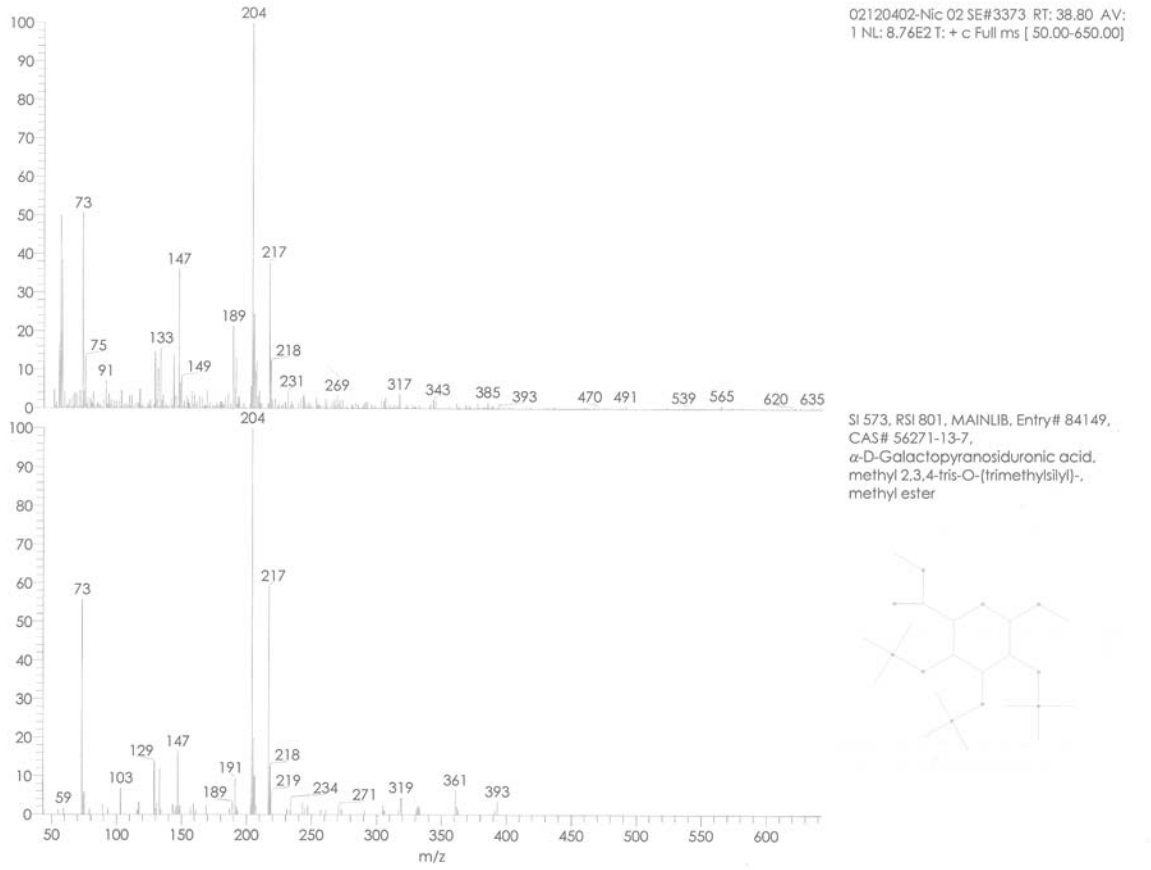

Figure 43 Mass Spectra of EPS from *S. elongatus* at for gas chromatography peak at 38.80 minutes

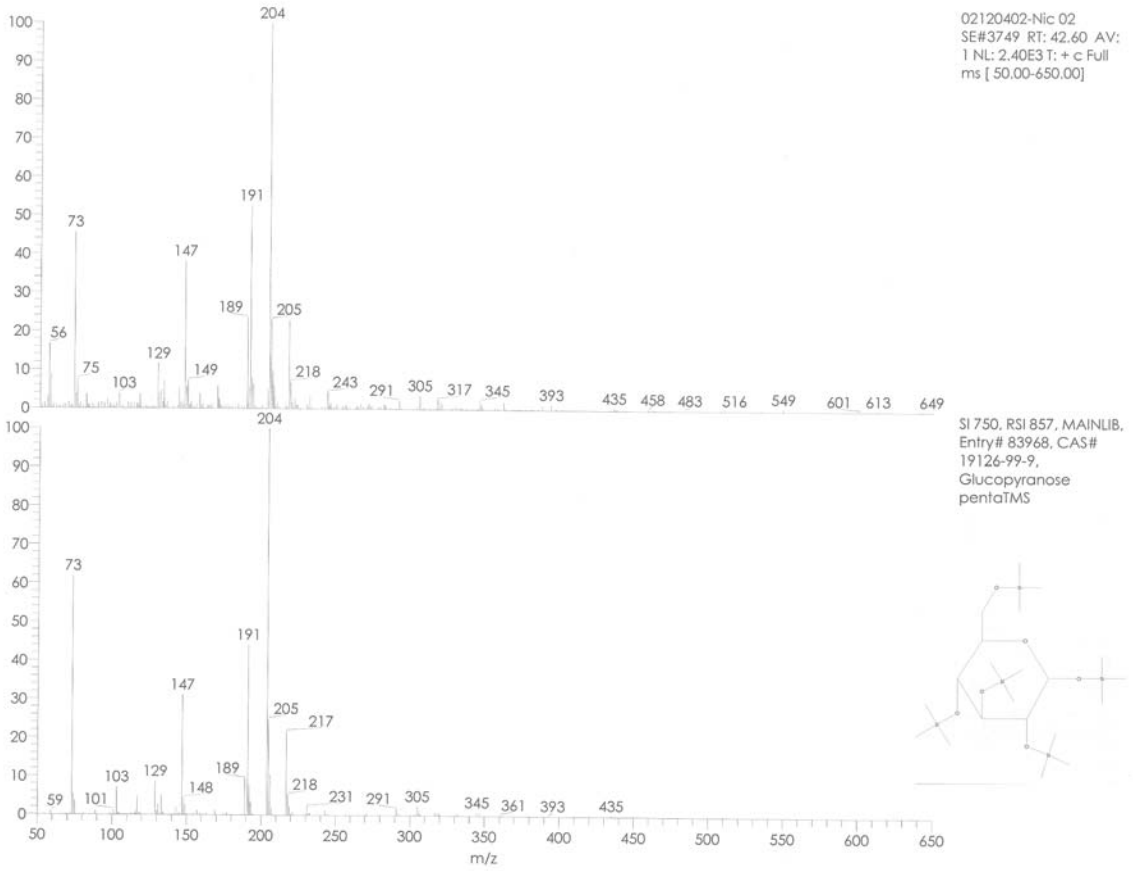

Figure 44 Mass Spectra of EPS from *S. elongatus* at for gas chromatography peak at 42.60 minutes

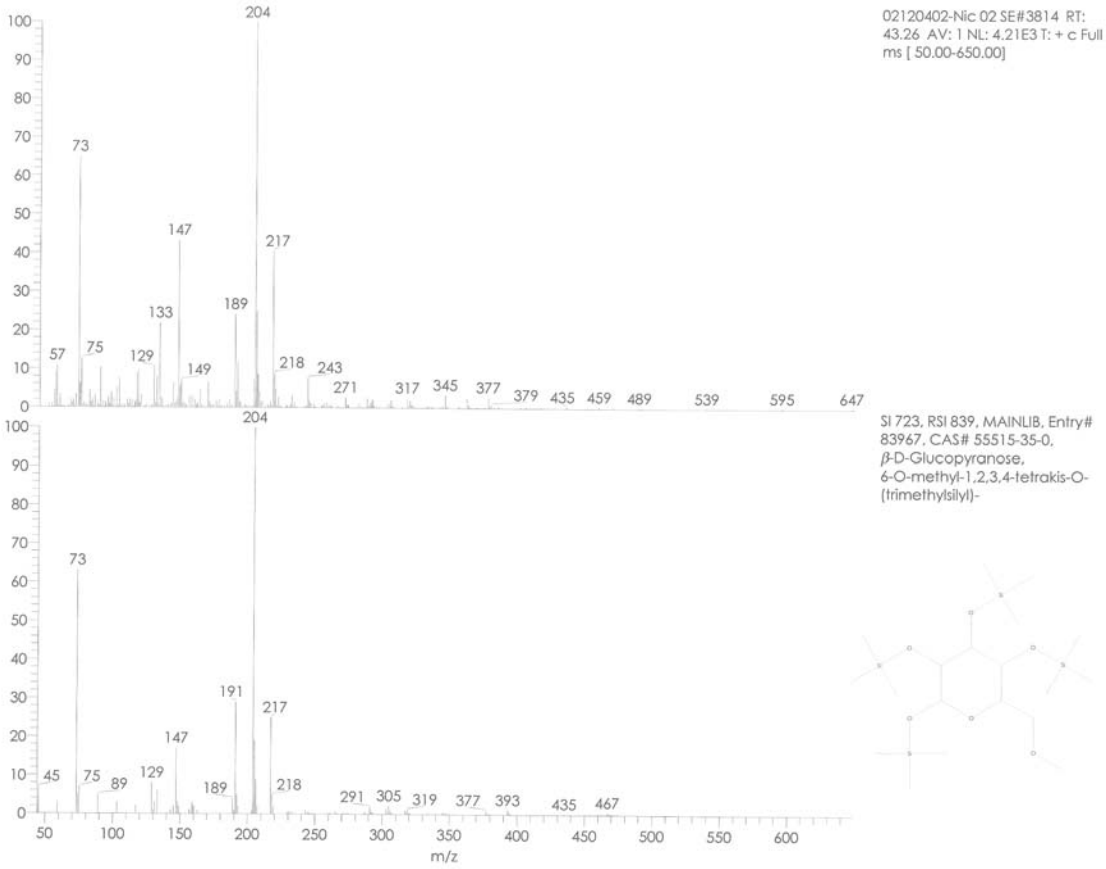

Figure 45 Mass Spectra of EPS from *S. elongatus* at for gas chromatography peak at 43.26 minutes

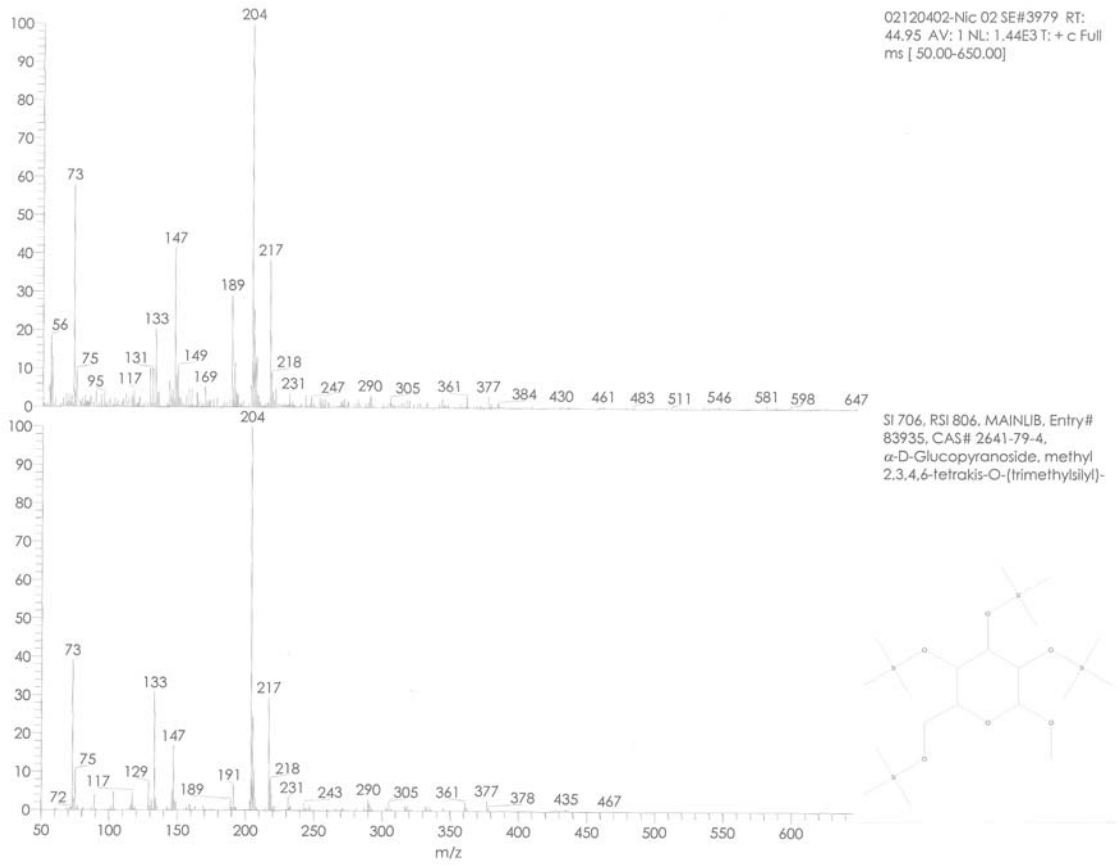

Figure 46 Mass Spectra of EPS from *S. elongatus* at for gas chromatography peak at 44.95 minutes

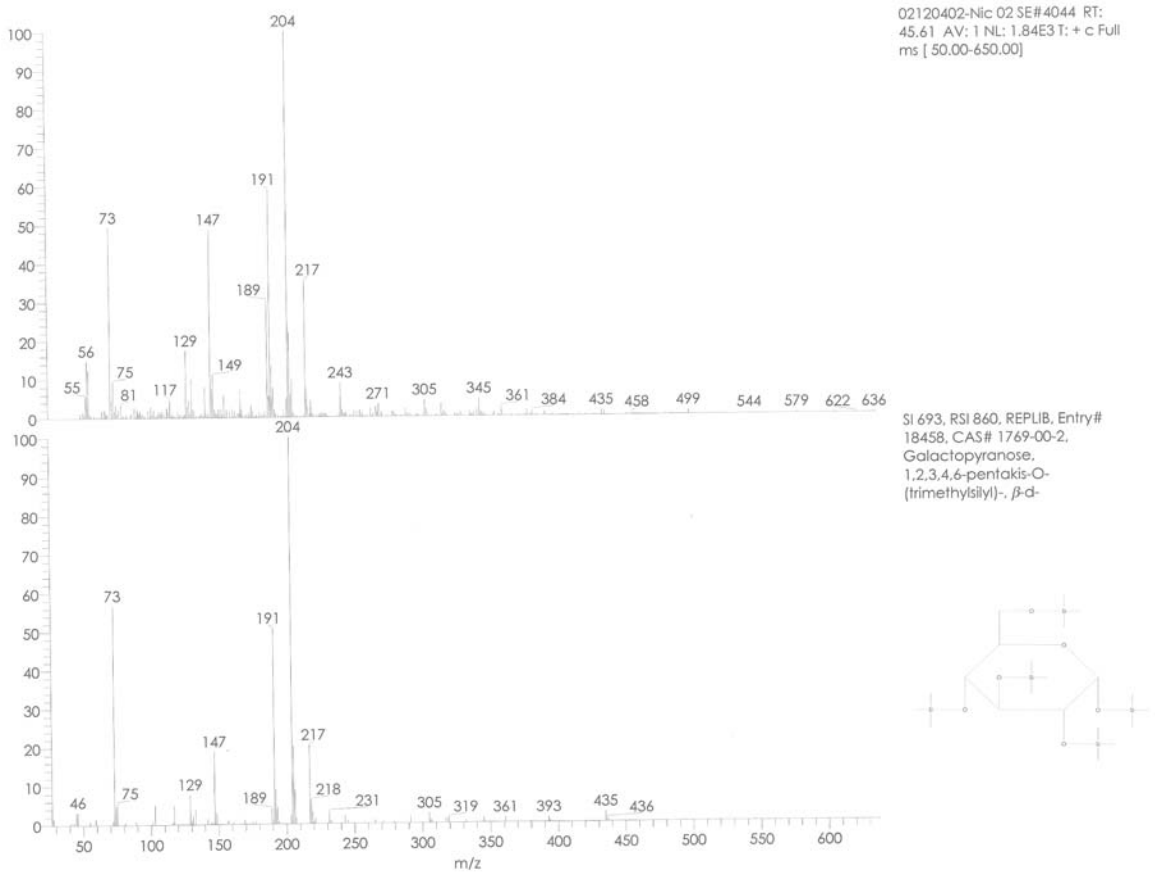

Figure 47 Mass Spectra of EPS from *S. elongatus* at for gas chromatography peak at 45.61 minutes

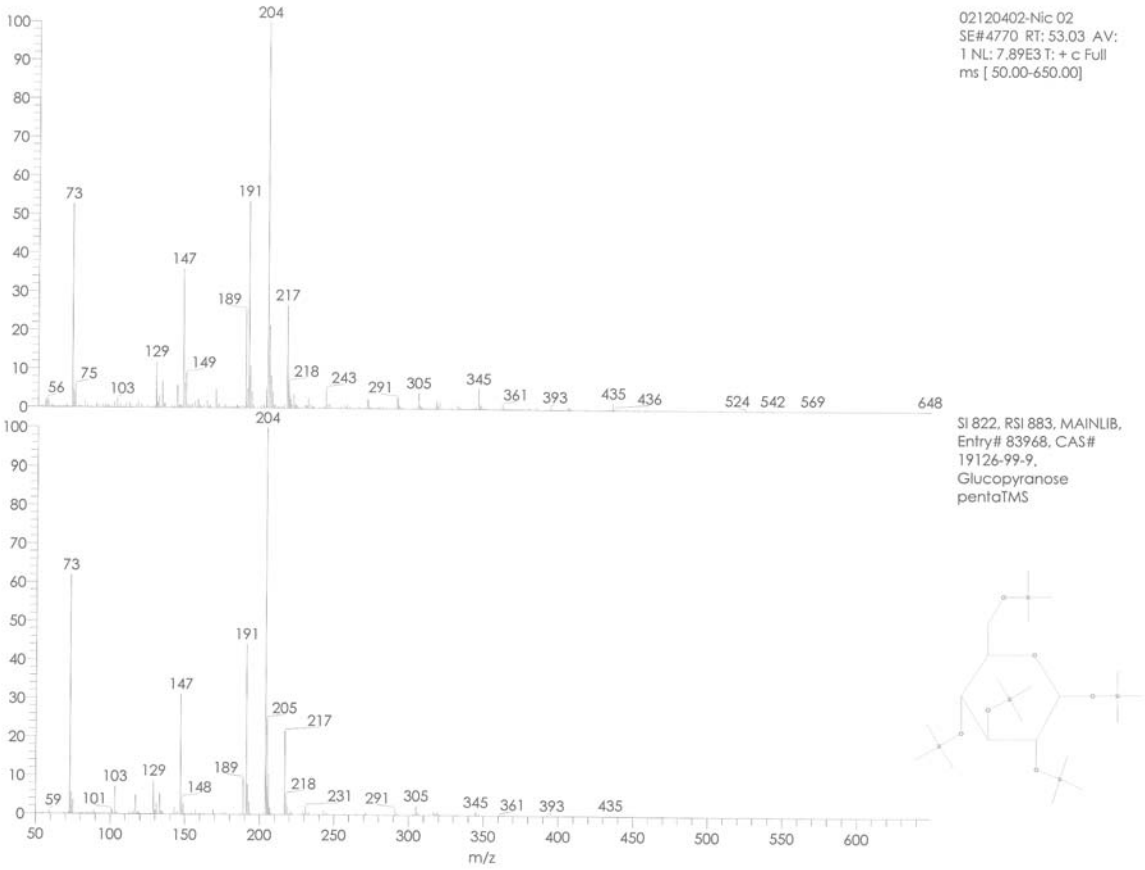

Figure 48 Mass Spectra of EPS from *S. elongatus* at for gas chromatography peak at 53.03 minutes

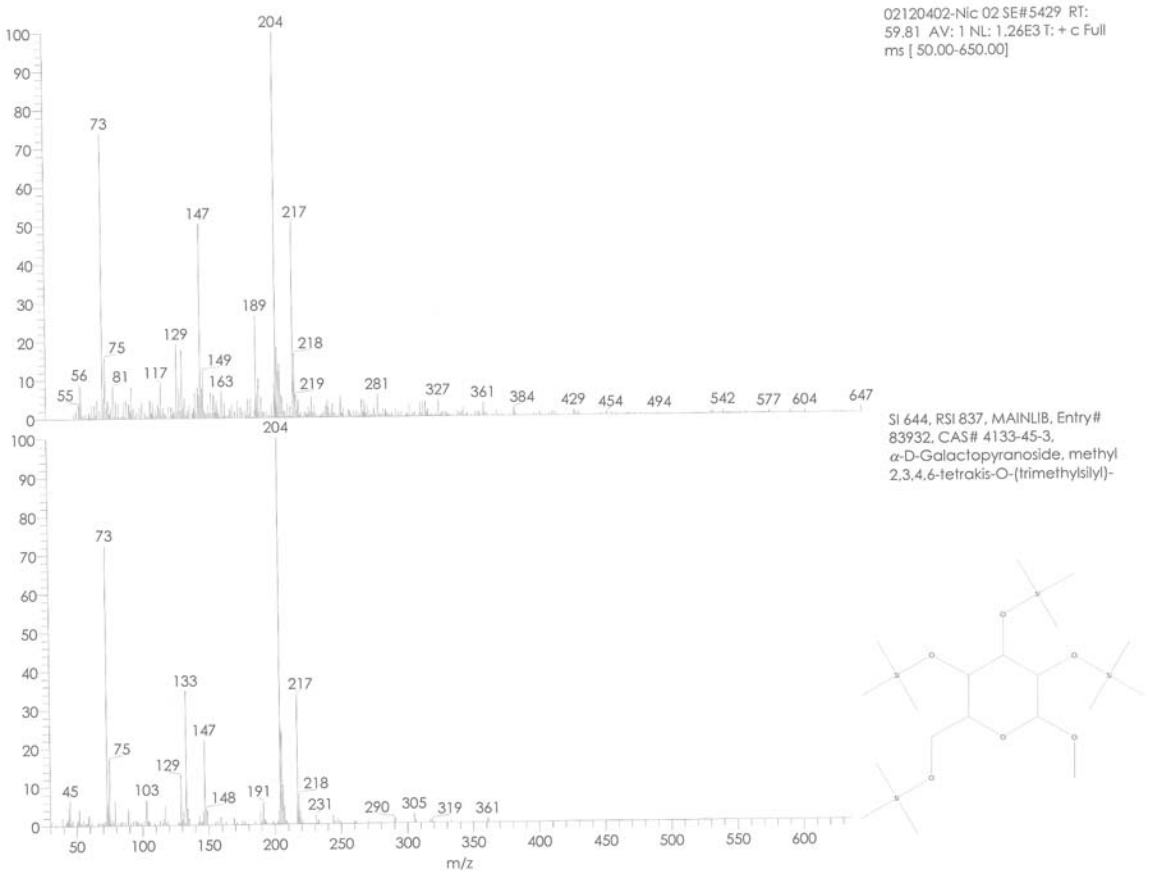

Figure 49 Mass Spectra of EPS from *S. elongatus* at for gas chromatography peak at 59.81 minutes

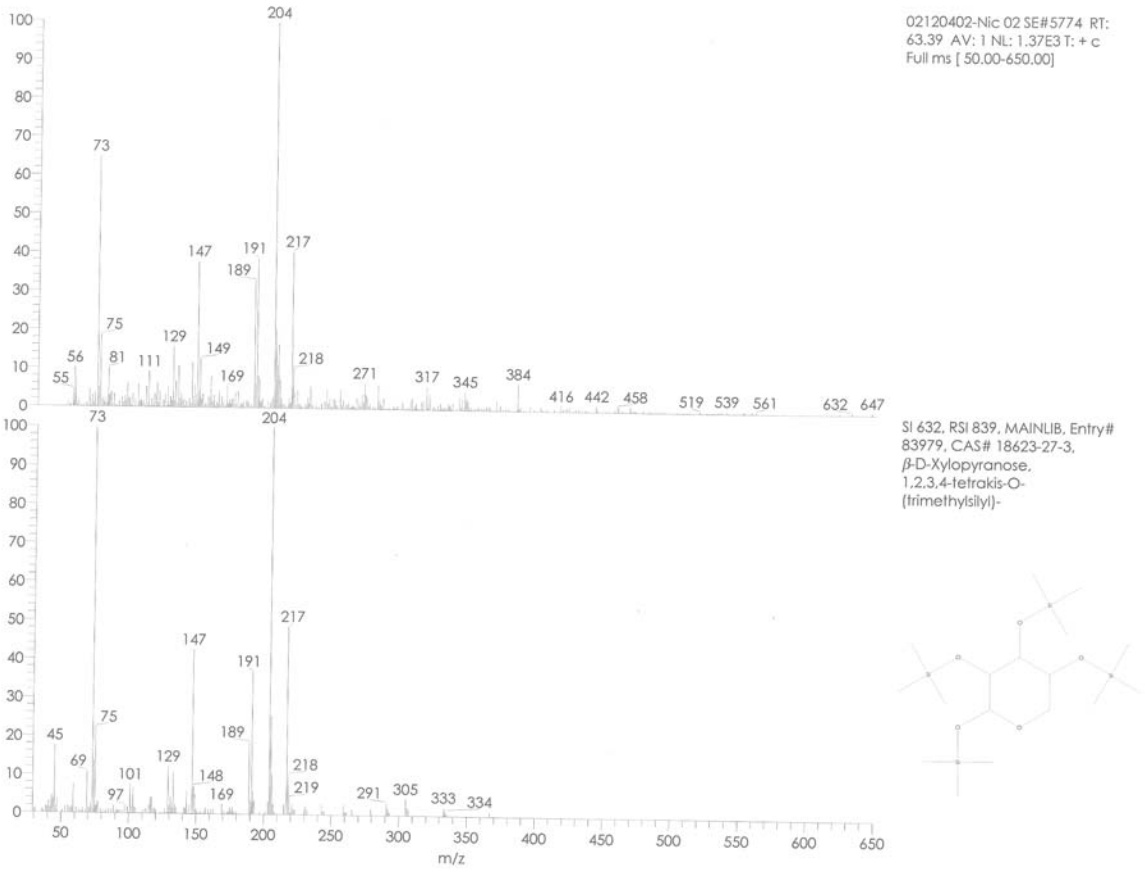

Figure 50 Mass Spectra of EPS from *S. elongatus* at for gas chromatography peak at 63.39 minutes

VITA

NICOLÁS GABRIEL ALVARADO QUIROZ

847 N. Humboldt, Suite 310
San Mateo, CA 94401

3549 Holmead Place
Washington, DC 20010

E-mail: nicolas.alvarado@noaa.gov

EDUCATION

- **Ph.D. in Chemical Oceanography, 1999-2004**
  Texas A & M University, College Station, TX
- **M.Sc. in Earth Sciences, 1997-1999**
  University of Ottawa, Ottawa, ON
- **B.Sc. (Hon.) in Chemistry, 1990-1995**
  University of Ottawa, Ottawa, ON

CONFERENCE PRESENTATIONS

2002 Ocean Sciences Meeting, Transport and Transformation of Biogeochemically Important Materials in Coastal Waters I Session OS22D-226. Honolulu HI (Poster) Abstract # 244 "Characterization of Marine Acid Polysaccharides Responsible for Binding Th Isotopes"

SELECTED PUBLICATIONS

Santschi, P.H., Hung, C.-C., Schultz, G., **Alvarado Quiroz, N. G.**, Guo, L., Pinckney, J., Walsh, I. (2003). Control of acid polysaccharide production and ^{234}Th and POC export fluxes by marine organisms, *Geophyical Research Letters*, **30**, dio, 10.1029/2002GL016046.

Hung C.-C., Guo L., Santschi P. H., **Alvarado Quiroz N. G.**, and Haye J. M. (2003) Distribution of carbohydrate species in the Gulf of México. *Marine Chemistry* **81**, 119-135.

Alvarado Quiroz, N. G., Kotzer, T., Milton, G., Clark, I.D. and D. Bottomley (2002). Partitioning of ^{127}I and ^{129}I in an unconfined glaciofluvial aquifer on the Canadian Shield. *Radiochimica Acta*. **90**, 469-478.

AWARDS & HONORS

- Dean John A. Knauss Marine Policy Fellow National Sea Grant Program (2004)
- Texas Institute of Oceanography Graduate Fellowship (Spring and Summer 2003)
- Texas A&M University Graduate Assistantship (1999-2003)
- Texas Institute of Oceanography Travel Grant (2002)
- Oceanography Graduate Council Travel Grant (2002)

LANGUAGES

- Fluent in English, French, Spanish, and working knowledge of Italian

PROFESSIONAL ACTIVITIES

- American Geophysical Union
- American Association for Underwater Sciences